Small Engine Technology (SET) Task 23 ANOPP Noise Prediction for Small Engines

Wing Reflection Code

L. Lieber and D. Brown
Honeywell Engines and Systems, Phoenix, Arizona

November 2000

The NASA STI Program Office ... in Profile

Since its founding, NASA has been dedicated to the advancement of aeronautics and space science. The NASA Scientific and Technical Information (STI) Program Office plays a key part in helping NASA maintain this important role.

The NASA STI Program Office is operated by Langley Research Center, the lead center for NASA's scientific and technical information. The NASA STI Program Office provides access to the NASA STI Database, the largest collection of aeronautical and space science STI in the world. The Program Office is also NASA's institutional mechanism for disseminating the results of its research and development activities. These results are published by NASA in the NASA STI Report Series, which includes the following report types:

- TECHNICAL PUBLICATION. Reports of completed research or a major significant phase of research that present the results of NASA programs and include extensive data or theoretical analysis. Includes compilations of significant scientific and technical data and information deemed to be of continuing reference value. NASA counterpart of peer-reviewed formal professional papers, but having less stringent limitations on manuscript length and extent of graphic presentations.

- TECHNICAL MEMORANDUM. Scientific and technical findings that are preliminary or of specialized interest, e.g., quick release reports, working papers, and bibliographies that contain minimal annotation. Does not contain extensive analysis.

- CONTRACTOR REPORT. Scientific and technical findings by NASA-sponsored contractors and grantees.

- CONFERENCE PUBLICATION. Collected papers from scientific and technical conferences, symposia, seminars, or other meetings sponsored or co-sponsored by NASA.

- SPECIAL PUBLICATION. Scientific, technical, or historical information from NASA programs, projects, and missions, often concerned with subjects having substantial public interest.

- TECHNICAL TRANSLATION. English-language translations of foreign scientific and technical material pertinent to NASA's mission.

Specialized services that complement the STI Program Office's diverse offerings include creating custom thesauri, building customized databases, organizing and publishing research results ... even providing videos.

For more information about the NASA STI Program Office, see the following:

- Access the NASA STI Program Home Page at *http://www.sti.nasa.gov*

- E-mail your question via the Internet to help@sti.nasa.gov

- Fax your question to the NASA STI Help Desk at (301) 621-0134

- Phone the NASA STI Help Desk at (301) 621-0390

- Write to:
  NASA STI Help Desk
  NASA Center for AeroSpace Information
  7121 Standard Drive
  Hanover, MD 21076-1320

NASA/CR-2000-210630

Small Engine Technology (SET) Task 23 ANOPP Noise Prediction for Small Engines

Wing Reflection Code

L. Lieber and D. Brown
Honeywell Engines and Systems, Phoenix, Arizona

November 2000

The use of trademarks or names of manufacturers in the report is for accurate reporting and does not constitute an official endorsement, either expressed or implied, of such products or manufacturers by the National Aeronautics and Space Administration.

TABLE OF CONTENTS

TABLE OF CONTENTS (CONT)

LIST OF FIGURES

LIST OF FIGURES (CONT)

Acknowledgements

1. INTRODUCTION AND OBJECTIVES

1.1 Introduction

This Final Report has been prepared by Honeywell Engines & Systems, Phoenix, Arizona, a unit of Honeywell International Inc., documenting work performed during the period August 1999 through December 1999 for the National Aeronautics and Space Administration (NASA) Glenn Research Center, Cleveland, Ohio, under the Small Engine Technology Program, Contract No. NAS3-27483, Task Order 23, Wing Reflection Code. The NASA Task Monitor was Mr. Robert A. Golub, NASA Langley Research Center, Mail Code 461, Hampton, Virginia 23681-0001; telephone: (757)864-5281. The NASA Contract Officer was Ms. Linda M. Kendrick, NASA Glenn Research Center, Mail Code 500-305, Cleveland, Ohio 44135-3191; telephone: (216)433-2407.

The work performed under Task 23 consisted of the development and demonstration of improvements for the NASA Aircraft Noise Prediction Program (ANOPP), specifically targeted to the modeling of engine noise enhancement due to wing reflection.

This report focuses on development of the model and procedure to predict the effects of wing reflection, and the demonstration of the procedure, using a representative wing/engine configuration.

1.2 Objectives

The primary function of the ANOPP program[1, 2]* is to provide the best, currently-available methods to predict aircraft noise. As new methods and engine acoustic data become available, ANOPP prediction modules can be improved or new modules can be added.

One aspect of noise modeling that has not previously been addressed in ANOPP is the effect of engine noise reflected from the wing surface, as perceived by a ground observer. Noise at the receiver is enhanced due to reflection of the noise incident on the wing surface.

The objective of this task was to develop a procedure to predict the effects of wing reflection on farfield acoustics, and to provide a Fortran prediction code to the ANOPP noise prediction program for wing reflection modeling.

1.3 Summary

A wing reflection model was successfully developed and prepared for installation in the ANOPP program. The model represents the increase in noise at a ground observer position that results when the aft fan duct source reflects off of the wing surface.

The degree of modeling accuracy required to predict the wing reflection behavior was determined using the Raynoise®[3] ray tracing program. This tool was applied to a series of wing/engine configurations to assess the impact of extended flaps, etc., on the noise reflected by the wing. The wing reflection studies performed with Raynoise® showed the importance of the

---

*References are listed in Section 8.

1

wing and flap as reflecting surfaces. As a result, the wing reflection model developed for ANOPP included multiple reflecting surfaces, in order to adequately represent the wing geometry.

Based on the conclusions reached in the Raynoise® study, ANOPP-compatible software was developed to model the wing reflection, in order to obtain more accurate farfield acoustics predictions. The wing reflection model was initially implemented in the Engines & Systems noise prediction program, GASP[4], and was demonstrated with a typical high-wing regional transport aircraft. Use of the wing reflection model resulted in an increase in observed noise from the aft fan duct, which was consistent with the predictions from the Raynoise® analyses.
Along with the wing reflection software, documentation was prepared, including a User Manual and a Technical Manual for the ANOPP wing reflection module.

2. TECHNICAL APPROACH

2.1 Approach

Experimental investigations have shown that the impact of wing reflection on farfield acoustics can be significant[5]. In particular, for regional aircraft with engines mounted under the wing, engine noise reflected from the wing can make a substantial contribution to the total noise detected by a ground observer.

NASA's ANOPP noise prediction program does not currently have a model to predict noise due to wing reflection. In order to improve the prediction capability of ANOPP, for under-the-wing engine mount configurations, a wing reflection model was needed.

As a first step toward developing the wing reflection model, a study was performed to determine the degree of modeling accuracy required to capture the primary elements of the reflected noise. The Raynoise® ray-tracing program was applied to examine a series of wing/engine configurations, and assess the impact of extended flaps, etc. on the noise reflected by the wing. This effort is discussed in more detail in Section 3.

In addition, various effects were examined using simple analytical estimates to determine what assumptions were justified, and whether a particular effect had to be included in the final reflection model. A criterion for determining the level of accuracy required involved the determination of the impact of the contribution from a particular source, during a 2-second integration of flyover noise exposure. If a particular source was not estimated to contribute measurably to the 2-second integrated noise level at the ground observer, then the contribution was considered to be secondary, and was not included in the model. Details of the model development are presented in Section 4.

The general model for wing reflection that was developed, based on the conclusions reached in the Raynoise® studies and the additional analytical estimates, then formed the foundation of the wing reflection analysis procedure that was implemented in a Fortran software module compatible with the ANOPP program. The wing reflection module was first installed in the Engines & Systems noise prediction program, GASP, where a series of analyses were performed to demonstrate that the farfield acoustics predictions accurately modeled the wing reflection effects. The results were compared with Raynoise® predictions for equivalent wing/engine configurations. The GASP analyses are summarized in Section 5.

After demonstrating the method in the GASP program, the wing reflection module was installed in ANOPP. This effort is discussed in Section 6.

2.2 Selection of Configurations

Relevant wing/engine configurations were required for both the Raynoise® studies and the demonstration cases for the new wing reflection model. It was desired to use a typical regional configuration, with engines mounted under-the-wing. The RJ100 regional transport, shown in Figure 1, was selected for the wing reflection studies. It is a high-wing transport with four engines mounted under-the-wing. The wing has a single, unbroken, tabbed Fowler flap system, which

3

extends over 78 percent of the wing span. Engines & Systems' LF507 engines are on the aircraft, and therefore sufficient information is available to model the aircraft and engine geometry.

For purposes of the Raynoise® studies and new wing reflection model predictions, the aircraft is modeled as simply a wing/engine combination. The fuselage and empennage are not included.

The certification flight profiles were used for take-off, sideline, and approach flight conditions. Analyses were performed for configurations with and without flaps, as appropriate to the flight condition. The primary flight conditions and wing configurations analyzed were as follows:

- Cutback Take-Off: Wing with Flaps Retracted
- Sideline: Wing with Flaps Retracted
- Approach: Wing with Full Flaps (33 Degrees)

Figure 1. The RJ100 Regional Transport Served as the Basis for the Wing/Engine Configuration Used in the Wing Reflection Studies.

3. WING REFLECTION USING RAY-TRACING PROGRAM

3.1 Ray-Tracing Predictions

The commercial acoustic ray-tracing program Raynoise® from LMS was used to predict the effects of engine noise reflections off an aircraft wing. The detailed noise contours provided by Raynoise® gave an understanding of both the gross effects of wing reflections as well as some of the nuances related to source position and wing geometry. Results from the ray-tracing program were used to optimize the methodology for the wing reflection model to be developed for NASA's ANOPP noise prediction program.

3.2 Description of Raynoise® Program

Raynoise® models the physics of acoustical propagation, including specular and diffuse reflections against physical boundaries, wall absorption and air absorption, diffraction, and transmission through walls.

Raynoise® combines a mirror image source method (MISM) with a ray tracing method (RTM), called the triangular beam method. Beams having a triangular cross section are emitted from the noise source. The number of beams the user selects determines the angular coverage of each beam. Having a triangular shape allows for complete coverage of the surrounding volume without the beams overlapping. The axis of each beam is traced while assuming spherical divergence and the corresponding decrease of sound intensity with distance. Absorptive properties of surrounding surfaces are accounted for with appropriate energy reductions with each reflection. Receiver locations are modeled as points and the contributions from all beams arriving at each receiver point are summed. Use of beams eliminates the need for time-consuming visibility testing inherent in the MISM while maintaining the advantage of simple receiver definition (point definition for MISM vs. volume required by RTM).

Single point sources are used in Raynoise® to model compact noise sources, while an array of point sources is used to model a distributed source. Both incoherent and coherent sources are available. Only incoherent sources were used in the analyses presented here, because it was assumed the relative phase between direct and reflected rays is not preserved in actual atmospheric propagation. The user may specify the angular extent of the source propagation (i.e., spherical, hemispherical radiation). Raynoise® can handle both specular and diffuse reflections of multiple order – beams can reflect more than once. Specular reflection was assumed for all studies reported here.

The geometry of a model along with the receiver locations can be constructed in Raynoise®; however, it was found that creation of these components using another piece of software was more efficient. MSC Patran® was used to manipulate IGES files for the aircraft under study and to generate the necessary model and receiver meshes.

3.3 Raynoise® Models of the RJ100

The model that was used for the Raynoise® study was derived from the RJ100 regional transport. The aircraft model was simplified to include only the port wing, flaps, outboard LF507

engine, and pylon (Figure 2). The wing and flaps were modeled as flat plates, and the engine nacelle and pylon surfaces were approximated by sets of planar surfaces (Figure 3).

Two models were considered for the pressure side of the wing. Simple connection of the leading and trailing edges produced the first wing model, described by a single element (Figure 3). The second wing model was slightly more complex and used two elements to estimate the curvature of the wing (Figure 4). Both models were run in three different configurations: engine-wing, engine-wing-flaps, and engine-wing-flaps-pylon. Flaps were modeled in the fully extended position.

Material properties were assigned to elements within the model. The wing and flaps were treated as perfectly reflective surfaces. All other surfaces were modeled as completely absorptive. This eliminated the possibility of reflections from the planar surfaces that represented the nacelle and pylon surface curvatures.

Raynoise® was used to model fan discharge noise from the LF507 engine. Because the LF507 installation has a separate flow nozzle, the source was placed in the fan bypass exit plane and the core nozzle was removed. A 4000 Hz tone was modeled to simulate the fan blade passage frequency. However, since an incoherent source was assumed, the predictions are valid for any frequency.

Three different source configurations were used. The first was a point source located on the centerline of the outboard engine in the plane of the fan bypass duct exit, as is shown in Figure 3. The point source was configured to radiate over the aft-facing hemisphere. The second source model included both the inboard and outboard engines modeled using two point sources that both radiated only to the aft-facing hemisphere (Figure 5). The inboard point source was positioned on the centerline of the inboard engine in the plane of the fan bypass duct exit. A more realistic distributed source was also used to model the outboard engine, making up the third source model. Twelve point sources were aligned in a ring representing the annular fan bypass duct exit (Figure 6).

A ground plane was modeled as shown in Figure 7. The aircraft was positioned at an altitude of 394 feet above a plane extending 700 feet in every direction. Grid spacing on the ground was 20 feet.

3.4 Model of Single-Element Wing with Point Source

As a baseline, noise contours were generated for the engine only with a single point source (no wing reflection), as shown in Figure 8.

The effect of reflections off the single-element wing (no flaps or pylon) is shown in Figure 9. With the source located just forward of the wing leading edge (Figure 3), the boundary of the region affected by wing reflections was apparent in both the contour and delta plots. Noise levels were increased by approximately 3 dB at each receiver location in the affected region, because each receiver (grid point) "saw" two rays that had traveled nearly the same distance from the engine.

Addition of the flaps increased noise levels on the ground plane, immediately aft of the aircraft position, as three and sometimes four rays propagated to the same location (Figure 10). Rays initially reflected to the aft starboard side of the ground plane were shielded by the flaps.

6

Single reflections were directed forward of the aircraft by the flaps. The widths of these forward regions, where noise levels increased, were 40 to 60 feet for a flyover altitude of 394 ft.

In an attempt to determine the influence of an engine pylon on the reflection of fan exit noise off a wing, the geometry of the RJ100 pylon was described using a simple four-element model (Figure 3). The beam method of Raynoise® breaks down for sharply curved surfaces like the underside of the engine pylon, thus the simple model. Because the pylon could not be accurately simulated, it was decided that the assignment of a completely absorptive material to the four pylon surfaces would be sufficient to determine the extent of the ground plane affected by this region of the wing. Figure 11 shows that, with a point source located in the lateral center of the pylon, a "trough of silence" was predicted behind the aircraft. This trough was approximately 160-feet wide. In actuality, the fan exit noise source is not a point but is rather a distributed source having a diameter nearly three times the width of the pylon. The results with a distributed source are given later.

3.5 Model of Double-Element Wing with Point Source

Division of the underside of the wing into two elements produced two distinct regions affected by reflections. Figure 12 shows that the forward portion of the wing reflected fan noise down to the region below and just aft of the aircraft, while reflections off the aft portion of the wing increased noise in the region farther behind the aircraft. A large region unaffected by reflections was predicted between them. Reflections were directed forward of the aircraft on the starboard side, due to the slope of the forward wing surface.

Addition of flaps and an absorptive pylon produced similar trends to those with the single element wing. The flaps increased noise forward and just aft of the aircraft while the absorptive pylon created a trough that was unaffected by reflections (Figure 13). An interesting result was the appearance of reflections between the regions influenced by the forward and rearward wing elements. These were the result of double reflections off the wing and flaps and influenced isolated areas approximately 40-feet wide.

3.6 Model of Inboard and Outboard Engines with Point Sources, Single Element Wing

Inclusion of the inboard engine produced very similar noise contours to those predicted with only the outboard engine (Figure 14). The close proximity of the two noise sources and the wing relative to their altitude resulted in only slight changes in the sizes of the regions affected by wing reflections. A comparison was made between the noise contours predicted with both the inboard and outboard engines and the contours predicted with only the outboard engine having twice the source strength (plus 3 dB). Figure 15 shows that over most of the ground plane the two models gave the same results. Differences arose in narrow regions near the edges of those areas influenced by reflections because of the differences in source locations.

3.7 Model of Outboard Engine with Ring Source, Single Element Wing

The point sources used in the 12-point distributed ring source model each had the same sound power level as the single point source used in the models presented above. For that reason, the overall noise levels along the ground plane were higher, as shown in Figure 16 for the distributed source baseline with no wing reflection.

7

Use of a spatially distributed source served to "blur" the edges of the regions affected by wing reflections (Figure 17), but produced essentially the same gross behavior as seen for the point source.

With flaps deployed, the area forward of the aircraft that was influenced by reflections off the aft flap (tab) became wider (Figure 18). Recall that the single point source was predicted to create a band approximately 40-feet wide (Figure 10). The ring source produced a band four times that wide. The radius of the distributed source was of the same order of magnitude as the chord length of the tab, and the two were relatively close to each other. Therefore, the range of possible reflection angles off the tab relative to the engine centerline was much greater than was produced with the single point source. A decrease was seen in the ratio of rays reflecting off the wing to those reflecting off the flaps and propagating to locations just aft and starboard of the aircraft. This is shown in Figure 18, where the maximum increase in noise due to wing-flap reflections was predicted to be just over 4 dB. Compare this result with the result from the single point source model (Figure 10), which showed a predicted increase of 6 dB at some locations. These predictions indicate that modeling the fan exit noise as a point source may give a conservative (high) estimate.

It was seen that the presence of an engine pylon did not have a significant effect when the fan source was modeled as a ring of point sources with diameter approximately three times the width of the pylon (Figure 19). The "trough of silence" directly behind the aircraft essentially disappeared. The pylon provided some shielding of rays propagating from one side of the pylon to the wing on the opposite side, resulting in a slight depression of the noise in the region behind the aircraft. It is likely that in reality, reflections from the pylon would make up for the noise decreases due to shielding, thereby giving a result very similar to that for the model without a pylon (Figure 18).

3.8 Effect of Double Reflections

It was discovered that rays that had reflected twice – first off the wing and then off a flap – influenced noise levels over a certain area of the ground plane. The locations where this was true are shown in Figure 20 for the single-element wing and flaps model. A narrow strip of the ground plane (never more than 40-feet wide) just aft of the aircraft was affected. Extraction of the noise contributions of the rays that reflected twice from the total noise levels at each affected point gave the deltas shown in Figure 21. Double reflections were predicted to increase noise levels 1.2 dB at most of the locations marked in Figure 20. For an aircraft forward velocity of 300 ft/sec, the region influenced by double reflections would propagate over a stationary ground point in 0.13 second.

3.9 Conclusions

Several conclusions were reached, based on the results of the Raynoise® analyses.

1) Many of the issues examined produced only localized effects, which would have minimal impact when integrated over a 2-second time interval:

   - Fully-extended flap surfaces
   - Engine position relative to the wing (i.e., inboard versus outboard mount locations)
   - Multiple reflections of a single ray

8

2) Use of a point source, as opposed to a distributed source, provided greater simplicity for the model, and produced the same general behavior for wing reflection effects, although it possibly caused predictions to be somewhat conservative.

3) Modeling of the pylon was somewhat misleading, because the pylon surfaces were treated as completely absorptive. In reality, the reflections off the pylon surfaces would eliminate much of the "trough of silence", and a realistic distributed source would also reduce the trough effect. Thus, eliminating the pylon from the point-source model would very likely produce more accurate results than attempting to model it in a simplified manner.

4) For this aircraft configuration, use of the double-element wing showed major changes in the predicted noise behavior. However, modeling requirements may differ from case to case, and would be expected to be a function of the given wing geometry. Therefore, the accuracy of the noise predictions will be dependent on the establishment of best practices regarding modeling of the wing. Similarly, the impact of extended flaps may vary from case to case, and also should be examined in more detail, to establish best practices.

5) In general, it may be observed that there is no significant benefit to analyzing a complex geometric model with a simple point source. Instead, application of a simple planar wing/flap model produces reasonable results with a point source.

The insight into wing reflection modeling gained through the Raynoise® studies was applied to the development of the reflection model for the ANOPP noise prediction program.
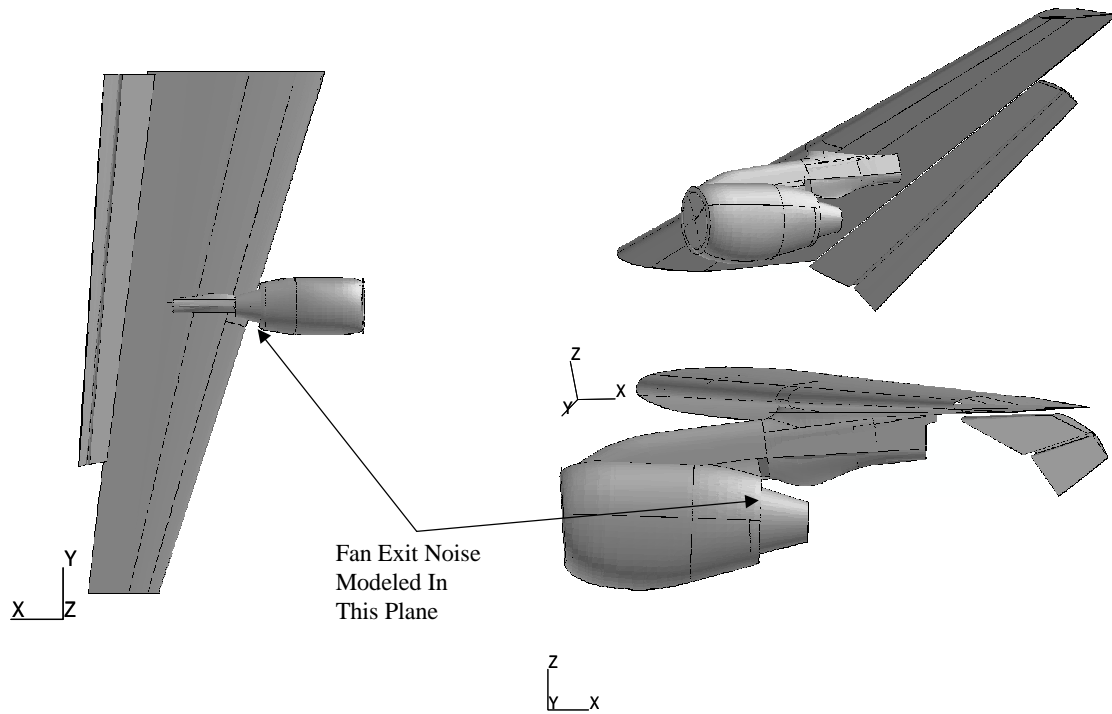
Figure 2. Outboard LF507 Engine on RJ100 Aircraft.
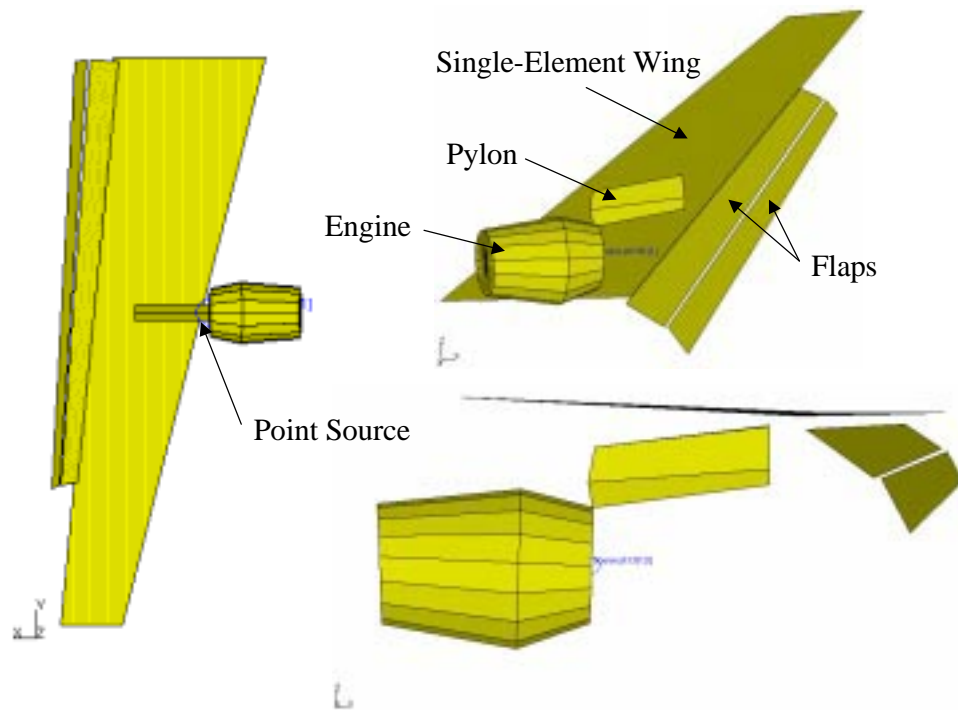
Figure 3. Raynoise® Model of the RJ100 Outboard Engine With Single-Element Wing.
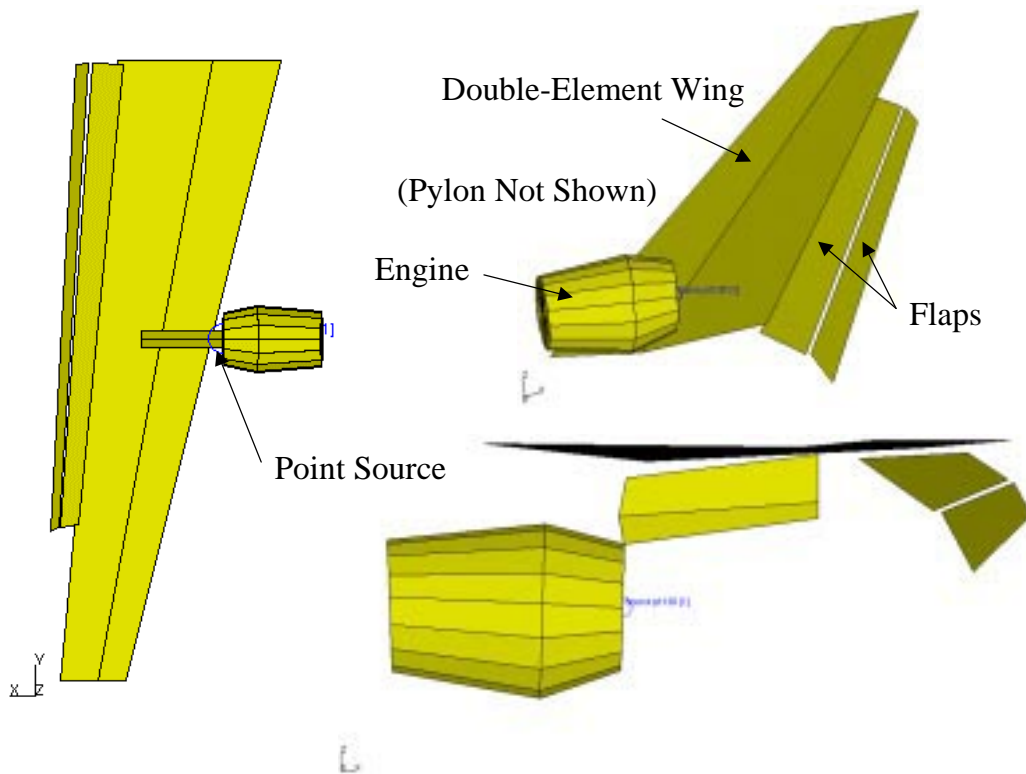
Figure 4. Raynoise® Model of the RJ100 Outboard Engine With Double-Element Wing.
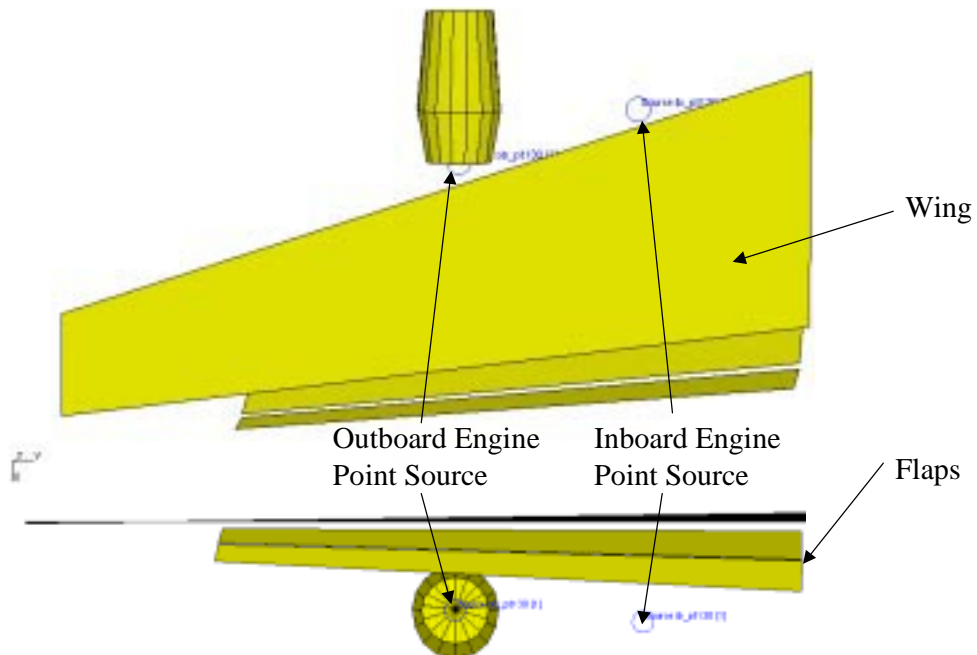
Figure 5. Raynoise® Model of the RJ100 Inboard and Outboard Engines, With Single-Element Wing.
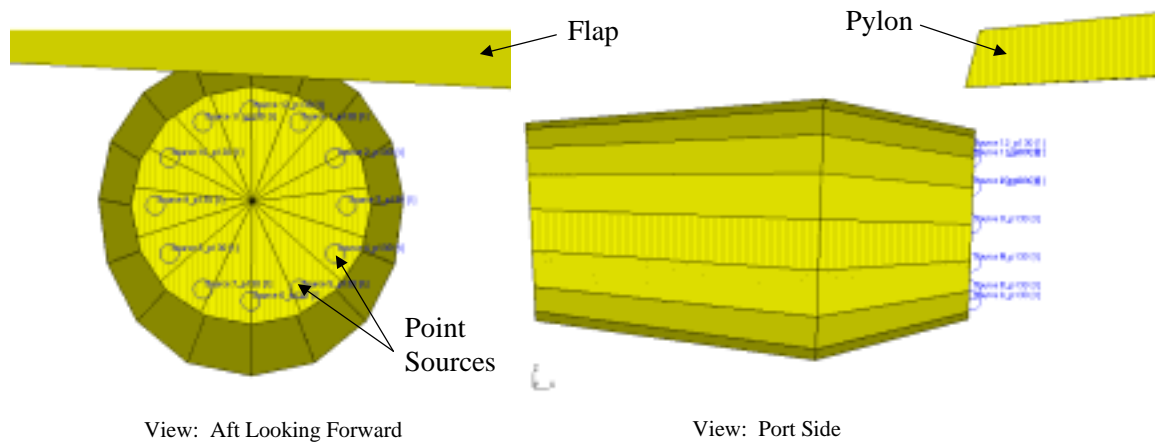
Figure 6. Raynoise® Model of the RJ100 Outboard Engine Using a Distributed Source, With Single-Element Wing.
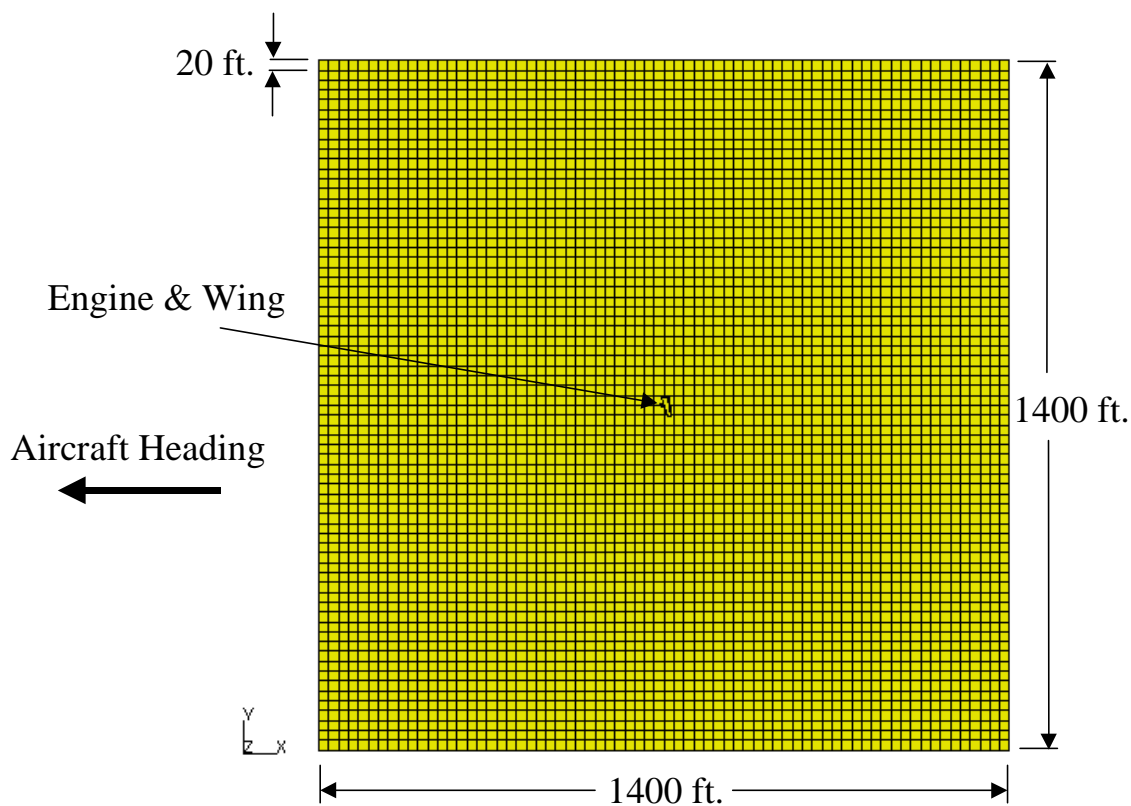
Figure 7. Ground Plane for All Predictions, Aircraft at Altitude of 394 Ft.
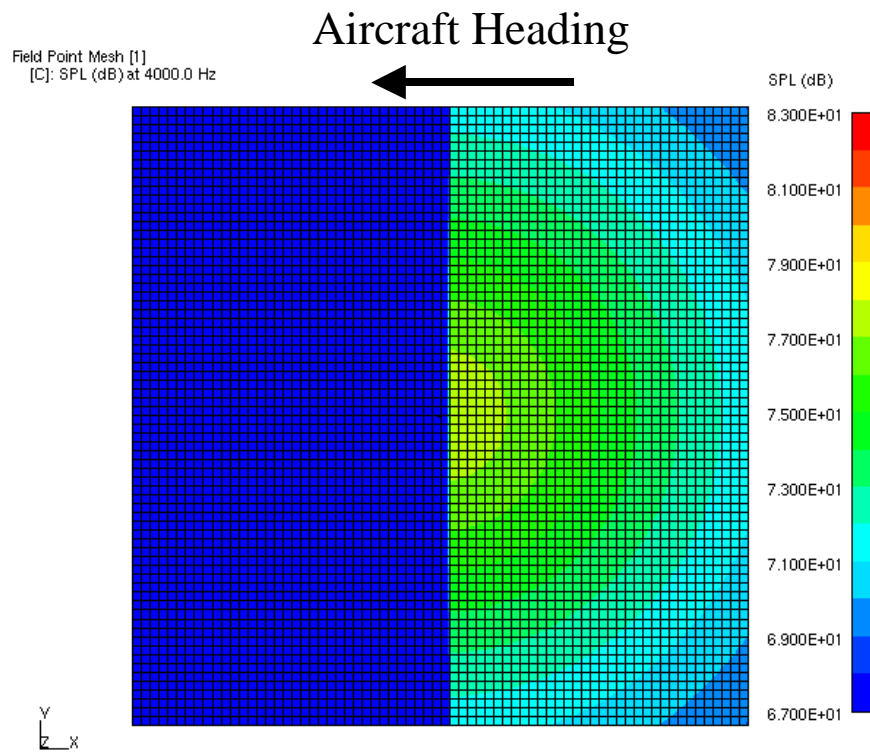
Figure 8. Noise Contours for Engine-Only Configuration, With Point Source.
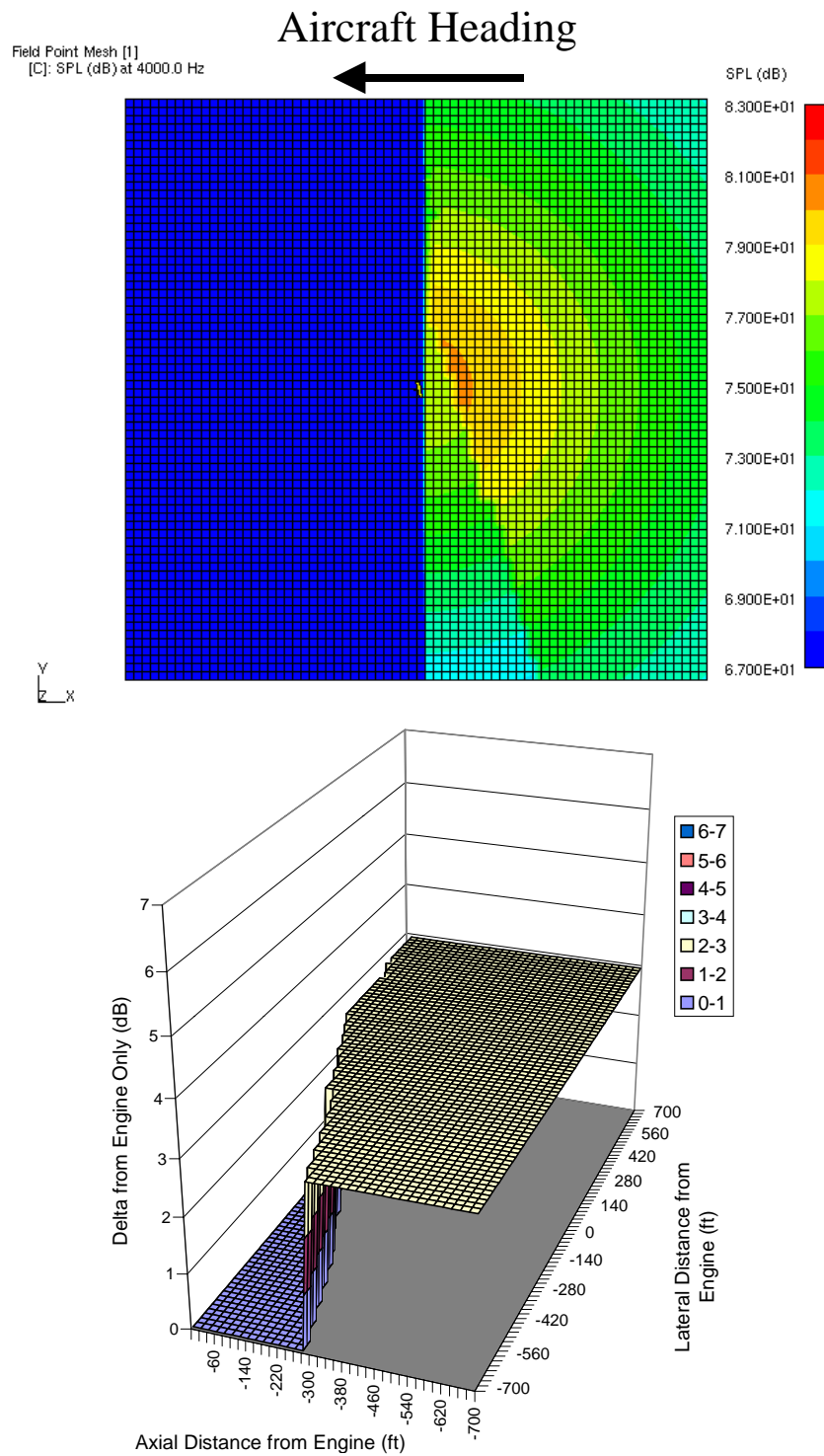
Figure 9. Engine With Single-Element Wing: Noise Contours, Noise Deltas From Engine-Only Configuration.

Aircraft Heading

Field Point Mesh [1]
[C]: SPL (dB) at 4000.0 Hz

SPL (dB)

8.300E+01
8.100E+01
7.900E+01
7.700E+01
7.500E+01
7.300E+01
7.100E+01
6.900E+01
6.700E+01
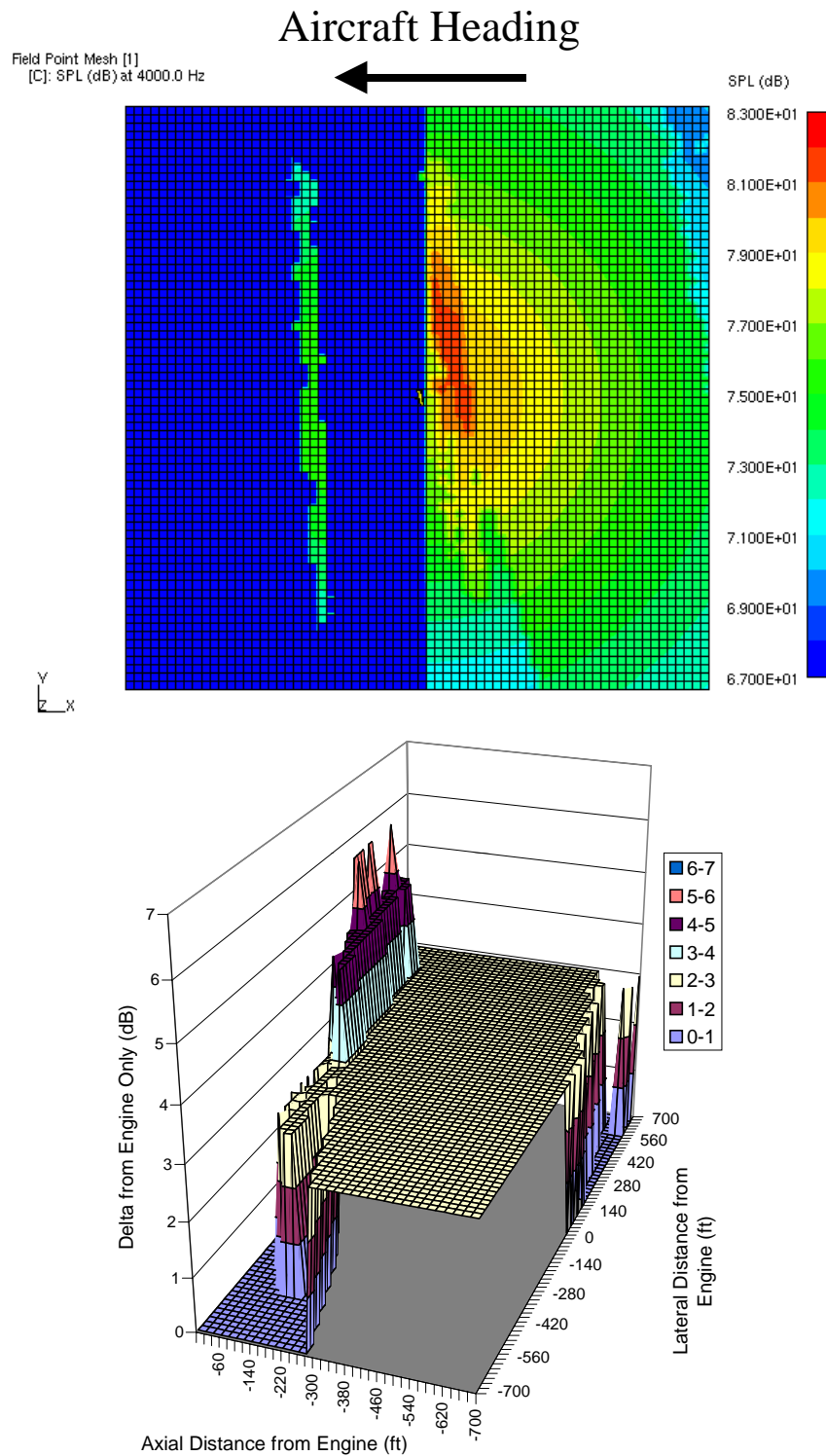
Figure 10. Engine With Single-Element Wing and Flaps: Noise Contours, Noise Deltas From Engine-Only Configuration.

15

Aircraft Heading

Field Point Mesh [1]
[C]: SPL (dB) at 4000.0 Hz

SPL (dB)

6.300E+01
8.100E+01
7.900E+01
7.700E+01
7.500E+01
7.300E+01
7.100E+01
6.900E+01
6.700E+01

Quiet trough
- no reflections
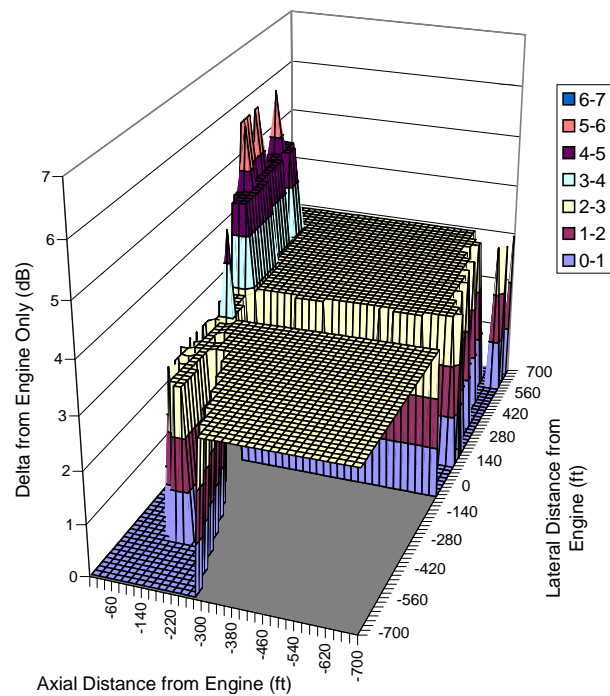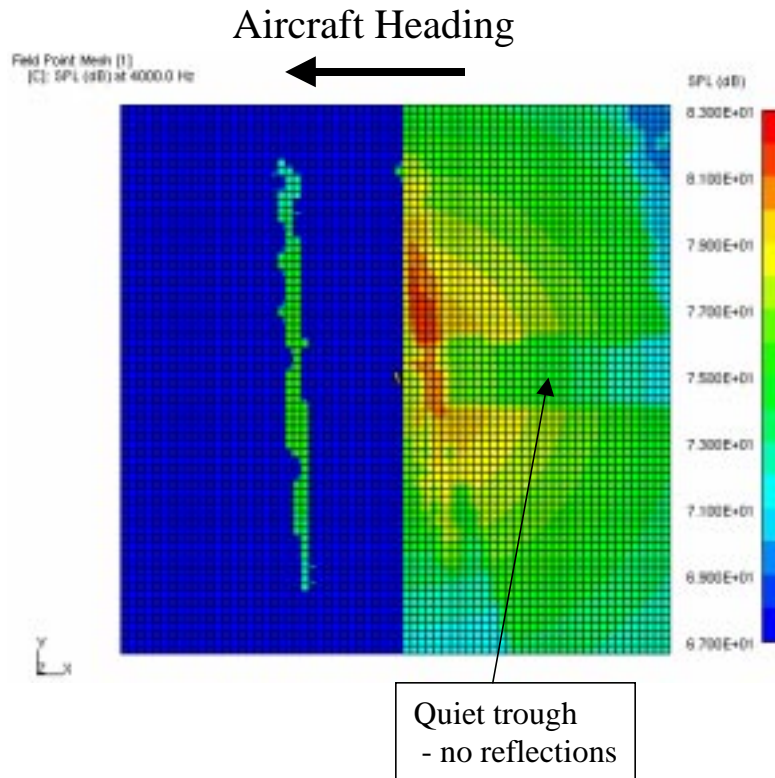
Figure 11. Engine With Single-Element Wing, Flaps, and Absorptive Pylon: Noise Contours, Noise Deltas from Engine-Only Configuration.
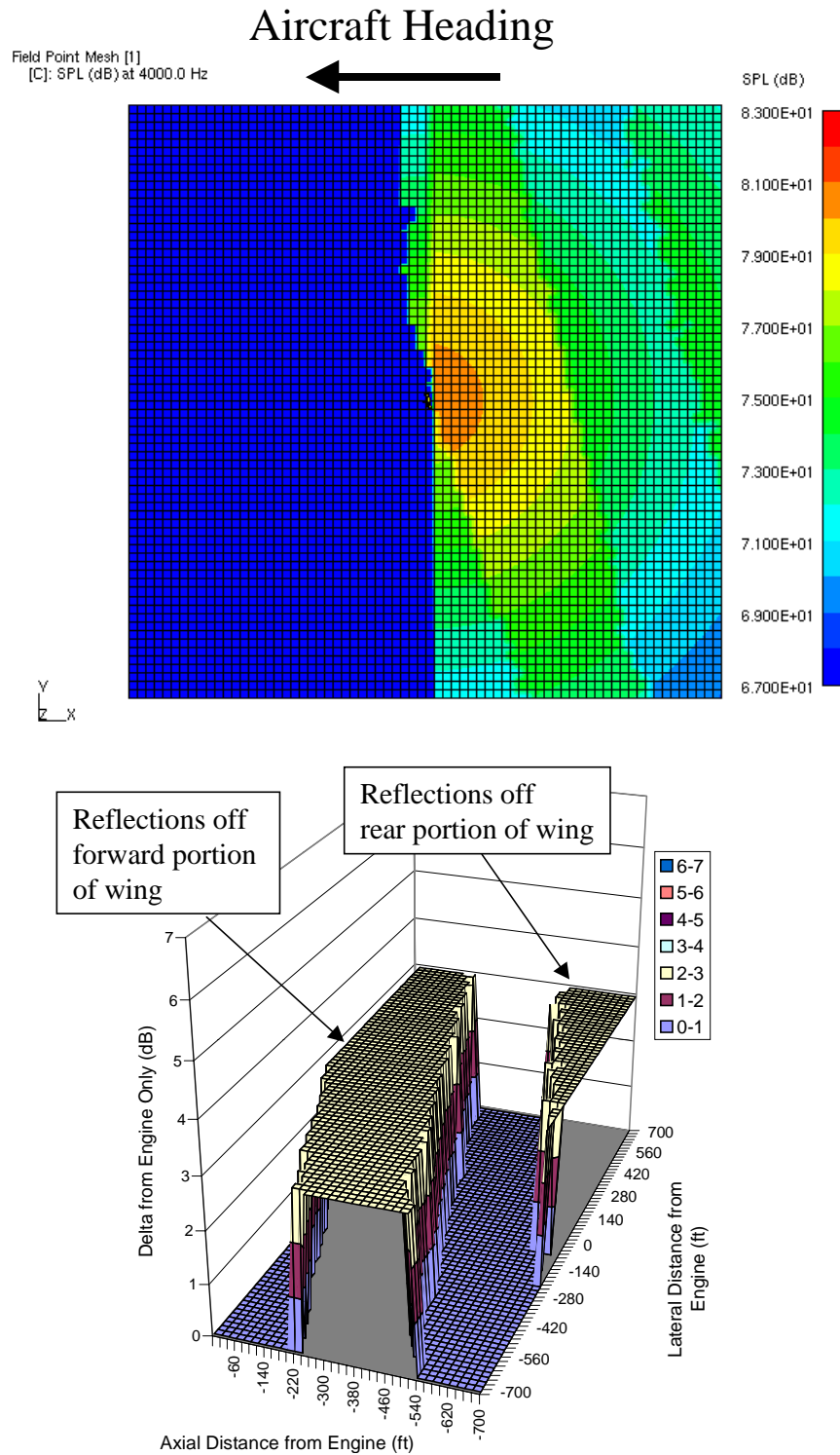
Figure 12. Engine With Double-Element Wing: Noise Contours, Noise Deltas From Engine-Only Configuration.

Aircraft Heading

Red Point Mesh [1]
[C] SPL (dB) at 4000.0 Hz

SPL (dB)

Double Reflection
Off Wing & Flap

Quiet trough
- no reflections

Double Reflection
Off Wing & Flap

Delta from Engine Only (dB)

6-7
5-6
4-5
3-4
2-3
1-2
0-1

Lateral Distance from Engine (ft)

Axial Distance from Engine (ft)
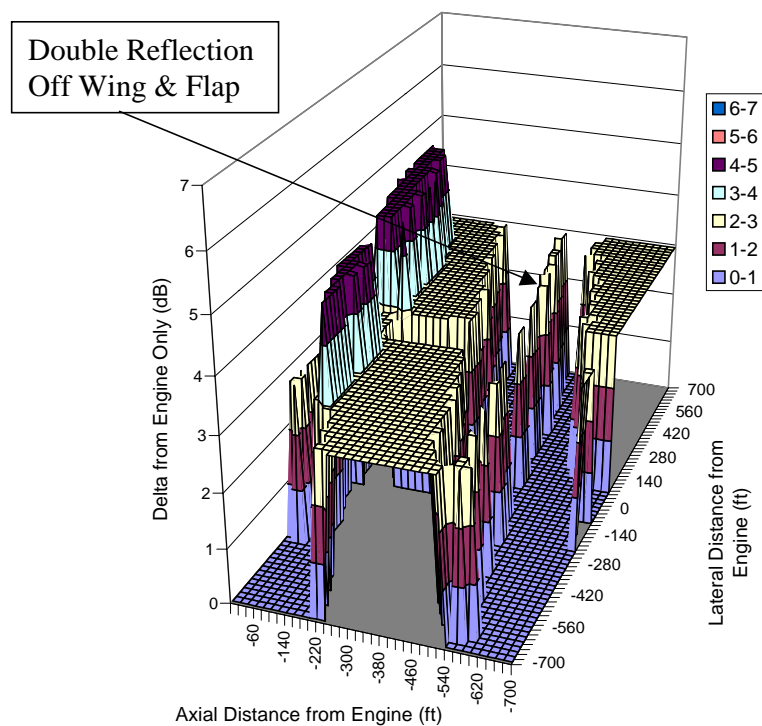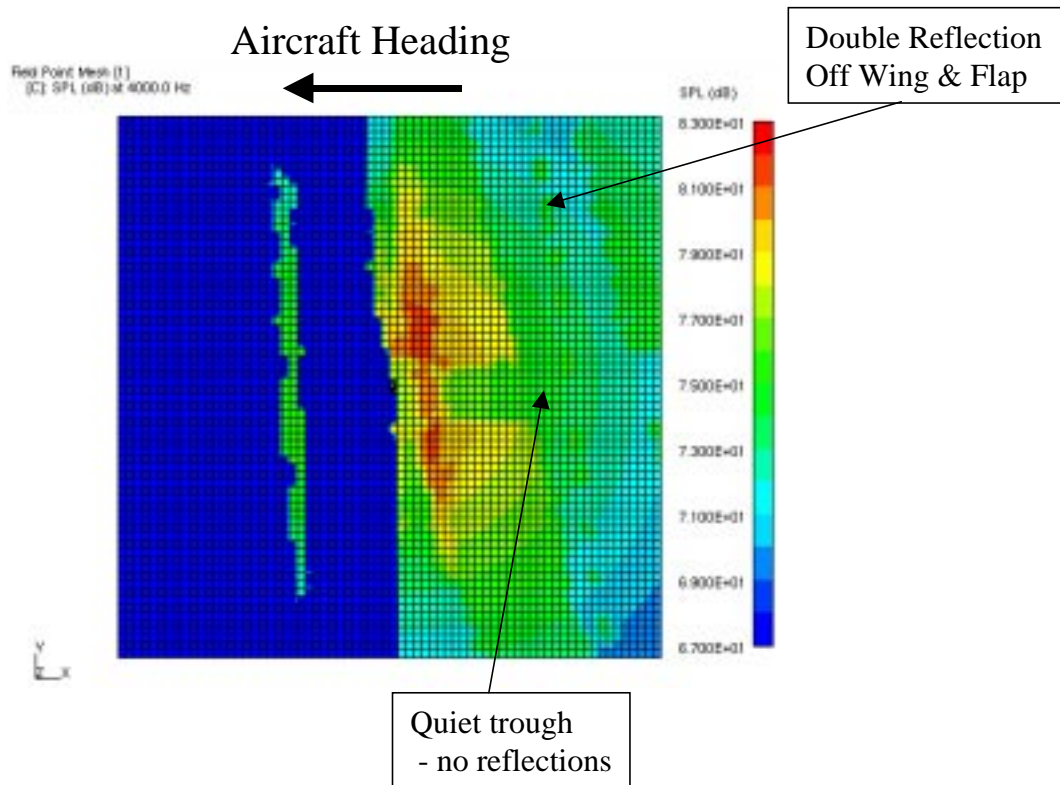
Figure 13. Engine With Double-Element Wing, Flaps, and Absorptive Pylon: Noise Contours, Noise Deltas From Engine-Only Configuration.

18
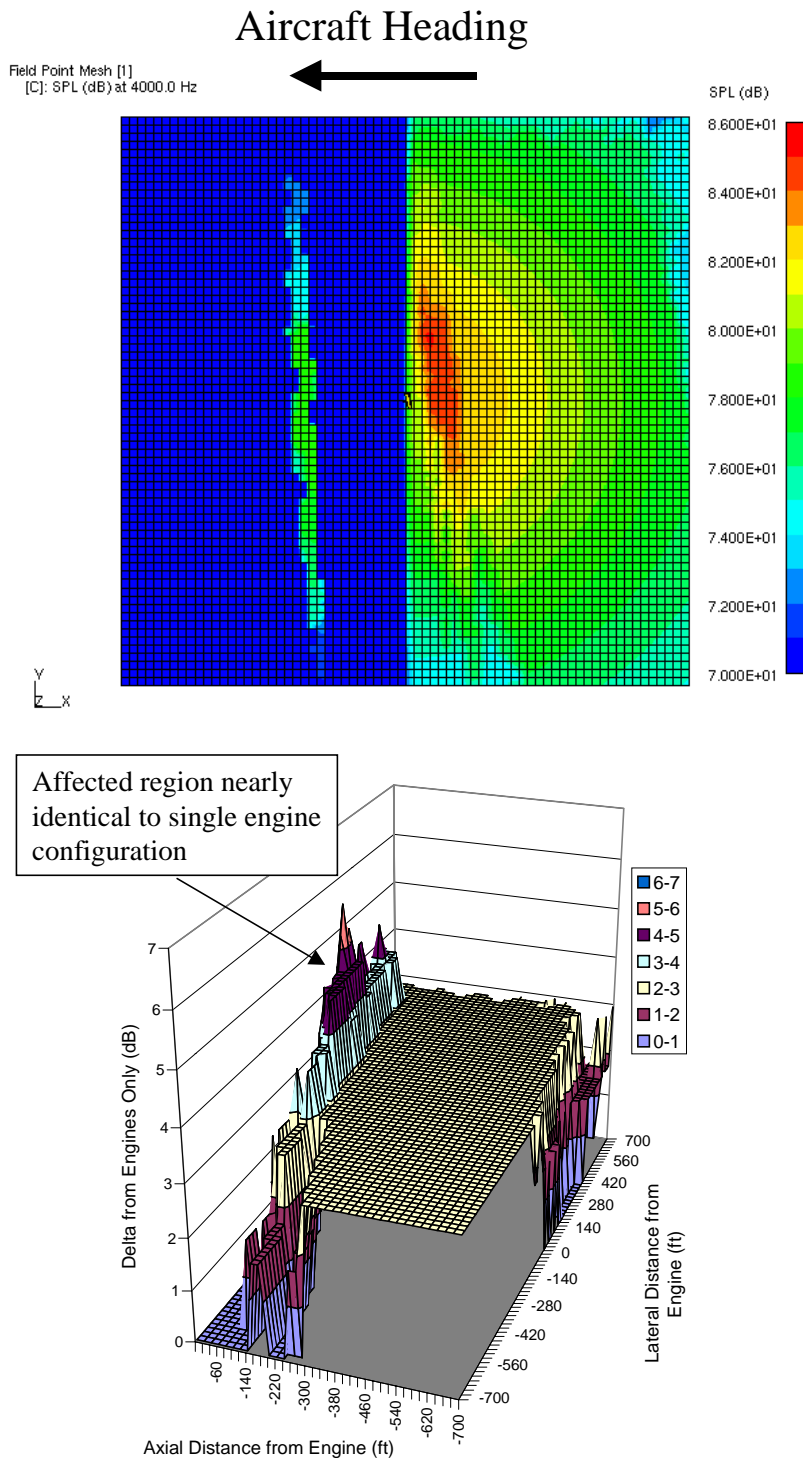
Figure 14. Inboard and Outboard Engines With Single-Element Wing, Flaps: Noise Contours, Noise Deltas From Engine-Only Configuration.
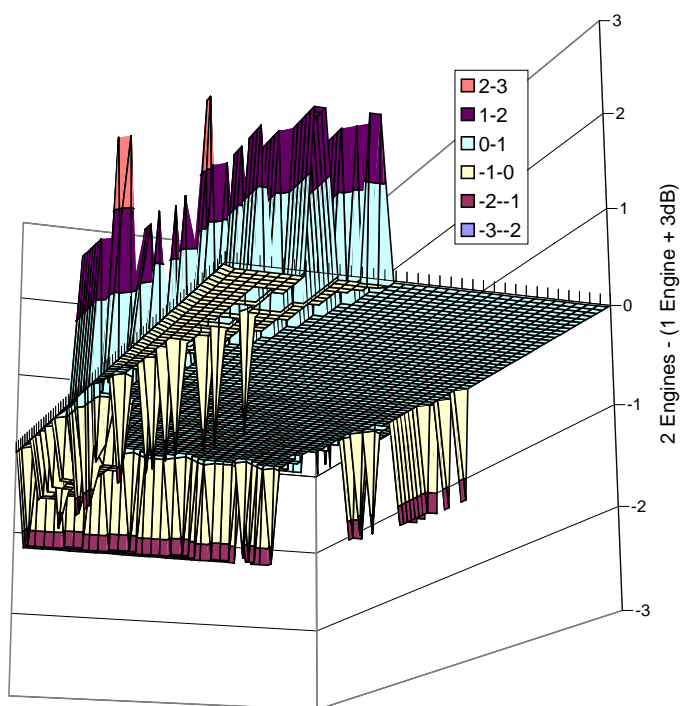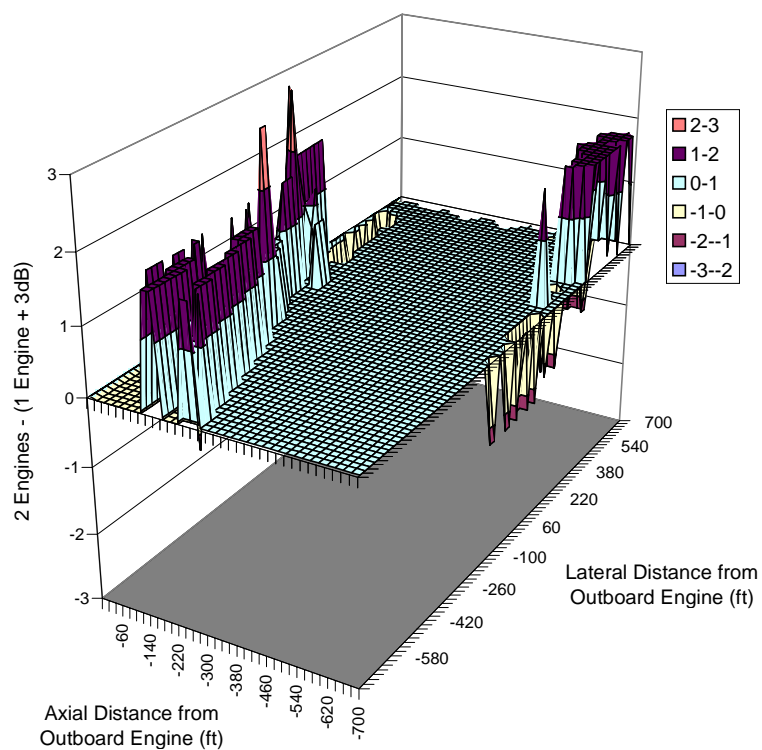
Figure 15. Differences Between Inboard + Outboard Engines and Outboard + 3 dB, Single-Element Wing, Flaps.

Aircraft Heading
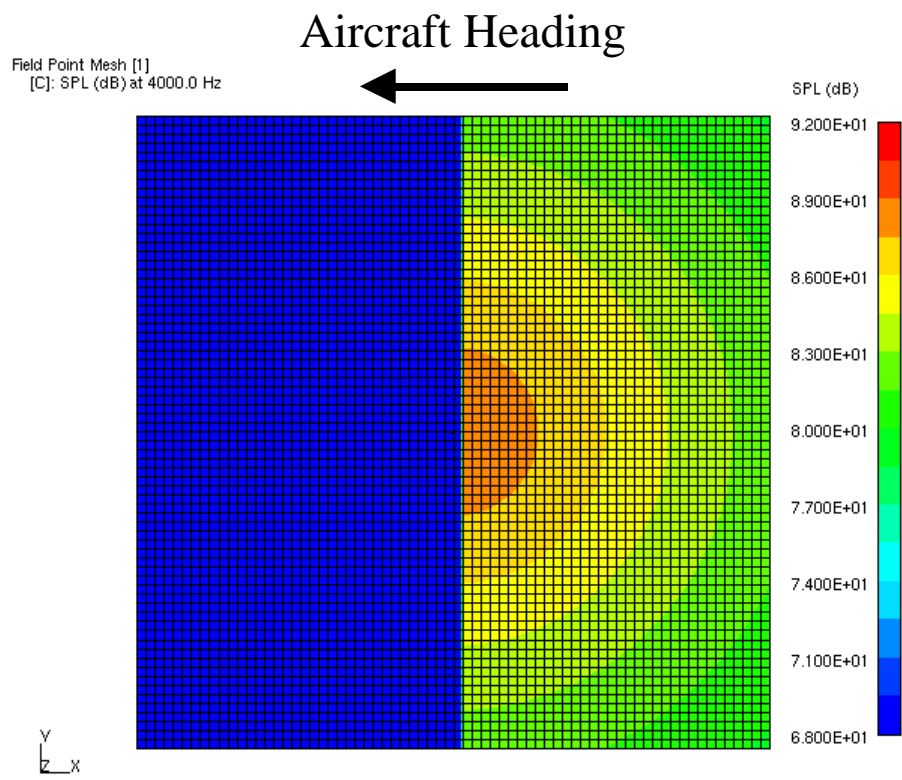
Figure 16. Noise Contours for Engine Only, 12-Point Ring Source.

Aircraft Heading

Field Point Mesh [1]
[C]: SPL (dB) at 4000.0 Hz

SPL (dB)

9.200E+01
8.900E+01
8.600E+01
8.300E+01
8.000E+01
7.700E+01
7.400E+01
7.100E+01
6.800E+01

Slight "blurring" of edges of region affected by reflections

6-7
5-6
4-5
3-4
2-3
1-2
0-1

Delta from Engines Only (dB)

Lateral Distance from Engine (ft)

Axial Distance from Engine (ft)
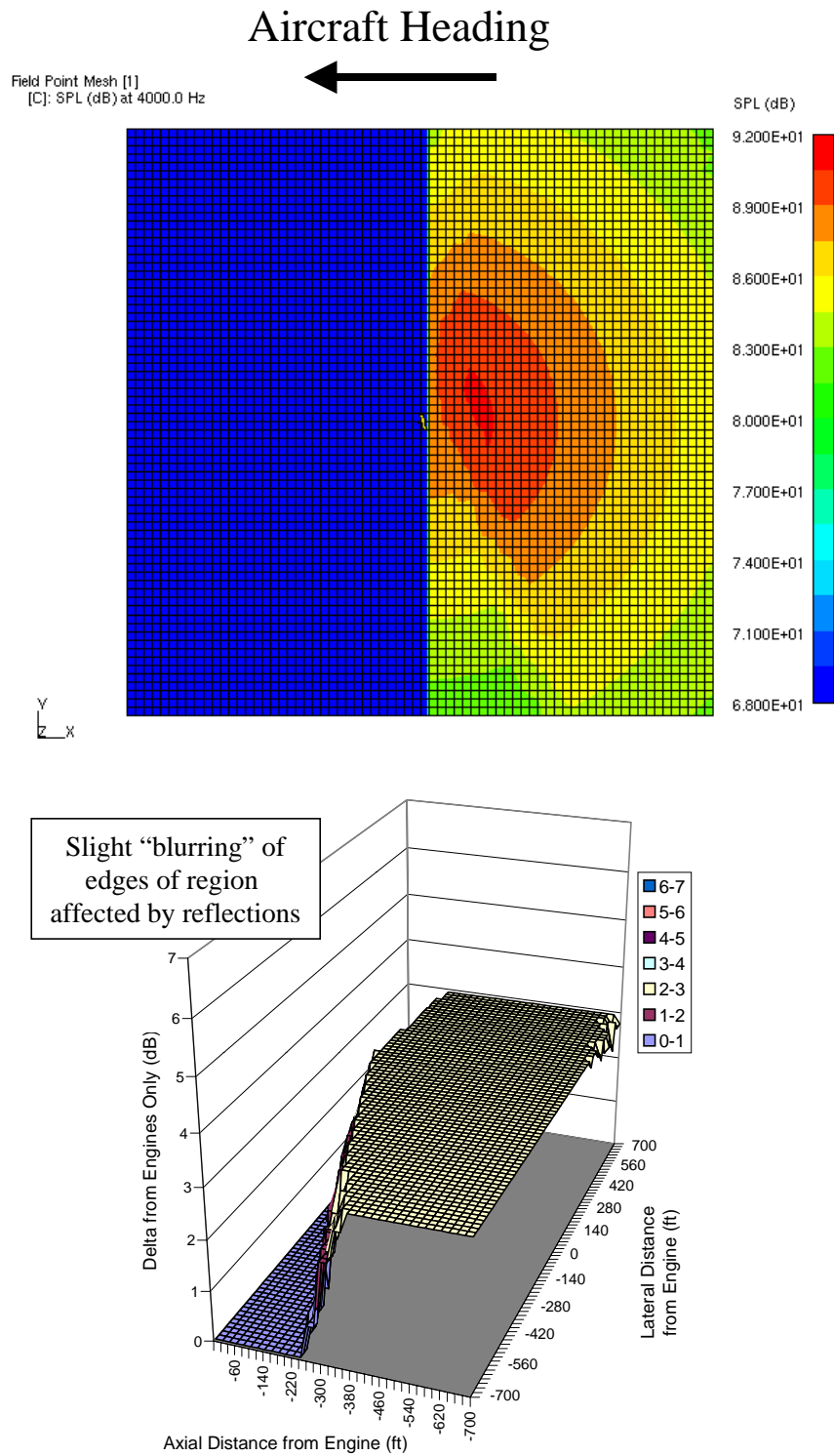
Figure 17. Outboard Engine, 12-Point Source, Single-Element Wing: Noise Contours, Noise Deltas from Engine-Only Configuration.

Aircraft Heading

Field Point Mesh [1]
[C]: SPL (dB) at 4000.0 Hz

SPL (dB)

9.200E+01

8.900E+01

8.600E+01

8.300E+01

8.000E+01

7.700E+01

7.400E+01

7.100E+01

6.800E+01
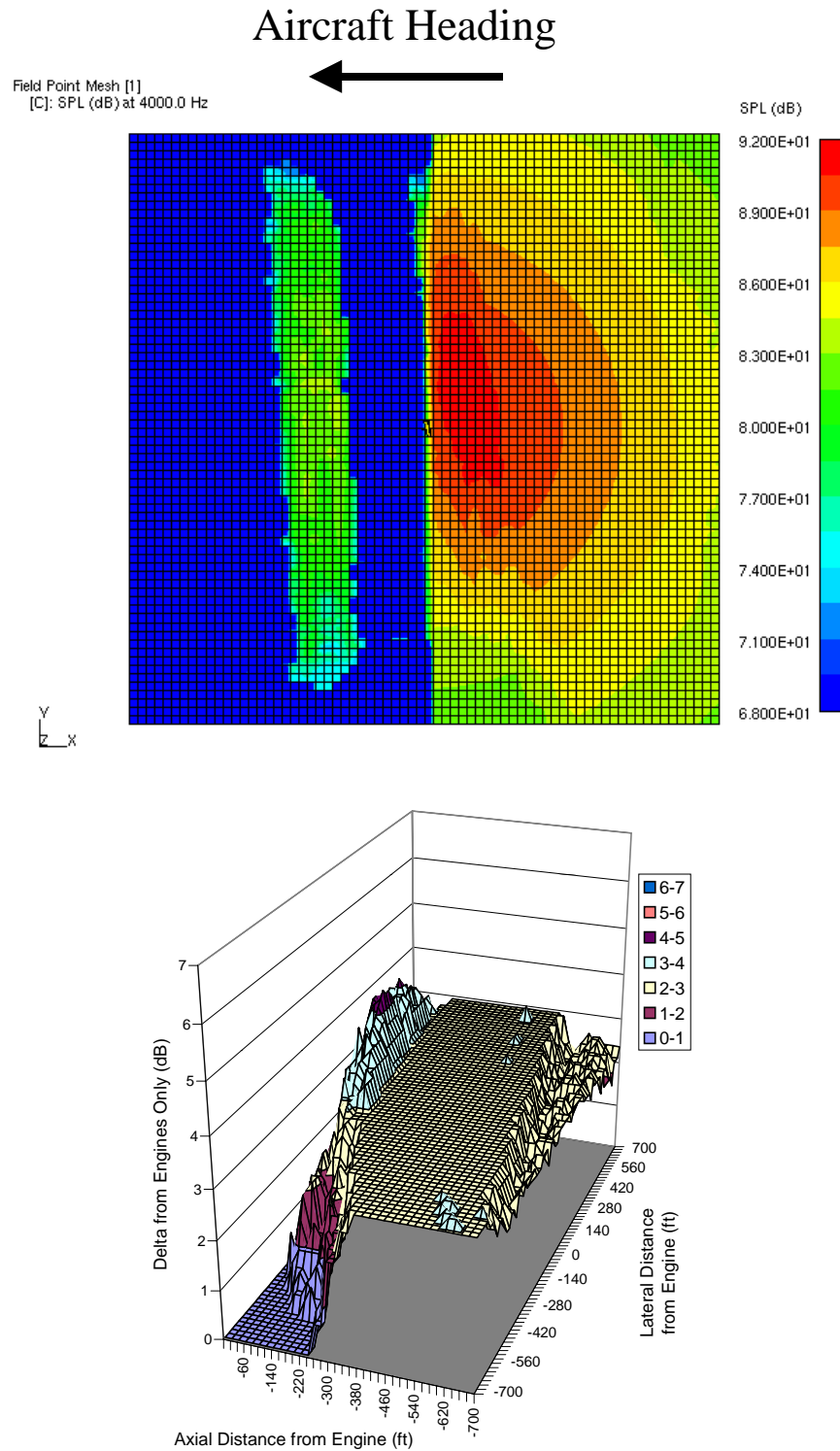
Figure 18. Outboard Engine, 12-Point Source, Single-Element Wing and Flaps: Noise Contours, Noise Deltas From Engine-Only Configuration.

23

Quiet trough seen with point source disappears using ring source since diameter of bypass exit larger than thickness of engine pylon

Reflections from Half of Point Sources Shielded by Pylon
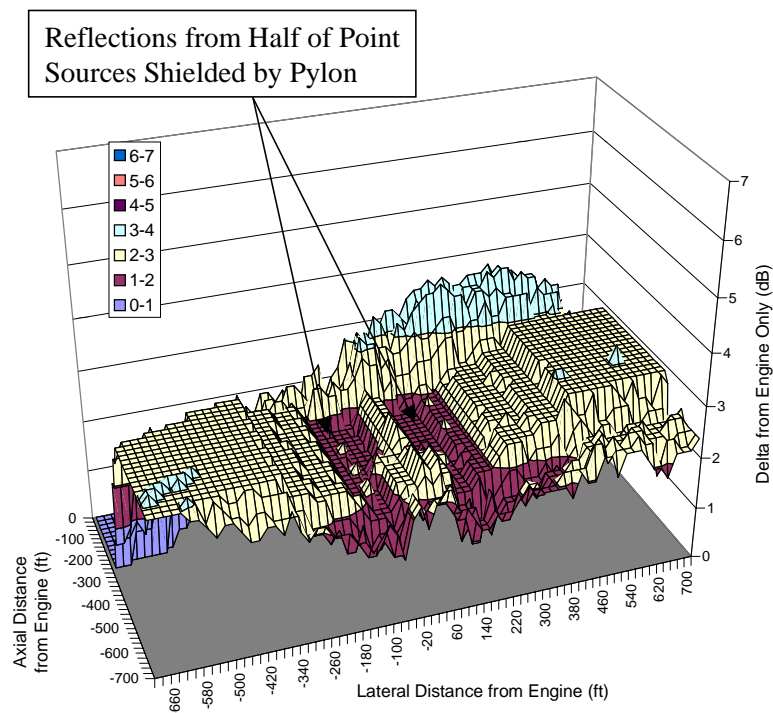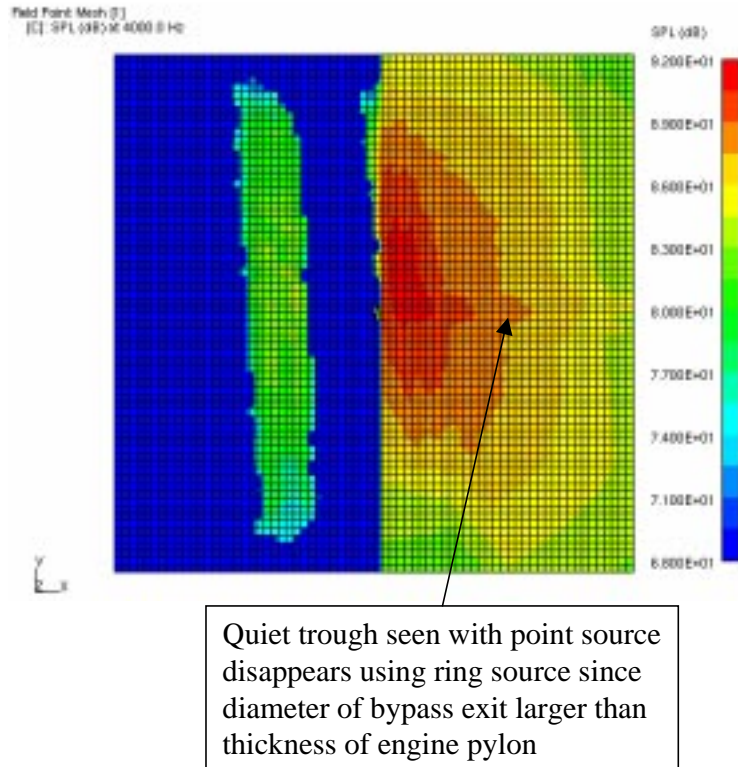
Figure 19. Outboard Engine, 12-Point Source, Single-Element Wing, Flaps, Absorptive Pylon: Noise Contours, Noise Deltas From Engine-Only Configuration.
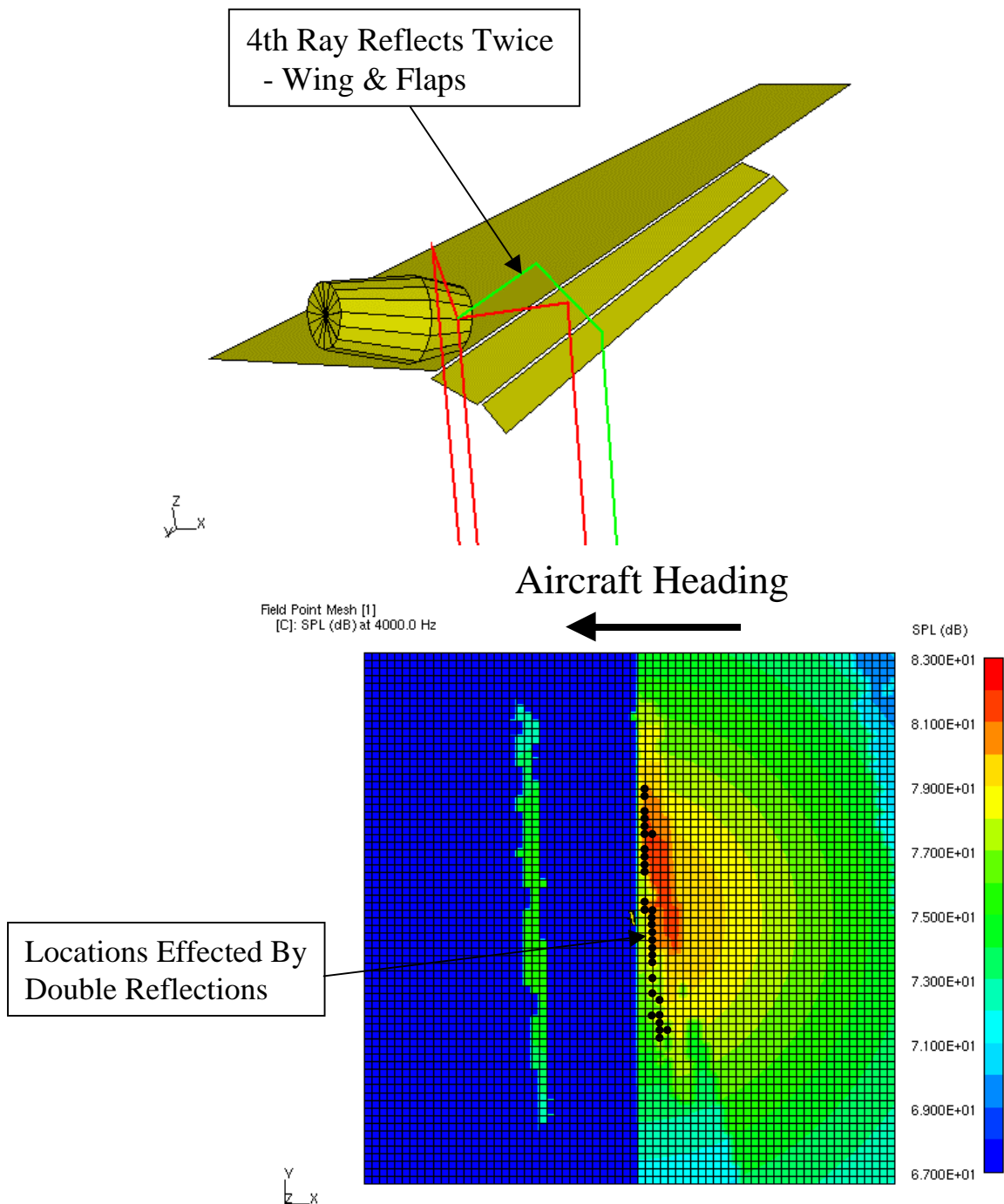
Figure 20. Double Reflections and the Locations Influenced by Them, Single Element Wing and Flaps, Point Source.
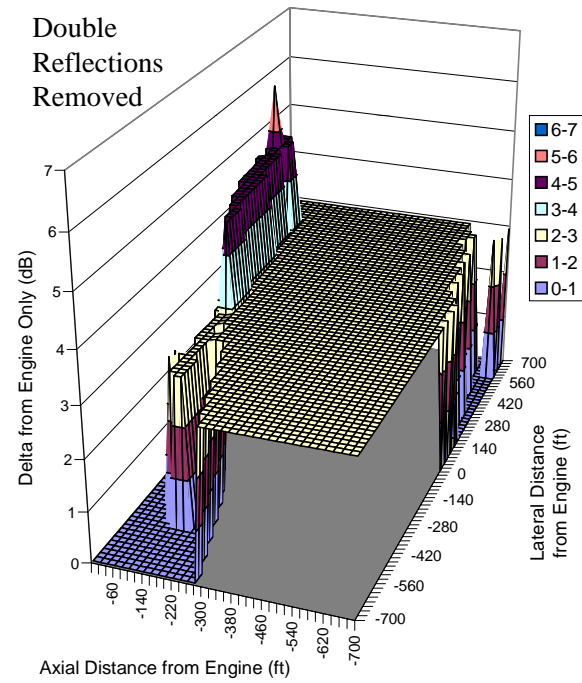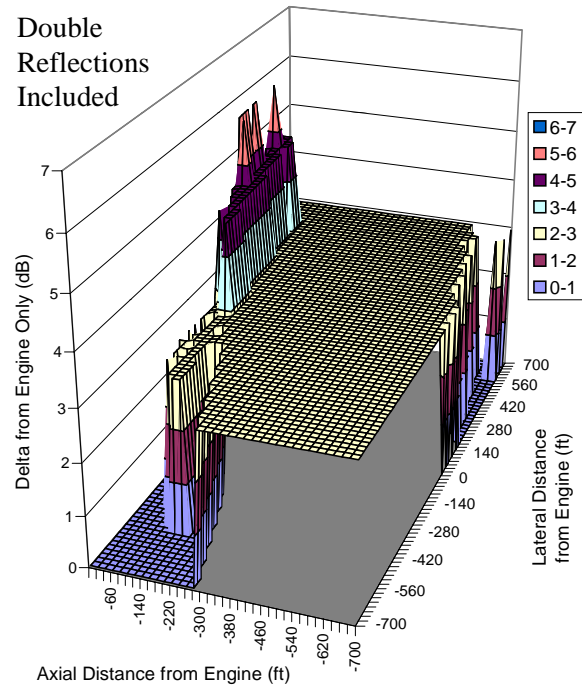
Figure 21. Comparison of Wing-Flap Reflections With and Without Double Reflections, Single-Element Wing and Flaps, Point Source.

4. DESCRIPTION OF WING REFLECTION MODEL FOR ANOPP

4.1 Aspects of Noise Modeling for Engine Under-the-Wing Configurations

As shown in Figure 22, wing reflection was but one of many issues which needed to be addressed, in developing the prediction module for an engine under-the-wing configuration, including the noise source, the directly-radiated wave, the reflected wave, entrainment-induced noise, and various effects on noise propagation. Each of these will be discussed in more detail in the following sections.

4.1.1 Noise Source

The noise source was limited to fan bypass duct noise, which is the main contributor to wing reflection noise. A point source was assumed, with a spherical sound wave radiating in an aft-facing hemisphere, as shown in Figure 23. This was consistent with Heidmann's[6] observation that the fan discharge duct broadband noise at 90 degrees was reduced approximately 5 dB from its maximum level, and the contribution at angles less than 90 degrees (forward of the duct exit) was negligible.

The sound field was assumed to be axisymmetric, in the azimuthal direction; however, polar directivity was accounted for in the model.

4.1.2 Directly-Radiated Wave

In the wing reflection model, the directly-radiated wave was treated in a manner consistent with the current ANOPP program. All of the significant effects were accounted for, including directivity, atmospheric attenuation, spherical spreading between the source location and the ground observer location, ground reflection, and extra-ground attenuation (for sideline predictions).

4.1.3 Reflected Wave

Among the modeling considerations which had to be taken into account for the reflected wave were the nature of the reflecting surfaces, the directivity of the source, and the issue of single versus multiple reflections of a single ray.

The aircraft configuration itself had to be modeled, as part of the definition of reflecting surfaces. For the ANOPP model, it was assumed that reflection could occur only from the wing/flap system. There would be no contribution from the fuselage, empennage, or engine pylon surfaces. Influence of the pylon was examined during the Raynoise® studies, and it was concluded that the pylon could be neglected in the final wing reflection model.

A maximum of three wing/flap panels were included in the model. The flap system was assumed to consist of continuous spanwise flap panels on each wing, with no jet efflux cut-outs. Tabbed Fowler flaps could be modeled, including gaps along the hinge centerlines.

The effect of leading edge slats on the wing was neglected. The slats would have a secondary effect as reflecting surfaces, relative to the wing/flap system. In addition, the assumption of an aft-facing hemispherical source model would limit the range of directivity angles at which a slat reflection would occur. The size of the slats would also limit the time interval during which flyover noise reflected from the slat would reach the receiver.

27

The characteristics of the reflecting surfaces also had to be considered, when developing the wing reflection model. The wing and flap panels were modeled as planar reflecting surfaces. Each reflecting panel was assumed to be an infinitely hard acoustic surface (i.e., perfectly reflecting).

Directivity of the source noise had to be included in the wing reflection model, because the polar angle at which the reflected ray leaves the engine may vary significantly from that of the direct ray, as shown in Figure 24. The difference in angle would depend on the position of the reflecting surface relative to the source, and the position of the source relative to the receiver. This difference in angle would result in different source strengths for the direct and reflected rays.

The issue of single versus multiple reflections was considered during the Raynoise® studies. It was determined that the impact of multiple reflections of a single ray was negligible, for the case under study. As a result, the ANOPP wing reflection model assumed that a single ray would reflect from at most one surface (wing, flap, or flap tab), and reflections of a single ray off of multiple surfaces would be neglected. In addition to the Raynoise studies, a similar case (RJ100 wing with LF507 engine) was modeled for a two-dimensional wing/flap system with fully-deployed flaps, as shown in Figure 25. A geometrical study of the reflected rays showed that instances of multiple reflections would occur for a range of approximately 2 degrees, in terms of aircraft-observer angle. This is small compared to the changes in angle during each ½ second interval of flyover noise predictions. Therefore, neglecting the multiple reflections should have no significant impact on the noise predictions.

4.1.4 Entrainment-Induced Noise

Entrainment-induced noise represents an additional noise source for engine under-the-wing configurations. This phenomenon occurs when flow is entrained between the nacelle and the wing, due to jet exhaust velocity. The entrainment-induced boundary layer on the wing surface is responsible for the noise. Entrainment effects are a function of the jet exhaust velocity, the axial wing position relative to the engine exhaust, and the normal distance between the wing and engine centerline.

According to Wang[5], entrainment-induced noise predominates at low frequencies. In scaled-nozzle tests, Wang found that the frequencies were below 500 Hz. When the data are scaled up for typical aircraft configurations, the frequencies at which entrainment has an impact are lowered (below approximately 170 Hz, for the RJ100 with LF507 engines). Therefore, the impact is at low enough frequencies to be of no consequence at full scale.

In addition, this noise source is distinct from the direct and reflected-wave noise, and therefore is beyond the scope of the current modeling effort.

4.1.5 Effects on Propagation

Propagation of the reflected wave is influenced by the same effects as the directly radiated wave, i.e., spherical spreading, atmospheric attenuation, and ground reflection. In the ANOPP model, these effects were treated for the reflected wave in the same manner as they were for the direct wave.

In addition, other effects had to be considered, which are more specific to the reflected wave. These included noise transmission through the jet, one aspect of which is refraction of the reflected wave through the jet, and interference between the directly radiated and reflected waves.

Some of the noise reflected from the wing is transmitted through the jet as it propagates to the receiver. During transmission through the jet, various frequency components of reflected noise are either absorbed, reflected, or refracted by the jet. As noted by Wang, high-frequency components of noise (wavelengths small compared to the dimension of the jet) are most susceptible. Therefore, high-frequency sound waves would experience more attenuation when transmitted through the jet than when their paths do not pass through the jet. However, these effects are outside the scope of the current wing reflection model, and will not be addressed.

One aspect of noise transmission through the jet, that of refraction, can be assessed in an approximate fashion to determine whether the impact would be significant. A reflected wave passing through the jet undergoes refraction, which alters the directivity and distance that the reflected wave travels (Figure 26). The jet exhaust velocity changes the direction of the ray, and the jet temperature alters the local speed of sound. For a typical flyover case, this change in distance compared to the overall distance traversed by the reflected wave was negligible. In addition, the shift in ray position was negligible compared to the distance traveled by the source in a ½ second interval of the flyover. Therefore, it may be assumed that refraction effects are negligible, in terms of distance and directivity, in the wing reflection model.

Interference can occur due to different path lengths between the directly radiated and reflected noise. However, the coherence coefficient for a typical case with the RJ100/LF507 configuration was estimated to be 0.0257, which implies that the uncorrelated energy is within approximately 0.11 dB of the initial acoustic energy. Therefore, it may be assumed that interference effects are essentially negligible. In addition, no evidence of attenuation due to interference was seen in the jet noise test data of Wang. Thus, the effect was not modeled in ANOPP.

4.2 Implementation in Wing Reflection Algorithm

4.2.1 Procedure for Calculation of Wing Reflection

Based on the modeling assumptions discussed above, the wing reflection algorithm for the ANOPP noise prediction program was developed. The primary steps in the procedure are presented in the flowchart of Figure 27, and include the following:

- Define the geometry for each reflecting panel (wing, flap, flap tab)
- Create the image source for each reflecting panel, at each flyover location
- Determine if a reflection will occur for a given panel
- Compute the path length of the reflected ray, for a given panel
- Obtain the source strength for the reflected ray, based on directivity
- Compute the strength at the receiver, by applying appropriate corrections
- Combine the contributions from the reflected ray(s) and the direct ray

Each of these steps is discussed in more detail in the following sections.

4.2.2 Geometry Definition for Reflecting Panels

The reflecting panels that represent the wing/flap system are modeled as planar surfaces. The geometry definition for each panel consists of the specification of the Cartesian coordinates (X, Y, Z) of each corner point of the panel; i.e., coordinates are defined for the Root Leading Edge (RLE), Root Trailing Edge (RTE), Tip Leading Edge (TLE), and Tip Trailing Edge (TTE), as shown in Figure 28. The coordinates of the Tip Trailing Edge are used only to define the wing boundary. The plane of the wing is defined by the three points: RLE, RTE, and TLE. Any twist in the wing is ignored.

The Cartesian coordinates of the wing boundary points are defined relative to the local origin of the engine centerline at the fan bypass duct exit plane. Local axes are shown in Figure 28. Then, the engine fan duct exit and wing coordinates are transformed into a global coordinate system consistent with the receiver location on the ground (Point R). This transformation must take into account the aircraft attitude and position at the particular time of the observation. Therefore, the global coordinates must be calculated at every flyover position.

Three wing/flap panels are currently permitted in the model. This allows the description of a main wing panel, a flap panel, and a flap tab panel. However, if flaps are not included in the model, or are considered to have negligible impact on reflection compared to the wing itself, the wing may be modeled using multiple panels, instead.

4.2.3 Creation of Image Source

The reflection model uses an image source point, which is positioned on a normal to the reflecting plane, at a distance equivalent to that between the source and the reflecting plane, but located on the opposite side of the reflecting plane. The orientation of the image source is shown in Figure 29.

To obtain the image source point, a normal to the reflecting plane is created, which intersects the original source point (S). Then Point IS, the image source, is located on the normal line. Points S and IS are equidistant from the reflecting panel. Note that the normal line between Points S and IS does not have to intersect the wing panel itself, only the plane extending through the wing panel.

First, obtain the components of a vector normal to the reflecting surface, by computing the cross-product of vectors along the wing root and leading edge:

$$\Delta x_n = \Delta y_{root} * \Delta z_{LE} - \Delta y_{LE} * \Delta z_{root}$$
$$\Delta y_n = -\left(\Delta x_{root} * \Delta z_{LE} - \Delta x_{LE} * \Delta z_{root}\right)$$
$$\Delta z_n = \Delta x_{root} * \Delta y_{LE} - \Delta x_{LE} * \Delta y_{root}$$

where:

$$\Delta x_{root} = x_{RTE} - x_{RLE}$$
$$\Delta y_{root} = y_{RTE} - y_{RLE}$$
$$\Delta z_{root} = z_{RTE} - z_{RLE}$$
$$\Delta x_{LE} = x_{TLE} - x_{RLE}$$

$$\Delta y_{LE} = y_{TLE} - y_{RLE}$$
$$\Delta z_{LE} = z_{TLE} - z_{RLE}$$

Next, the coordinates of a point, N, on a line normal to the reflecting surface and passing through the engine source point, S, are obtained as follows:

$$x_N = x_S + \Delta x_N$$
$$y_N = y_S + \Delta y_N$$
$$z_N = z_S + \Delta z_N$$

Then, the coordinates of the intersection of the line S-N with the plane of the reflecting surface are computed. The intersection point is identified as Point I. The coordinates of the intersection point are determined by solving a set of three equations in three unknowns (x_I, y_I, and z_I). Two of the equations are produced by the two-point form of the equation for the line S-N:

$$\frac{x_I - x_S}{x_N - x_S} - \frac{y_I - y_S}{y_N - y_S} = 0$$
$$\frac{x_I - x_S}{x_N - x_S} - \frac{z_I - z_S}{z_N - z_S} = 0$$

The other equation comes from the three-point form of the equation for the reflecting plane:

$$\begin{vmatrix} x_I - x_{RLE} & y_I - y_{RLE} & z_I - z_{RLE} \\ x_{RTE} - x_{RLE} & y_{RTE} - y_{RLE} & z_{RTE} - z_{RLE} \\ x_{TLE} - x_{RLE} & y_{TLE} - y_{RLE} & z_{TLE} - z_{RLE} \end{vmatrix} = 0$$

Once the coordinates of the intersection point have been determined, the components of the vector between the source point, S, and the intersection point, I, may be computed:

$$\Delta x_I = x_I - x_S$$
$$\Delta y_I = y_I - y_S$$
$$\Delta z_I = z_I - z_S$$

Finally, the image source point, IS, may be positioned on the normal to the reflecting surface, through the source point, S, by adding the above vector components to the coordinates of the Point I:

$$x_{IS} = x_I + \Delta x_I$$
$$y_{IS} = y_I + \Delta y_I$$
$$z_{IS} = z_I + \Delta z_I$$

4.2.4 Will Reflection Occur?

Once the image source is located, it is necessary to determine if a reflection will actually occur for the reflecting panel under consideration. A reflection will occur if the line passing between the receiver and the image source at a given flyover location intersects the plane of the reflecting panel within the boundaries of the actual panel, as shown in Figure 30. The orientation of image source and receiver changes at each interval during the flyover, and therefore, must be recomputed for each flyover position.

To determine if a reflection will occur, the coordinates of the reflection point (W) on the plane of the wing panel must first be obtained, by determining the intersection point of the line formed by IS-R and the plane of the wing panel. The coordinates of the intersection point, W, are determined by solving a set of three equations in three unknowns (x_W, y_W, and z_W). Two of the equations are produced by the two-point form of the equation for the line IS-R:

$$\frac{x_W - x_R}{x_{IS} - x_R} - \frac{y_W - y_R}{y_{IS} - y_R} = 0$$

$$\frac{x_W - x_R}{x_{IS} - x_R} - \frac{z_W - z_R}{z_{IS} - z_R} = 0$$

The other equation comes from the three-point form of the equation for the reflecting plane:

$$\begin{vmatrix} x_W - x_{RLE} & y_W - y_{RLE} & z_W - z_{RLE} \\ x_{RTE} - x_{RLE} & y_{RTE} - y_{RLE} & z_{RTE} - z_{RLE} \\ x_{TLE} - x_{RLE} & y_{TLE} - y_{RLE} & z_{TLE} - z_{RLE} \end{vmatrix} = 0$$

After the coordinates of the reflection point, W, have been determined, the point must be tested to establish whether or not it lies within the boundaries of the reflecting plane. To accomplish this, the point on each wing boundary that is nearest to Point W must be located. Each of these points (Points W_{LE}, W_{TE}, and W_{TIP}) is computed by solving a set of three equations in three unknowns (e.g., $x_{W_{LE}}$, $y_{W_{LE}}$, and $z_{W_{LE}}$ for the leading edge boundary). The equations are obtained by imposing the following conditions, e.g. for the leading edge boundary:

1) The line W-W_{LE} must be perpendicular to the wing boundary. This condition is represented by setting the dot product of the line W-W_{LE} vector and the wing boundary line vector equal to zero, e.g.:

$$\left(x_W - x_{W_{LE}}\right)\left(x_{RLE} - x_{TLE}\right) + \left(y_W - y_{W_{LE}}\right)\left(y_{RLE} - y_{TLE}\right) + \left(z_W - z_{W_{LE}}\right)\left(z_{RLE} - z_{TLE}\right) = 0$$

2) The point W_{LE} must lie on the wing boundary. This condition is met when the coordinates of the point W_{LE} satisfy the two-point equation of the line representing the wing boundary edge, e.g.:

$$\frac{x_{W_{LE}} - x_{RLE}}{x_{TLE} - x_{RLE}} - \frac{y_{W_{LE}} - y_{RLE}}{y_{TLE} - y_{RLE}} = 0$$

$$\frac{x_{W_{LE}} - x_{RLE}}{x_{TLE} - x_{RLE}} - \frac{z_{W_{LE}} - z_{RLE}}{z_{TLE} - z_{RLE}} = 0$$

The coordinates of the reflection point, W, are then tested against the coordinates of the three nearest boundary points to determine if Point W is actually located on the wing or flap reflecting surface.

If the reflection point W is contained within the wing panel boundaries, the reflection computation may continue. If Point W is outside the wing panel boundaries, no contribution to reflected noise occurs, and the algorithm proceeds to consider the next reflecting panel.

4.2.5 Computation of Reflected Ray Path Length

If a reflection has occurred for a particular wing panel, the path length of the reflected ray must be determined. The path length is the combined distance from the source to the reflection point, S-W, and from the reflection point to the receiver, W-R, as shown in Figure 31. This is equivalent to the distance from the image source point, IS, to the receiver point, R.

Thus, the reflected ray path length may be computed from:

$$d_r = \sqrt{(\Delta x_r)^2 + (\Delta y_r)^2 + (\Delta z_r)^2}$$

where:

$$\Delta x_r = x_{IS} - x_R$$
$$\Delta y_r = y_{IS} - y_R$$
$$\Delta z_r = z_{IS} - z_R$$

4.2.6 Determination of Source Strength for Reflected Ray

The strength of the point source, S, is a function of the directivity angle of the ray radiating from it. As illustrated in Figure 32, the directivity angles of the direct ray and the reflected ray could be different. Therefore, the source strength of the reflected ray must be computed separately from that of the direct ray.

To obtain the source strength, the directivity angle of the reflected ray must be computed in three-dimensional space. The directivity angle is equivalent to the 3-D included angle between the engine exhaust centerline and the reflected ray. Then, the reflected ray source strength is interpolated from an array of source strength versus directivity angle.

4.2.7 Computation of Strength at Receiver

To obtain the strength at the ground receiver, the source strength of the reflected ray must be corrected for the same propagation effects as the directly radiated ray, i.e., atmospheric attenuation, spherical spreading, and ground reflection. These are all functions of the path length of the reflected ray, and thus will have different values than for the direct ray. Existing algorithms are available in the ANOPP program to compute these correction values.

4.2.8 Combination of Contributions from Direct and Reflected Rays

After the corrected strength of each of the reflected rays has been computed, they must be combined with the strength of the direct ray, in order to obtain the total Sound Pressure Level (SPL) at the receiver.

The combined contribution of rays from each of the reflecting panels is computed using the following equation, for every 1/3-octave frequency band, k:

$$SPL_{k,REF,TOT} = 10 \log \sum_{IPANEL=1}^{NPANEL} 10^{(SPL_{k,IPANEL}/10)}$$

The total contribution from reflected rays may then be combined with the direct ray contribution, to yield the total SPL at the receiver. For every 1/3-octave band, the total SPL is given by:

$$SPL_{k,TOT} = 10 \log \left[10^{(SPL_{k,DIR}/10)} + 10^{(SPL_{k,REF,TOT}/10)} \right]$$

4.3 Conclusion

The wing reflection model to be applied in the ANOPP noise prediction program was formulated based on the results of the Raynoise® studies and additional analytical estimates. Reasonable assumptions were applied, and their impact on modeling accuracy was assessed.

The wing reflection algorithm described in this section was designed to be compatible with NASA's ANOPP noise prediction program. However, rather than installing it directly in ANOPP, a more expedient process was to first install the wing reflection module in Engines & Systems' noise prediction program, GASP. This permitted more efficient check-out and demonstration of the module. Then, after verifying its capability, the module was installed in ANOPP.
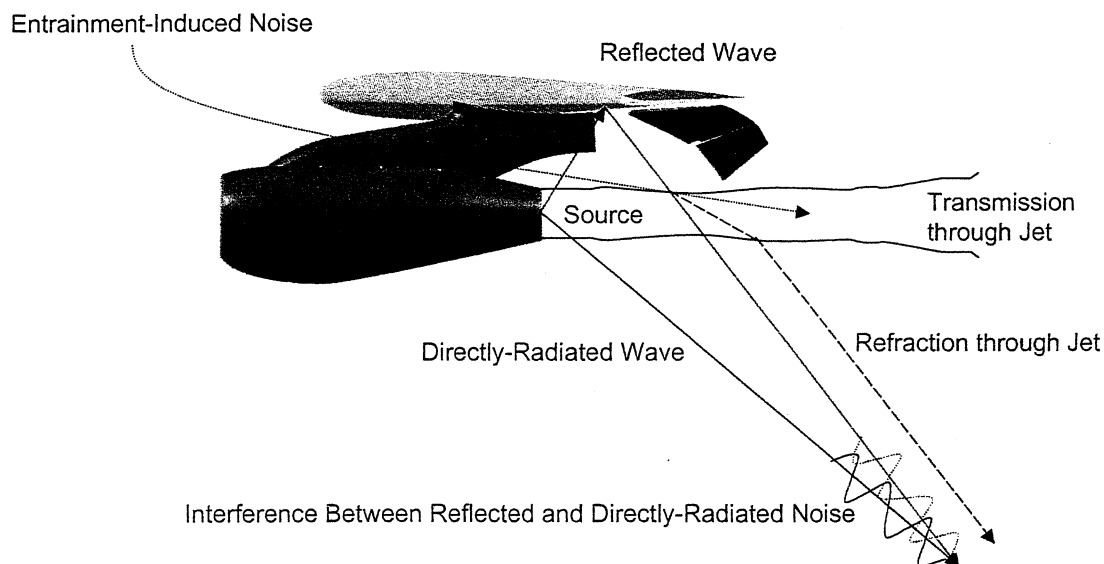
Figure 22. Issues To Be Considered for Noise Prediction With Engine Mounted Under-the-Wing.
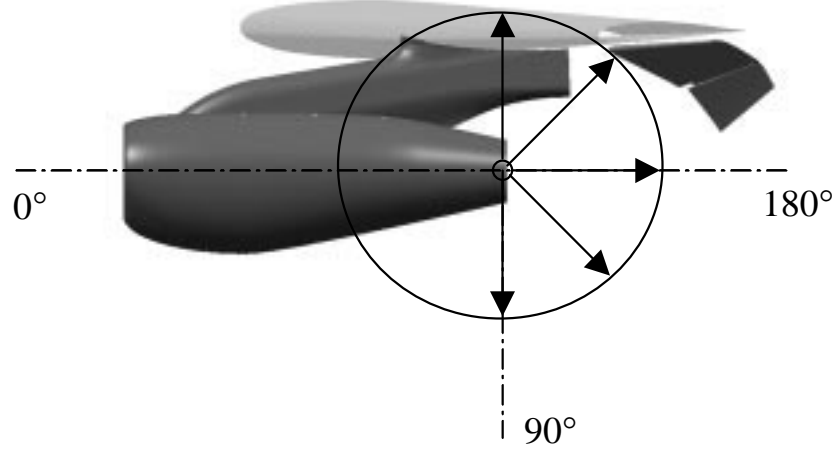
Figure 23. Point Source Model for Fan Bypass Noise at Fan Duct Exit.
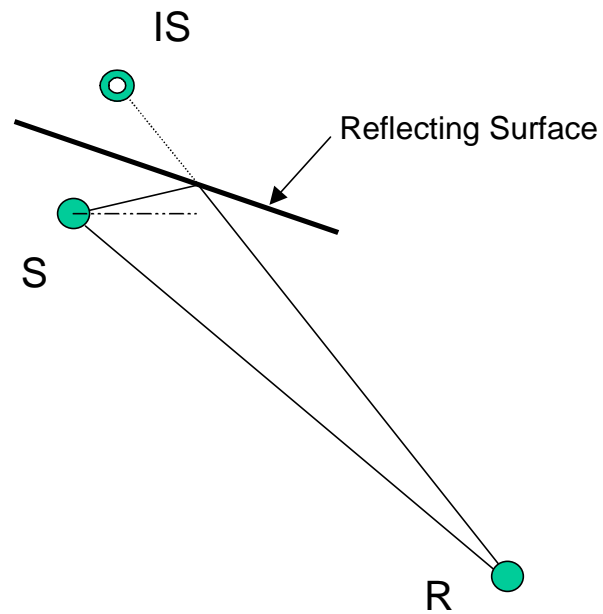
Figure 24. The Directivity Angle of the Reflected Ray May Differ From That of the Directly-Radiated Ray.
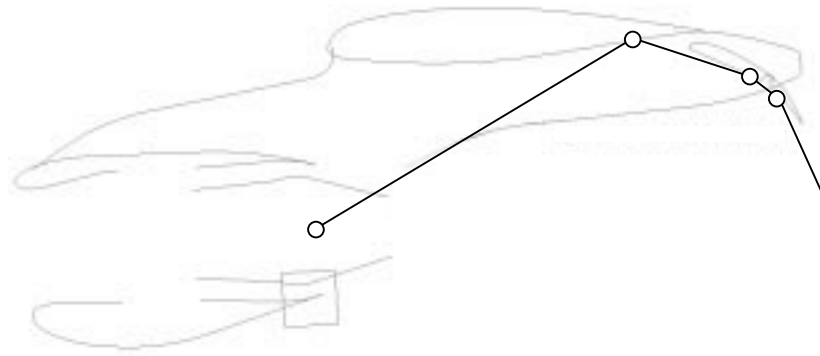
Figure 25. A 2-D Model of a Typical Wing/Flap System, With Fully-Extended Flaps, Illustrates the Occurrence of Multiple Reflections From a Single Ray.
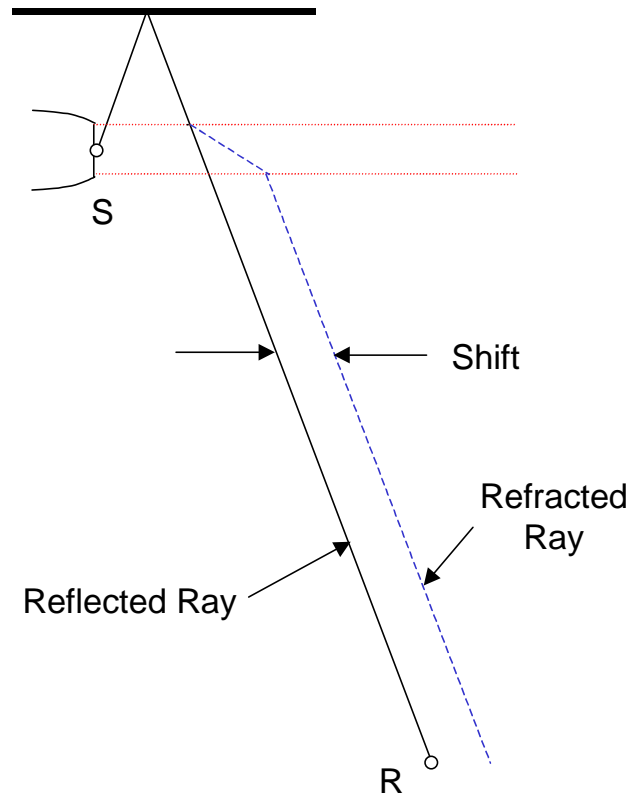
Figure 26. A Reflected Ray Experiences Refraction As It Passes Through the Exhaust Jet.
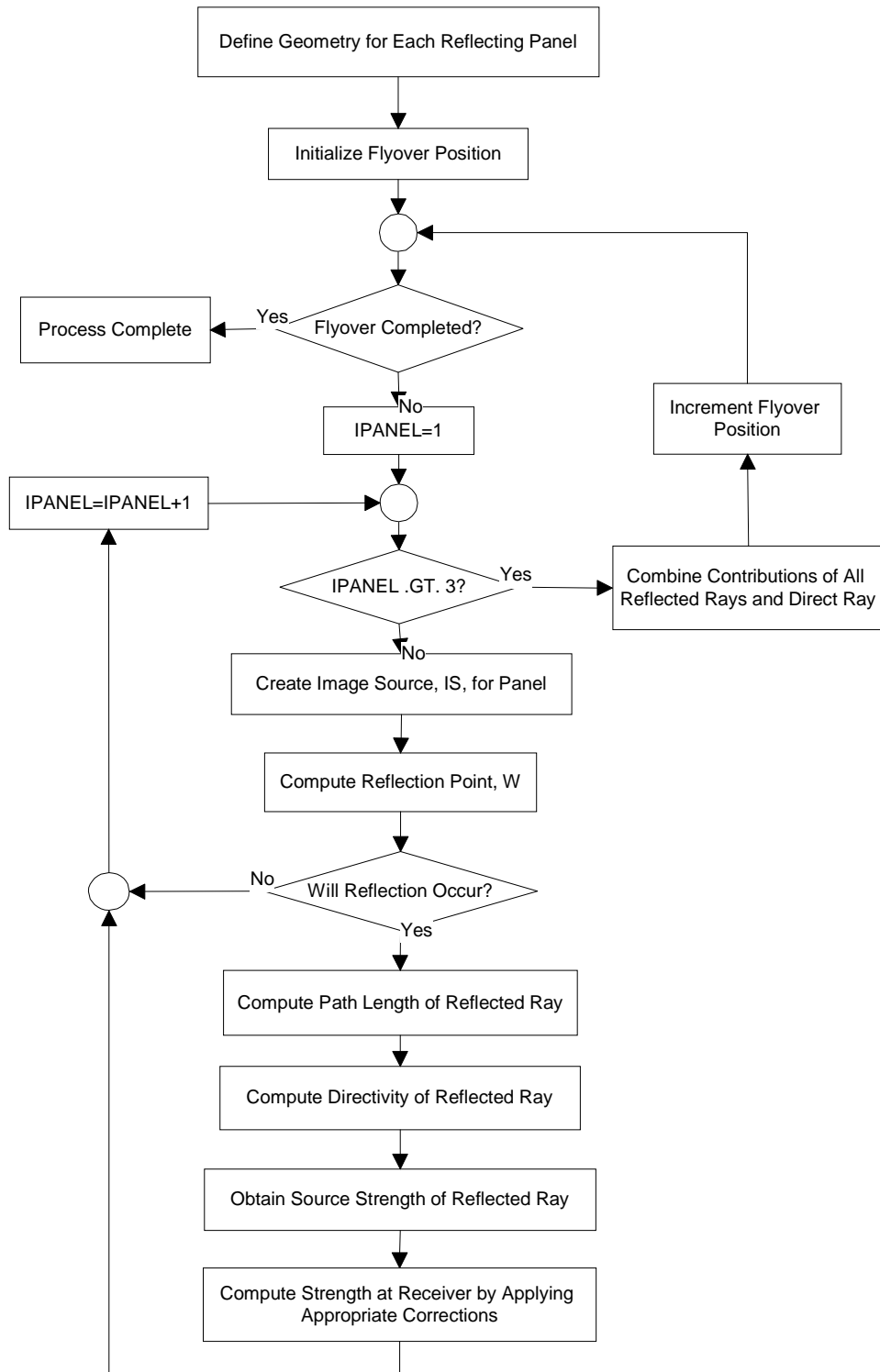
Figure 27. Flowchart for the Wing Reflection Algorithm.
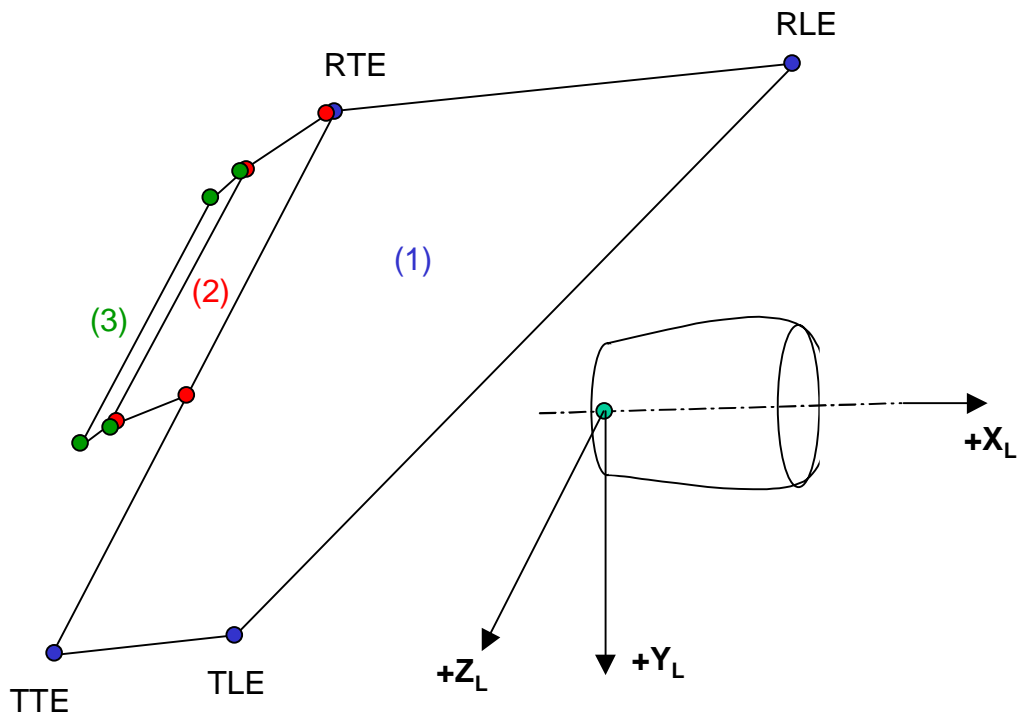
Figure 28. The Reflecting Panel Geometry Is Defined in Terms of Panel Boundary Points.
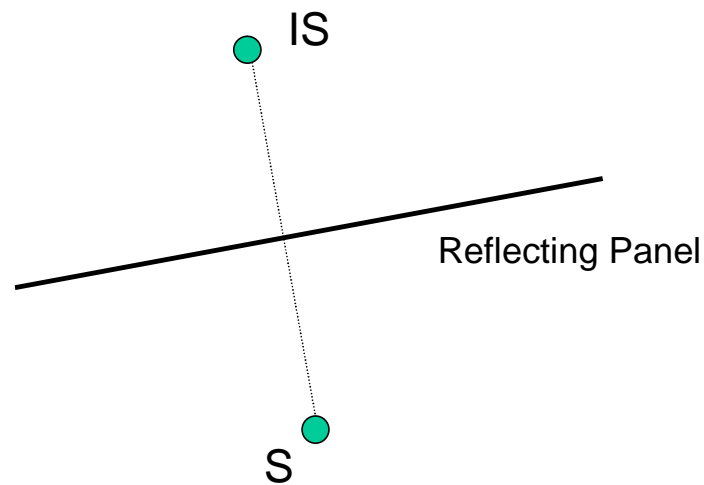
Figure 29. Orientation of the Image Source Point Relative to the Original Source and the Reflecting Panel.
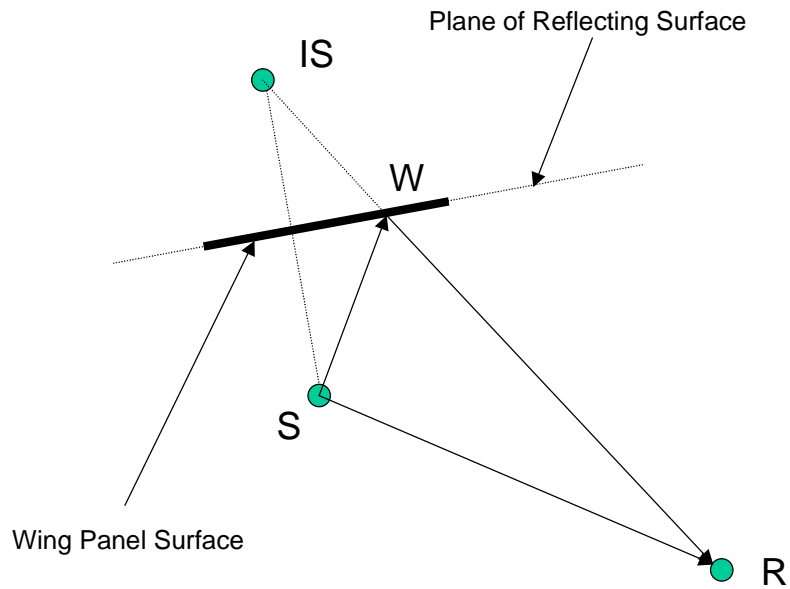
Figure 30. To Determine if a Reflection Will Occur, the Location of the Reflection Point W Must Be Determined Relative to the Wing Panel.
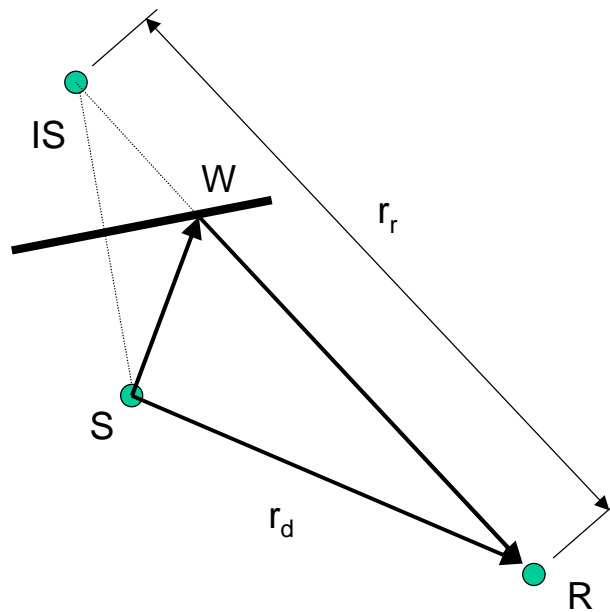
Figure 31. The Path Length of the Reflected Ray Is Equivalent to the Distance Between the Receiver, R, and the Image Source, IS.
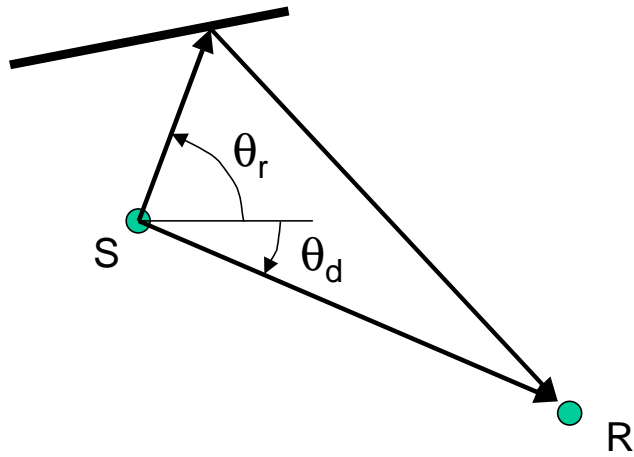
Figure 32. The Source Strength of the Reflected Ray Is a Function of the Directivity Angle, Which Can Differ From that of the Direct Ray.

5. DEMONSTRATION OF THE NEW MODEL IN GASP

5.1 Configurations and Operating Conditions

In order to demonstrate the new wing reflection model in GASP, a series of test cases was performed using the wing/engine configuration of the RJ100 regional transport with LF507 engines, as described in paragraph 2.2. For purposes of the GASP analyses, only the geometry of the wing/flap system and the position of the noise source were modeled. The wing and flap panels were defined using the four corner points on each panel, and the noise source was located on the outboard engine centerline at the aft fan duct exit plane.

The GASP analyses were performed at the operating conditions for the three FAA certification points:

- Cutback Takeoff
- Sideline
- Approach

The analyses were performed in three modes for each of the three operating conditions:

- No wing reflection
- Wing reflection with the wing panel only (i.e., flaps retracted)
- Wing reflection with the wing, flap, and flap tab panels (full flaps – 33 degrees)

Although full flaps are only appropriate for approach, and not for takeoff and sideline conditions, the full flap cases were analyzed for all points, in order to obtain an estimate of sensitivity to flap extension.

5.2 Results

For each operating condition, results of the three analyses were compared by computing deltas of EPNL and maximum PNLTC between the wing reflection model and no wing reflection model. Deltas were considered for both aft fan duct noise alone and total overall noise.

At the cutback takeoff condition, shown in Figure 33, the EPNL contribution from the aft fan duct increases by 2.4 dB when reflection from the wing panel (1 panel) is included. Full flap extension (three panels) has little impact, increasing the aft fan duct EPNL by only an additional 0.1 dB. Overall EPNL is only increased by 0.4 dB with the wing reflection option, and there is no additional impact from the flaps and flap tabs.

Figure 34 presents the results at the sideline condition. The aft fan duct contribution to EPNL increases by 1.9 dB when the wing panel reflection is included. Addition of the extended flap panels produces another 0.2 dB EPNL. For sideline, the wing reflection effect on total EPNL is minimal, with a prediction of 0.1 dB increase for wing reflection, and an additional 0.1 dB increase with full flaps.

At the approach condition, the EPNL increase in aft fan duct noise due to reflection from the single wing panel (shown in Figure 35) is 1.9 dB, and no additional increase is seen when the fully-

extended flap panels are included. Overall EPNL increases only 0.5 dB with wing reflection, and no additional increase is seen with flap extension. Examination of individual points along the approach path reveals local differences in wing-only and extended-flap reflected noise contributions; however, the integrated effect is negligible.

As would be expected, the maximum PNLTC deltas for each of the operating conditions are larger than the EPNL deltas, as shown in Figures 33 through 35. These maximum PNLTC values for aft fan duct noise range from 2.9 dB at approach to 3.5 dB at sideline, for reflection from the wing panel only. A maximum additional contribution of 0.2 dB with fully extended flaps is seen at cutback takeoff. The overall maximum PNLTC deltas range from 0.6 dB at sideline to 1.6 dB at approach.

It may be observed that the impact on maximum PNLTC is reasonable, representing an approximate doubling of the noise, due to the contribution of a reflected wave from the wing surface. Also, it may be noted that the impact of the flap and flap tab surfaces is not substantial, producing at most a 0.1 dB increase in total noise contributed from the wing reflection model. This appears quite reasonable, given the size of the flap reflecting surfaces relative to that of the wing surface. This result is also supported by the Raynoise[®] analyses, which showed only a small, localized effect from the flaps.

The effect of wing reflection on PNL for the approach flight profile is shown in Figure 36. In this case, the wing/flap system is modeled with fully extended flaps. The wing reflection contribution is evident after the aircraft has passed over the observer's position. The maximum increase in aft fan duct PNL occurs at an engine-observer angle of approximately 110 degrees, and at approximately 125 degrees for total PNL.

5.3 Conclusions

The results from the new wing reflection model are generally consistent with those of the Raynoise[®] analyses. However, these wing reflection results are a strong function of the wing/engine configuration analyzed. As was seen in the Raynoise[®] analyses (Section 3), different relative placement of the noise source and the reflecting surface boundaries can result in different contributions from wing reflection. Therefore, to more fully exercise the wing reflection module, and to establish best practices for its use, further analysis with other wing/engine configurations is recommended.

Noise Deltas at Cutback Takeoff Conditions
(Wing Reflection - No Wing Reflection)
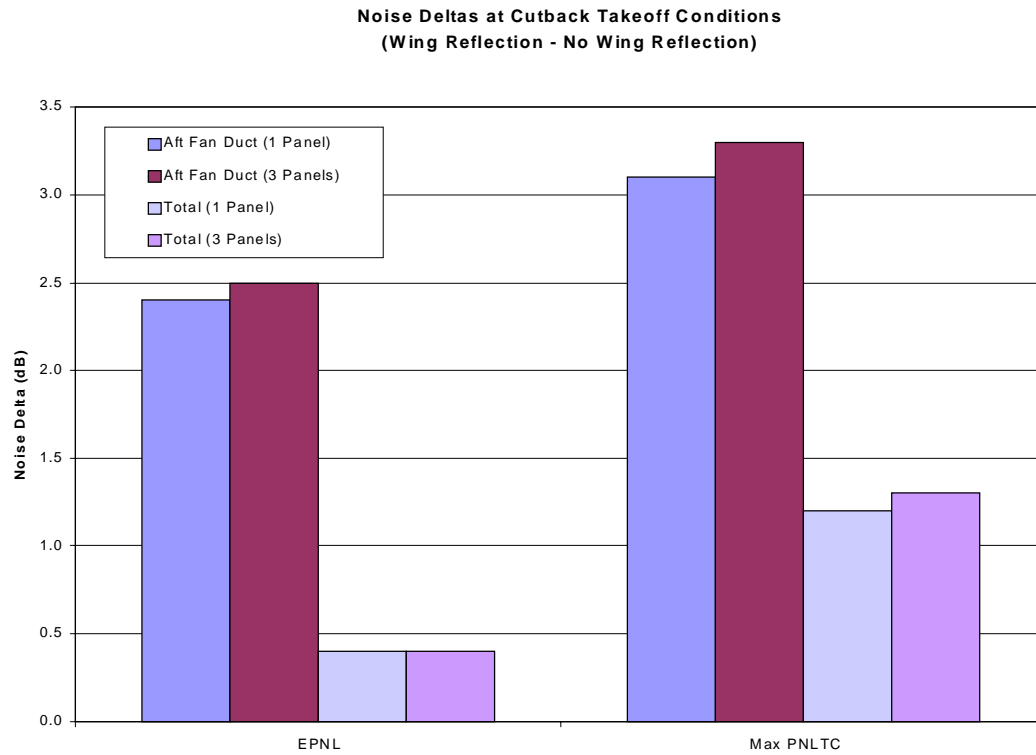
Figure 33. Effect of Wing Reflection at Cutback Takeoff Conditions for the Wing/Engine Configuration of the Regional Transport Test Case.
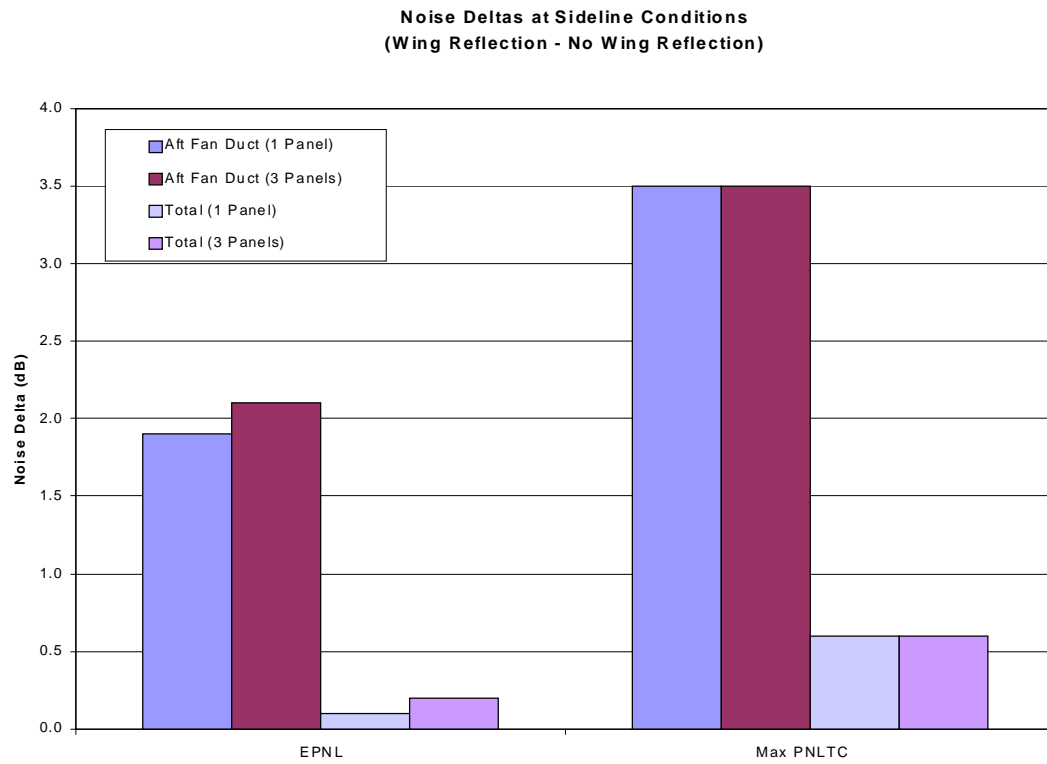
Figure 34. Effect of Wing Reflection at Sideline Conditions for the Wing/Engine Configuration of the Regional Transport Test Case.

Noise Deltas at Approach Conditions
(Wing Reflection - No Wing Reflection)
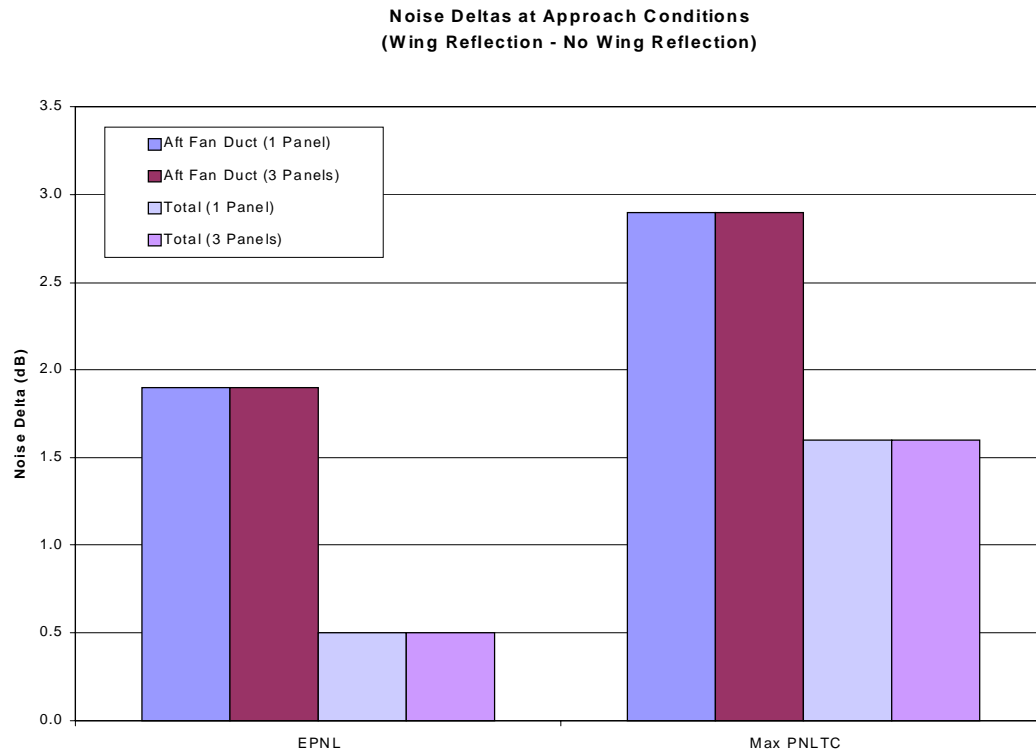
Figure 35. Effect of Wing Reflection at Approach Conditions for the Wing/Engine Configuration of the Regional Transport Test Case.
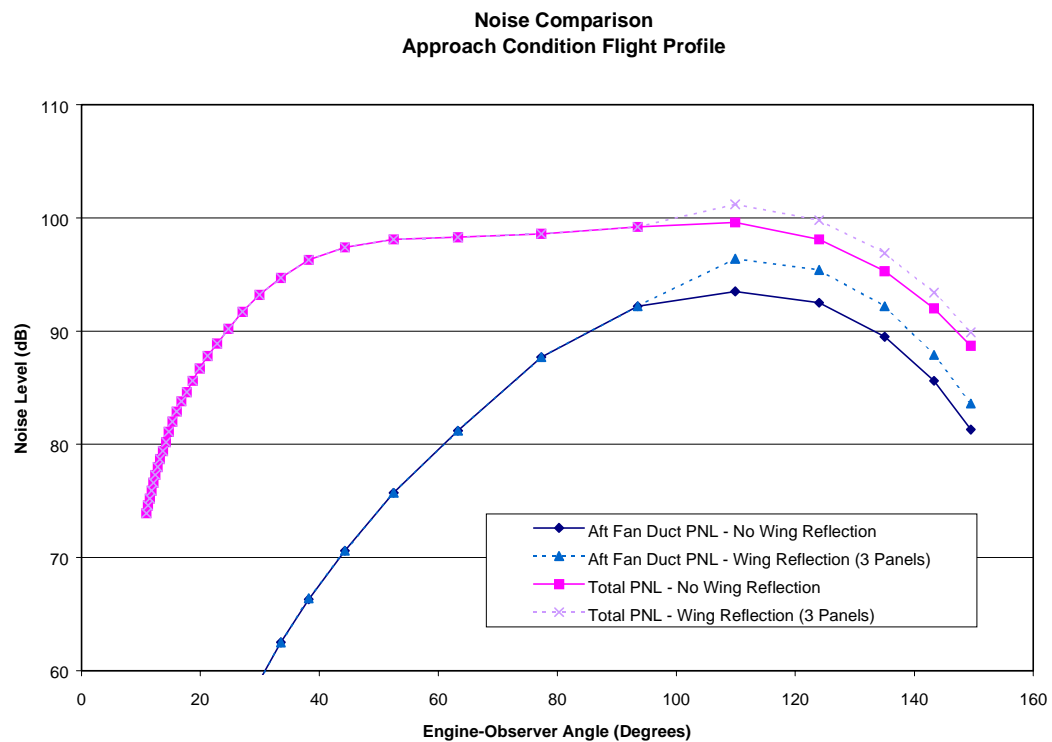
Figure 36. Impact of Wing Reflection on Noise for the Approach Flight Profile With the Wing/Engine Configuration of the Regional Transport Test Case.

6. APPLICATION IN THE ANOPP PROGRAM

After demonstration of the wing reflection model in the GASP program, the algorithm was then prepared for installation in the ANOPP program as the Wing Geometric Effects module, which is accessed with the "EXECUTE WING" command.

The Wing Geometric Effects module was designed to perform calculations using just the output from the Geometry (GEO) and Propagation (PRO) modules. The method for wing reflection required computing a directivity angle and adjusting the source noise level for the reflected ray. To implement this calculation, the noise level for the reflected ray was computed by interpolating the PRO received noise data table at the appropriate directivity angle. Then, a spherical spreading correction was applied to adjust the level for the appropriate path length. It was assumed that the original ground effects and atmospheric absorption calculations for the interpolated direct ray (at the reflected ray directivity angle) were valid for the reflected ray.

Following installation of the wing reflection module in ANOPP, an approach analysis was performed, using the RJ100 regional transport, to obtain predicted farfield noise levels with and without the wing reflection option. A plot of flyover noise levels comparing the two analyses is shown in Figure 37. These results were obtained directly from the Wing Geometric Effects module test case.

The ANOPP Theoretical Manual for the Wing Reflection module is included in Appendix I of this report. The ANOPP Wing Reflection User's Manual is contained in Appendix II, and the Wing Reflection Test Case Inputs and Outputs are in Appendix III.
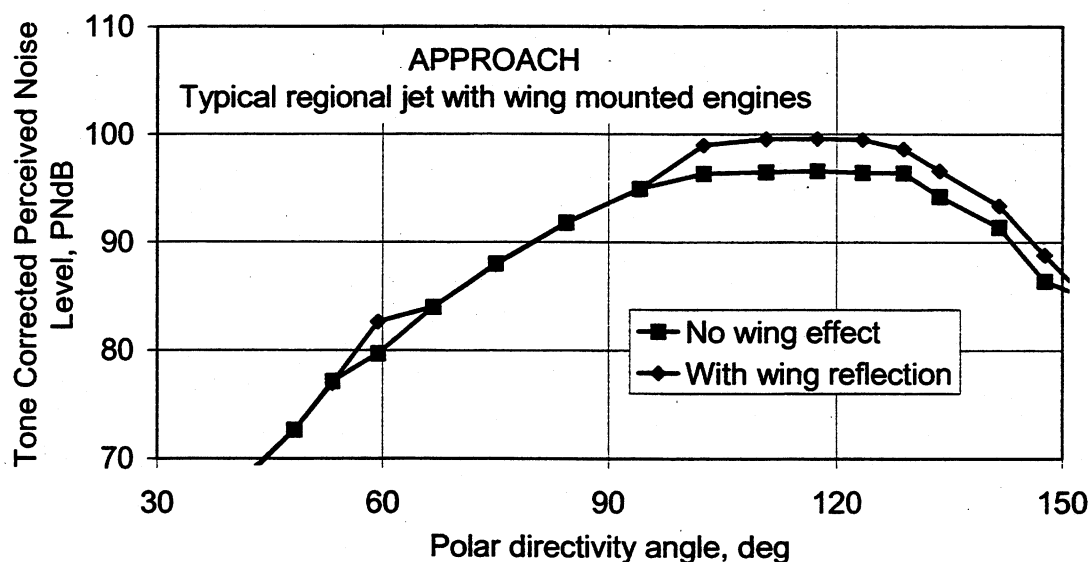
Figure 37. ANOPP Predictions of Flyover Noise Levels With and Without the Wing Reflection Option.

7. CONCLUSIONS AND RECOMMENDATIONS

Engines & Systems has completed Task Order 23, Wing Reflection Code, under the National Aeronautics and Space Administration (NASA)-sponsored Small Engine Technology (SET) Program, Contract No. NAS3-27483. This task focused on improving the engine noise prediction capabilities of the NASA ANOPP program through the introduction of a wing reflection model.

The wing reflection model accounts for flyover noise enhancement due to reflection of the aft fan duct noise off of the wing/flap system, for under-the-wing engine mount configurations.

The ray-tracing program Raynoise® was used to examine wing reflection behavior. Based on input from the Raynoise® study, the wing reflection model was successfully developed and installed in Engines & Systems' GASP noise prediction program. The model was then demonstrated for a typical regional transport with engines mounted under-the-wing. As expected, use of the wing reflection model resulted in enhancement of the aft fan duct noise, and thus the overall aircraft noise, at a ground receiver location, due to reflection from the wing/flap system.

The software module containing the wing reflection algorithm was then installed in the ANOPP program. In addition, ANOPP documentation for the wing reflection module was generated, including a Technical Manual, a User's Manual, and a listing of input and output for a test case.

Further analyses using the wing reflection module in ANOPP would be recommended, with different wing/engine configurations, in order to more fully exercise the model and determine its sensitivity to the relative placement of noise sources and reflecting surface boundaries. Also, further examination of the impact of flap system surfaces would be of value, to establish best practices for modeling small reflecting surfaces.

8. REFERENCES

1. Zorumski, W.E., "Aircraft Noise Prediction Program Theoretical Manual, Parts 1 and 2," NASA Technical Memorandums TM-83199-PT-1 and PT-2, National Aeronautics and Space Administration, Langley Research Center, Hampton, VA, February 1982.

2. Zorumski, W.E., and Weir, D.S., "Aircraft Noise Prediction Program Theoretical Manual, Part 3," NASA Technical Memorandum TM-83199-PT-3, National Aeronautics and Space Administration, Langley Research Center, Hampton, VA, June 1986.

3. Raynoise® is a product of LMS Numerical Technologies, a subsidiary of LMS International, Interleuvenlaan 70, 3001 Leuven, Belgium.

4. Mitchell, J.A., Barton, C.K., Kisner, L.S., Lyon, C.A., "Computer Program to Predict Noise of General Aviation Aircraft: Final Report and User's Guide," NASA Report CR-168050, National Aeronautics and Space Administration, Lewis Research Center, September 1982.

5. Wang, M.E., "Wing Effect on Jet Noise Propagation," AIAA-80-1047, AIAA 6th Aeroacoustics Conference, Hartford, Connecticut, June 1980.

6. Heidmann, M.F., "Interim Prediction Method For Fan and Compressor Source Noise," NASA TM X-71763, 1979.

APPENDIX I

ANOPP

WING GEOMETRIC EFFECTS MODULE
THEORETICAL MANUAL

INTRODUCTION

The Wing Geometric Effects Module computes the effects of wing shielding and reflection on the propagation of noise from the engine. The wing shielding model employs the Fresnel diffraction theory for a semi-infinite barrier, as described in Beranek (1) and Maekawa (2), with modifications to treat the finite barrier presented by the aircraft wing. In the wing reflection model, the directly radiated wave is treated in a manner consistent with the current ANOPP program. For the reflected wave, the nature of the reflecting surfaces and the directivity of the source are modeled as well as atmospheric absorption, ground effects, and source-to-observer geometry. It is assumed that reflection can occur only from the wing/flap system. A maximum of three wing/flap panels is included in the model. The flap system consists of continuous spanwise flap panels on each wing, with no jet efflux cut-outs. Tabbed Fowler flaps can be modeled, including gaps along the hinge centerlines. The effect of leading edge slats on the wing is neglected. The wing and flap panels are modeled as planar perfectly reflecting surfaces.

SYMBOLS

A	attenuation, dB
c_∞	ambient speed of sound, m/s (ft/s)
d	distance, m (ft)
f	frequency, Hz
N	Fresnel number
$<p^2>*$	mean-square acoustic pressure, re $\rho_\infty^2 c_\infty^4$
x, y, z	coordinate locations

GREEK

Δ	difference in source-receiver path length
ρ_∞	ambient density, kg/m^3 (slug/ft^3)

SUPERSCRIPT

*	dimensionless quantity

SUBSCRIPT

F	flap
1	source location
O	observer location
r	reference standard sea level
RLE	root leading edge
RTE	root trailing edge
T	flap tab
TLE	tip leading edge
TOT	total
TTE	tip trailing edge
W	wing

INPUT

The values of the wing (and the flap and flap tab for reflection) coordinates are provided by the user. The source-to-observer geometry is provided by the Geometry (GEO) Module and the one-third octave band noise levels being propagated to the observer are provided by the Propagation (PRO) Module. The frequency array establishes the independent variable values for the output table.

$(x_{RLE}, y_{RLE}, z_{RLE})$	coordinates of root leading edge
$(x_{RTE}, y_{RTE}, z_{RTE})$	coordinates of root trailing edge
$(x_{TLE}, y_{TLE}, z_{TLE})$	coordinates of tip leading edge
$(x_{TTE}, y_{TTE}, z_{TTE})$	coordinates of tip trailing edge

Independent Variable Array

f	frequency, Hz

Received Noise Data Table

f	frequency, Hz
t	reception time, s
o	observer index
$c_a^*(o)$	speed of sound at the observer, re c_r
$\rho_a^*(o)$	air density at the observer, re ρ_r
$<p^2(f,t,o)>^*$	mean square acoustic pressure, re $\rho_\infty^2 c_\infty^4$

OUTPUT

The output of this module is a table of the mean-square acoustic pressure as a function of frequency, reception time, and observer index corrected for wing geometry effects.

Attenuated (or Enhanced) Received Noise Data Table

f	frequency, Hz
t	reception time, s
o	observer index
$c_a^*(o)$	speed of sound at the observer, re c_r
$\rho_a^*(o)$	air density at the observer, re ρ_r
$<p^2(f,t,o)>^*$	mean square acoustic pressure, re $\rho_\infty^2 c_\infty^4$

METHOD

Wing Geometry

The wing (flap or flap tab) configuration is described in a local coordinate system with the origin positioned at the engine inlet (Point 1), as shown in Figure 1 for wing shielding. The origin of the local coordinate system for wing reflection is at the engine exhaust as shown in Figure 2. The local coordinate system origin is assumed to be the aircraft location specified in the body coordinate system (see the Geometry Module) for the propagation calculation. The user must specify the coordinates at the wing root leading edge, root trailing edge, tip leading edge, and tip trailing edge, relative to the location of the local coordinate system origin.

Then, the local origin and wing coordinates are transformed into a global coordinate system consistent with the observer location on the ground (Point O). This transformation must take into account the aircraft attitude and position at the particular time of the observation.
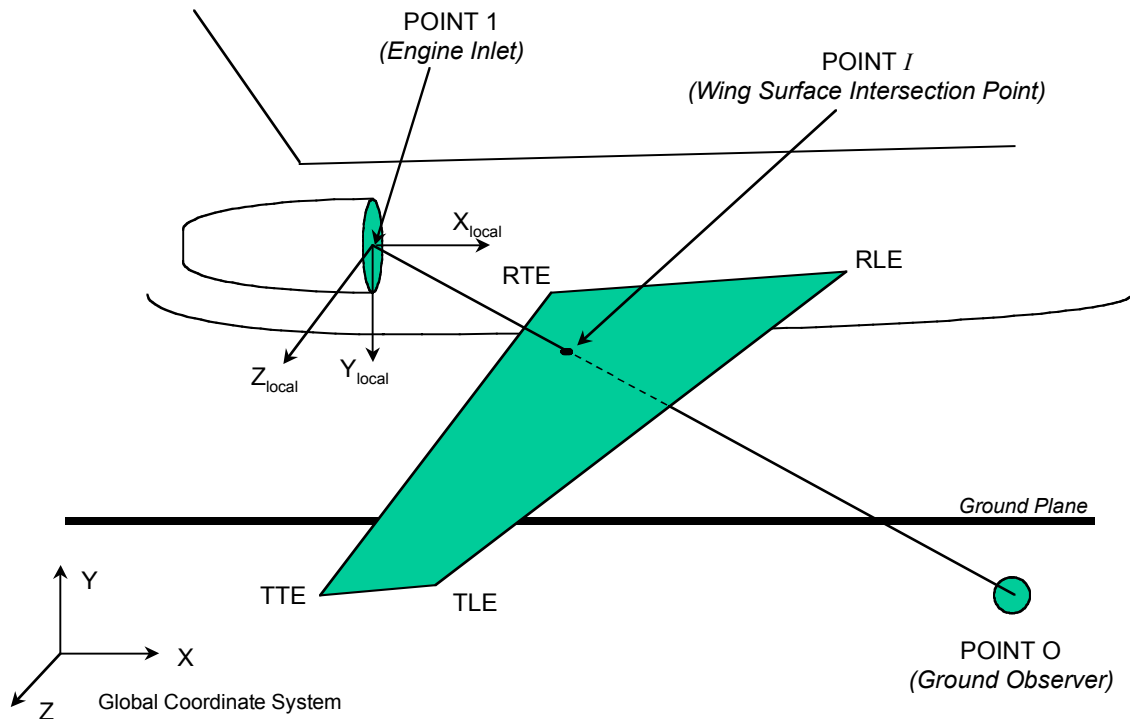
Figure 1. Coordinate System That Defines the Wing Geometry and Typical Sound Propagation Vector For Wing Shielding.

Figure 2. The Reflecting Panel Geometry Is Defined in Terms of Panel Boundary Points Similar to Wing Shielding.

Wing Shielding Model

The location of the point representing the intersection of the line between the engine inlet (Point 1) and the observer on the ground (Point O) with the plane of the wing must be computed. Figure 3 illustrates the configuration of line 1-O and the wing plane, with the intersection point (Point I). The coordinates of the intersection point are determined by solving a set of three equations in three unknowns (x_I, y_I, and z_I). Two equations are produced by the 2-point form for the equation for the line 1-O:

$$\frac{x_I - x_O}{x_1 - x_O} - \frac{y_I - y_O}{y_1 - y_O} = 0 \qquad (1)$$

$$\frac{x_I - x_O}{x_1 - x_O} - \frac{z_I - z_O}{z_1 - z_O} = 0 \qquad (2)$$

The other equation comes from the 3-point form of the equation for the wing plane:

$$\begin{vmatrix} x_I - x_{RLE} & y_I - y_{RLE} & z_I - z_{RLE} \\ x_{RTE} - x_{RLE} & y_{RTE} - y_{RLE} & z_{RTE} - z_{RLE} \\ x_{TLE} - x_{RLE} & y_{TLE} - y_{RLE} & z_{TLE} - z_{RLE} \end{vmatrix} = 0 \qquad (3)$$

Because four points have been specified to describe the boundaries of the wing, the wing surface may not actually be planar. However, for the purpose of determining the intersection Point I, the assumption is made that the wing plane is described by the points at the root leading and trailing edges, and the tip leading edge. The intersection point (Point I) may or may not be located within the boundaries of the wing surface.

Now, the point on each wing boundary which is nearest to Point I must be located, as shown in Figure 3. Each of these points (Points W_{LE}, W_{TE}, and W_{TIP}) is computed by solving a set of three equations in three unknowns (e.g., $x_{W_{LE}}$, $y_{W_{LE}}$, and $z_{W_{LE}}$). The equations are obtained by imposing the following conditions:

1) The line I-W must be perpendicular to the wing boundary. This condition is represented by setting the dot product of the line I-W vector and the wing boundary line vector equal to zero, e.g.:

$$\left(x_I - x_{W_{LE}}\right)\left(x_{RLE} - x_{TLE}\right) + \left(y_I - y_{W_{LE}}\right)\left(y_{RLE} - y_{TLE}\right) + \left(z_I - z_{W_{LE}}\right)\left(z_{RLE} - z_{TLE}\right) = 0 \quad (4)$$

2) The point W must lie on the wing boundary. This condition is met when the coordinates of the point W satisfy the two-point equation of the line representing the wing boundary edge, e.g.:

$$\frac{x_{W_{LE}} - x_{RLE}}{x_{TLE} - x_{RLE}} - \frac{y_{W_{LE}} - y_{RLE}}{y_{TLE} - y_{RLE}} = 0 \quad (5)$$

$$\frac{x_{W_{LE}} - x_{RLE}}{x_{TLE} - x_{RLE}} - \frac{z_{W_{LE}} - z_{RLE}}{z_{TLE} - z_{RLE}} = 0 \quad (6)$$

It is necessary then to determine if the intersection point I actually is located within the boundaries of the wing. If it is outside the wing, then no attenuation of the noise source is present. However, if Point I lies on the wing surface, then the Fresnel diffraction theory is applied to determine the level of attenuation.

Assuming that Point I is located within the boundaries of the wing, then the attenuation of the noise source due to wing shielding must be determined for each diffraction edge (i.e., wing boundary edge). For each diffraction edge, three distances must be computed, as shown in Figure 4:

1) The direct source-receiver path length, from Point 1 to Point O, d_{1O},

2) The distance from Point 1 to the closest point on the diffraction edge, Point W, d_{1W},

3) The distance from the point W on the diffraction edge to the observer location on the ground, Point O, d_{WO}.

From these three distances, the difference in source-receiver path length between the direct and diffracted sound fields may be computed:

$$\Delta = (d_{1W} + d_{WO}) - d_{1O} \qquad (7)$$

where $\Delta > 0$ when Point I lies on the wing surface, $\Delta = 0$ when Point I lies on the wing boundary edge, and $\Delta < 0$ when Point I is beyond the wing surface.
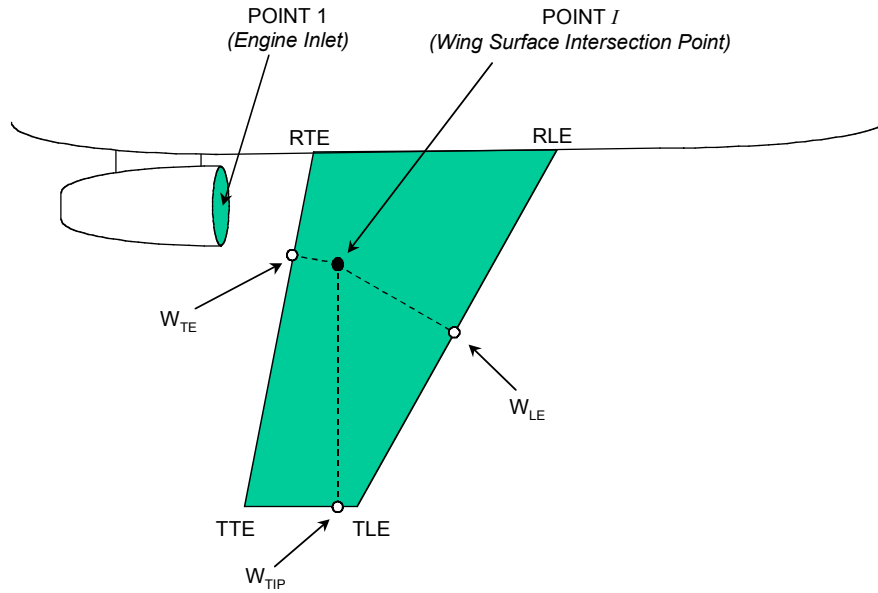
Figure 3. The Point That Is Nearest To The Ray Intersection Point With The Wing Is Determined.
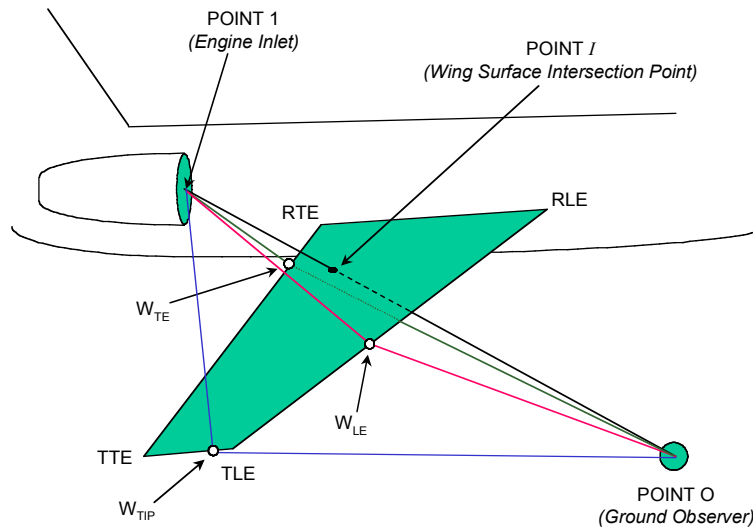
Figure 4. The Differences In Path Length Between The Direct And Diffracted Sound Rays Are Used To Calculate The Wing Shielding.

From this difference in distances, the Fresnel number is calculated as follows:

$$N = 2 \, f_i \, \Delta \, / \, c_\infty \qquad\qquad (8)$$

where f_i represents the frequency for each 1/3 octave band, in Hz, and c_∞ represents the ambient speed of sound.

The attenuation is computed for each 1/3 octave band frequency as follows:

$$A(f_i) = \begin{cases} 20 \, \log \dfrac{\sqrt{2\pi N}}{\tanh \sqrt{2\pi N}} + 5.0 & ; \; N \geq 0 \\[3mm] 20 \, \log \dfrac{\sqrt{2\pi |N|}}{\tan \sqrt{2\pi |N|}} + 5.0 & ; \quad -0.2 \leq N < 0 \\[3mm] 0. & ; \quad N < -0.2 \end{cases} \qquad (9)$$

This attenuation is the noise reduction due to a semi-infinite barrier. In this model, diffraction around three diffraction edges (wing leading edge, trailing edge, and tip) is included. In order to obtain an equivalent total attenuation from the combined effects of the three diffraction edges, the individual attenuations for each edge at any frequency f_i are combined as follows:

$$A_{TOT} = -10 \log \sum 10^{-\left(A_k / 10\right)} \qquad\qquad (10)$$

where k = LE, TE, and TIP.

Wing Reflection Model

The reflecting panels that represent the wing/flap system are modeled as planar surfaces. The geometry definition for each panel consists of the specification of the Cartesian coordinates (x, y, z) of each corner point of the panel. The coordinates are defined for the Root Leading Edge (RLE), Root Trailing Edge (RTE), Tip Leading Edge (TLE), and Tip Trailing Edge (TTE), as shown in Figure 2. The coordinates of the Tip Trailing Edge (TTE) are used only to define the wing boundary. Three points define the plane of the wing: RLE, RTE, and TLE. Any twist in the wing is ignored.

The Cartesian coordinates of the wing boundary points are defined relative to the local origin of the engine centerline at the exit plane of the fan bypass duct. Local axes are shown in Figure 2. Then, the engine fan duct exit and wing coordinates are transformed into a global coordinate system consistent with the receiver location on the ground (Point R). This transformation must take into account the aircraft attitude and position at the particular time of the observation. Therefore, the global coordinates must be calculated at every flyover position.

Three wing/flap panels are currently permitted in the model. This allows the description of a main wing panel, a flap panel, and a flap tab panel. However, if flaps are not included in the model, or are considered to have negligible impact on reflection compared to the wing itself, the wing may be modeled using multiple panels, instead.

The reflection model uses an image source point, which is positioned on a normal to the reflecting plane, at a distance equivalent to that between the source and the reflecting plane, but located on the opposite side of the reflecting plane. The orientation of the image source is shown in Figure 5.

To obtain the image source point, a normal to the reflecting plane is created, which intersects the original source point (S). Then Point IS, the image source, is located on the normal line. The points S and IS are equidistant from the reflecting panel. Note that the normal line between Points S and IS does not have to intersect the wing panel itself, only the plane extending through the wing panel.
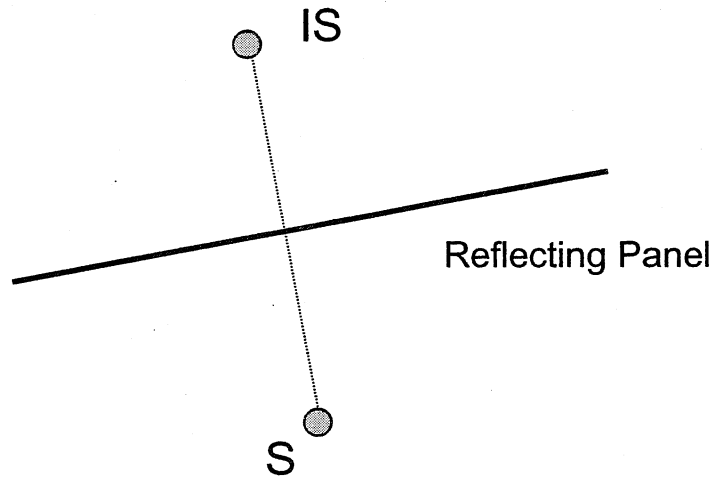
Figure 5. The Orientation of the Image Source Point is Shown Relative to the Original Source and the Reflecting Panel.

First, the components of a vector normal to the reflecting surface are obtained by computing the cross-product of vectors along the wing root and leading edge:

$$\Delta x_n = \Delta y_{root} * \Delta z_{LE} - \Delta y_{LE} * \Delta z_{root}$$

$$\Delta y_n = -\left(\Delta x_{root} * \Delta z_{LE} - \Delta x_{LE} * \Delta z_{root}\right)$$

$$\Delta z_n = \Delta x_{root} * \Delta y_{LE} - \Delta x_{LE} * \Delta y_{root}$$

where:

$$\Delta x_{root} = x_{RTE} - x_{RLE}$$

$$\Delta y_{root} = y_{RTE} - y_{RLE}$$

I-8

$$\Delta z_{root} = z_{RTE} - z_{RLE}$$

$$\Delta x_{LE} = x_{TLE} - x_{RLE}$$

$$\Delta y_{LE} = y_{TLE} - y_{RLE}$$

$$\Delta z_{LE} = z_{TLE} - z_{RLE}$$

Next, the coordinates of a point, N, on a line normal to the reflecting surface and passing through the engine source point, S, are obtained as follows:

$$x_N = x_S + \Delta x_N$$

$$y_N = y_S + \Delta y_N$$

$$z_N = z_S + \Delta z_N$$

Then, the coordinates of the intersection of the line S-N with the plane of the reflecting surface are computed. The intersection point is identified as Point I. The coordinates of the intersection point are determined by solving a set of three equations in three unknowns (x_I, y_I, and z_I). Two equations are produced by the 2-point form of the equation for the line S-N:

$$\frac{x_I - x_S}{x_N - x_S} - \frac{y_I - y_S}{y_N - y_S} = 0$$

$$\frac{x_I - x_S}{x_N - x_S} - \frac{z_I - z_S}{z_N - z_S} = 0$$

The other equation comes from the 3-point form of the equation for the reflecting plane:

$$\begin{vmatrix} x_I - x_{RLE} & y_I - y_{RLE} & z_I - z_{RLE} \\ x_{RTE} - x_{RLE} & y_{RTE} - y_{RLE} & z_{RTE} - z_{RLE} \\ x_{TLE} - x_{RLE} & y_{TLE} - y_{RLE} & z_{TLE} - z_{RLE} \end{vmatrix} = 0$$

Once the coordinates of the intersection point have been determined, the components of the vector between the source point, S, and the intersection point, I, may be computed:

$$\Delta x_I = x_I - x_S$$

$$\Delta y_I = y_I - y_S$$

$$\Delta z_I = z_I - z_S$$

Finally, the image source point, IS, may be positioned on the normal to the reflecting surface, through the source point, S, by adding the above vector components to the coordinates of the Point I:

$$x_{IS} = x_I + \Delta x_I$$

$$y_{IS} = y_I + \Delta y_I$$

$$z_{IS} = z_I + \Delta z_I$$

Once the image source is located, it is necessary to determine if a reflection will actually occur for the reflecting panel under consideration. A reflection will occur if the line passing between the receiver and the image source at a given flyover location intersects the plane of the reflecting panel within the boundaries of the actual panel, as shown in Figure 6. The orientation of image source and receiver changes at each interval during the flyover, and therefore must be recomputed for each flyover position.
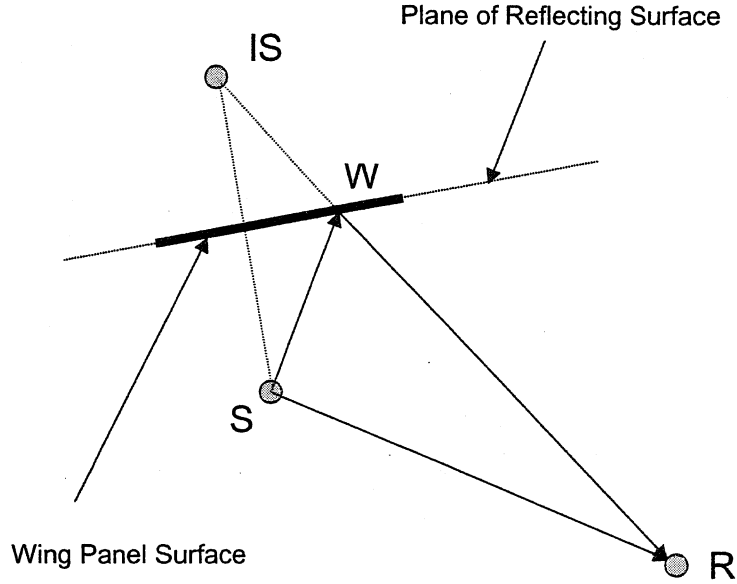
Figure 6. To Determine if a Reflection Will Occur, the Location of the Reflection Point W Must Be Determined Relative to the Wing Panel.

To determine if a reflection will occur, the coordinates of the reflection point (W) on the plane of the wing panel must first be obtained, by determining the intersection point of the line formed by IS-R and the plane of the wing panel. The coordinates of the intersection point, W, are determined by solving a set of three equations in three unknowns (x_W, y_W, and z_W). Two of the equations are produced by the 2-point form of the equation for the line IS-R:

$$\frac{x_W - x_R}{x_{IS} - x_R} - \frac{y_W - y_R}{y_{IS} - y_R} = 0$$

$$\frac{x_W - x_R}{x_{IS} - x_R} - \frac{z_W - z_R}{z_{IS} - z_R} = 0$$

The other equation comes from the 3-point form of the equation for the reflecting plane:

$$\begin{vmatrix} x_W - x_{RLE} & y_W - y_{RLE} & z_W - z_{RLE} \\ x_{RTE} - x_{RLE} & y_{RTE} - y_{RLE} & z_{RTE} - z_{RLE} \\ x_{TLE} - x_{RLE} & y_{TLE} - y_{RLE} & z_{TLE} - z_{RLE} \end{vmatrix} = 0$$

After the coordinates of the reflection point, W, have been determined, the point must be tested to establish whether or not it lies within the boundaries of the reflecting plane. To accomplish this, the point on each wing boundary that is nearest to Point W must be located. Each of these points (Points W_{LE}, W_{TE}, and W_{TIP}) is computed by solving a set of three equations in three unknowns (e.g., $x_{W_{LE}}$, $y_{W_{LE}}$, and $z_{W_{LE}}$ for the leading edge boundary). The equations are obtained by imposing the following conditions, e.g. for the leading edge boundary:

The line W-W_{LE} must be perpendicular to the wing boundary. This condition is represented by setting the dot product of the line W-W_{LE} vector and the wing boundary line vector equal to zero, e.g.:

$$\left(x_W - x_{W_{LE}} \right)\left(x_{RLE} - x_{TLE} \right) + \left(y_W - y_{W_{LE}} \right)\left(y_{RLE} - y_{TLE} \right) + \left(z_W - z_{W_{LE}} \right)\left(z_{RLE} - z_{TLE} \right) = 0$$

The point W_{LE} must lie on the wing boundary. This condition is met when the coordinates of the point W_{LE} satisfy the 2-point equation of the line representing the wing boundary edge, e.g.:

$$\frac{x_{W_{LE}} - x_{RLE}}{x_{TLE} - x_{RLE}} - \frac{y_{W_{LE}} - y_{RLE}}{y_{TLE} - y_{RLE}} = 0$$

$$\frac{x_{W_{LE}} - x_{RLE}}{x_{TLE} - x_{RLE}} - \frac{z_{W_{LE}} - z_{RLE}}{z_{TLE} - z_{RLE}} = 0$$

The coordinates of the reflection point, W, are then tested against the coordinates of the three nearest boundary points, to determine if Point W is actually located on the wing or flap reflecting surface.

If the reflection point W is contained within the wing panel boundaries, the reflection computation may continue. If Point W is outside the wing panel boundaries, no contribution to reflected noise occurs, and the algorithm proceeds to consider the next reflecting panel.

If a reflection has occurred for a particular wing panel, the path length of the reflected ray must be determined. The path length is the combined distance from the source to the reflection point, S-W, and from the reflection point to the receiver, W-R, as shown in Figure 7. This is equivalent to the distance from the image source point, IS, to the receiver point, R.
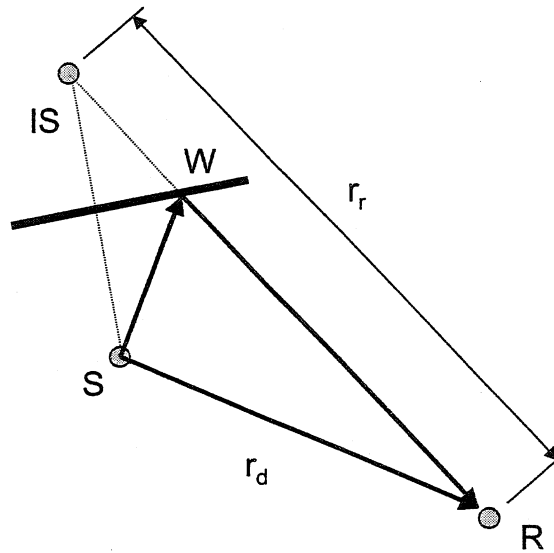
Figure 7. The Path Length of the Reflected Ray is Equivalent to the Distance Between the Receiver, R, and the Image Source, IS.

Thus, the reflected ray path length may be computed from:

$$d_r = \sqrt{\left(\Delta x_r\right)^2 + \left(\Delta y_r\right)^2 + \left(\Delta z_r\right)^2}$$

where:

$$\Delta x_r = x_{IS} - x_R$$

$$\Delta y_r = y_{IS} - y_R$$

$$\Delta z_r = z_{IS} - z_R$$

The strength of the point source, S, is a function of the directivity angle of the ray radiating from it. As illustrated in Figure 8, the directivity angles of the direct ray and the reflected ray could be different. Therefore, the source strength of the reflected ray must be computed separately from that of the direct ray.
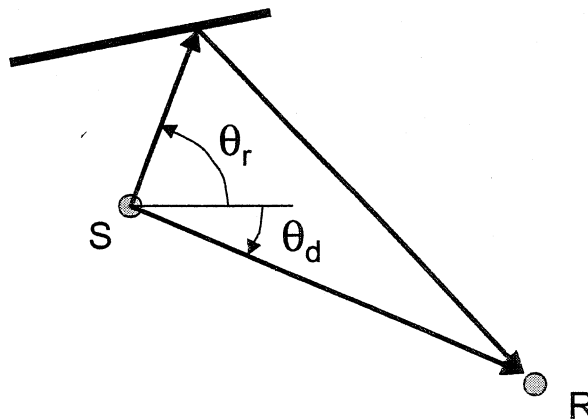
Figure 8. The Source Strength of the Reflected Ray is a Function of the Directivity Angle, Which Can Differ From That of the Direct Ray.

I-12

To obtain the source strength, the directivity angle of the reflected ray must be computed in three-dimensional space. The directivity angle is equivalent to the 3D included angle between the engine exhaust centerline and the reflected ray. Then, the reflected ray source strength is interpolated from an array of source strength vs. directivity angle.

To obtain the strength at the ground receiver, the source strength of the reflected ray must be corrected for the same propagation effects as the directly-radiated ray, i.e. atmospheric attenuation, spherical spreading, and ground reflection. These are all functions of the path length of the reflected ray, and thus will have different values than for the direct ray.

After the corrected strength of each of the reflected rays has been computed, they must be combined with the strength of the direct ray, in order to obtain the total Sound Pressure Level (SPL) at the receiver.

The combined contribution of rays from each of the reflecting panels is computed using the following equation, for every 1/3-octave frequency band, k:

$$SPL_{k,REF,TOT} = 10 \log \sum_{IPANEL=1}^{NPANEL} 10^{(SPL_{k,IPANEL}/10)}$$

The total contribution from reflected rays may then be combined with the direct ray contribution, to yield the total SPL at the receiver. For every 1/3-octave band, the total SPL is given by:

$$SPL_{k,TOT} = 10 \log \left[10^{(SPL_{k,DIR}/10)} + 10^{(SPL_{k,REF,TOT}/10)} \right]$$

Noise Prediction

The method for the preparation of the output noise results for the wing shielding model is as follows:

1. Obtain the geometry and received spectra data from the input files.
2. For each reception time value, calculate the point I and determine if the ray intersects the wing.
3. Compute the shielding attenuation using equation (10) at the desired values of frequency.
4. Apply the attenuation to the appropriate value of the received mean-square pressure.

The output values are the attenuated mean-square acoustic pressure values as a function of frequency, reception time, and observer position.

The method for the preparation of the output noise results for the wing reflection model is as follows:

1. Define the geometry for each reflecting panel (wing, flap, flap tab)
2. Create the image source for each reflecting panel, at each flyover location
3. Determine if a reflection will occur for a given panel

4. Compute the path length of the reflected ray, for a given panel
5. Obtain the source strength for the reflected ray, based on directivity
6. Compute the strength at the receiver, by applying appropriate corrections
7. Combine the contributions from the reflected ray(s) and the direct ray

REFERENCES

1. Beranek, L.L., Noise and Vibration Control, McGraw-Hill Book Company, 1971, pp. 174-180.

2. Maekawa, Z., "Noise Reduction By Screens," Applied Acoustics, Elsevier Publishing Co., Ltd., 1968, pp. 157-173.

APPENDIX II

ANOPP
WING GEOMETRIC EFFECTS MODULE
USER'S MANUAL

```
***
*          PURPOSE - WING TAKES NOISE DATA WHICH HAS BEEN PROPAGATED TO THE
*                    OBSERVER BY THE PROPAGATION (PRO) MODULE
*                    AND APPLIES CORRECTIONS FOR WING GEOMETRY EFFECTS.
*
*          AUTHOR  - DSW(L03/02/11)
*
*          INPUT
*            USER PARAMETERS
*              METHOD      OPTION FLAG FOR METHOD TO BE APPLIED
*                          (NOTE:  ORIGIN OF LOCAL COORDINATE SYSTEM FOR
*                                  WING BOUNDARY POINTS IS DIFFERENT FOR
*                                  WING SHIELDING AND WING REFLECTION.
*                                  REFER TO THEORETICAL MANUAL.)
*                          =1  WING SHIELDING AND DIFFRACTION
*                          =2  WING REFLECTION
*              IPRINT      OUTPUT PRINT OPTION CODE
*                          =0 NO PRINTED OUTPUT
*                          =1 PRINT INPUT DATA ONLY
*                          =2 PRINT OUTPUT DATA ONLY
*                          =3 PRINT BOTH INPUT AND OUTPUT DATA (DEFAULT)
*              IUNITS      =2HSI    , INPUTS ARE IN SI UNITS (DEFAULT)
*                          =7HENGLISH, INPUTS ARE IN ENGLISH UNITS
*              ROOTLE(3)   THREE ELEMENT PARAMETER WITH THE X,Y,Z
*                          COORDINATES OF THE WING ROOT LEADING EDGE (3RS)
*              ROOTTE(3)   THREE ELEMENT PARAMETER WITH THE X,Y,Z
*                          COORDINATES OF THE WING ROOT TRAILING EDGE (3RS)
*              TIPLE(3)    THREE ELEMENT PARAMETER WITH THE X,Y,Z
*                          COORDINATES OF THE WING TIP LEADING EDGE (3RS)
*              TIPTE(3)    THREE ELEMENT PARAMETER WITH THE X,Y,Z
*                          COORDINATES OF THE WING TIP TRAILING EDGE (3RS)
*
*          THE FOLLOWING PARAMETERS ARE USED FOR METHOD=2 ONLY
*
*              NPANEL      NUMBER OF WING PANELS USED IN WING REFLECTION
*                          MODEL (I)
*              FLPRLE(3)   THREE ELEMENT PARAMETER WITH THE X,Y,Z
*                          COORDINATES OF THE FLAP ROOT LEADING EDGE (3RS)
*              FLPRTE(3)   THREE ELEMENT PARAMETER WITH THE X,Y,Z
*                          COORDINATES OF THE FLAP ROOT TRAILING EDGE (3RS)
*              FLPTLE(3)   THREE ELEMENT PARAMETER WITH THE X,Y,Z
*                          COORDINATES OF THE FLAP TIP LEADING EDGE (3RS)
*              FLPTTE(3)   THREE ELEMENT PARAMETER WITH THE X,Y,Z
*                          COORDINATES OF THE FLAP TIP TRAILING EDGE (3RS)
*              TABRLE(3)   THREE ELEMENT PARAMETER WITH THE X,Y,Z
*                          COORDINATES OF THE FLAP TAB ROOT LEADING EDGE (3RS)
*              TABRTE(3)   THREE ELEMENT PARAMETER WITH THE X,Y,Z
*                          COORDINATES OF THE FLAP TAB ROOT TRAILING EDGE (3RS)
*              TABTLE(3)   THREE ELEMENT PARAMETER WITH THE X,Y,Z
*                          COORDINATES OF THE FLAP TAB TIP LEADING EDGE (3RS)
*              TABTTE(3)   THREE ELEMENT PARAMETER WITH THE X,Y,Z
*                          COORDINATES OF THE FLAP TAB TIP TRAILING EDGE (3RS)
*
```

```
*        DATA BASE UNITS AND MEMBERS
*           GEO(BODY)        GEOMETRY DATA FOR ALL OBSERVERS RELATIVE
*                            TO THE AIRCRAFT BODY COORDINATE SYSTEM
*                               SEE DESCRIPTION IN DATA BASE STRUCTURES.
*                            (SEE MODULE GEO)
*           PRO(PRES)        DIMENSIONLESS MEAN SQUARE PRESSURE AT THE
*                            OBSERVER AS A FUNCTION OF FREQUENCY AND
*                            TIME. (SEE DESCRIPTION IN DATA BASE
*                            STRUCTURES.)
*     OUTPUT
*        USER PARAMETERS
*           NERR             =.TRUE. , ERROR ENCOUNTERED, PRO
*                            TERMINATED ABNORMALLY
*                            =.FALSE., NO ERRORS ENCOUNTERED, PRO
*                            TERMINATED SUCCESSFULLY
*
*        DATA BASE UNITS AND MEMBERS
*           WING(PRES)       DIMENSIONLESS MEAN SQUARE PRESSURE AT THE
*                            OBSERVER, CORRECTED FOR WING EFFECTS
*                            AS A FUNCTION OF FREQUENCY AND
*                            TIME. (SEE DESCRIPTION IN DATA BASE
*                            STRUCTURES.)
*           SCRATCH(XXXNNN)  UNIT SCRATCH CONTAINS THE RESULT OF SUMMING
*                            NOISE TABLES
*     DATA BASE STRUCTURES
*        THE FORMAT OF GEO(BODY) IS AS FOLLOWS:
*
*           RECORD    WORD                    DESCRIPTION
*             1                    RECORD FORMAT IS I,3RS,I,RS
*                        1         OBSERVER INDEX FOR FIRST OBSERVER
*                        2         X COORDINATE OF OBSERVER
*                        3         Y COORDINATE OF OBSERVER
*                        4         Z COORDINATE OF OBSERVER
*                        5         NUMBER OF RECEPTION TIMES ASSOCIATED WITH
*                                  THIS OBSERVER (ASSUME VALUE IS N)
*                        6         OBSERVER'S HEIGHT
*
*             2                    RECORD FORMAT IS *RS
*                        1
*                        .         RECEPTION TIMES FOR CURRENT OBSERVER
*                        .         INDEX
*                        N
*
*           RECORDS 3 THROUGH  N+2  CONTAIN GEOMETRY DATA FOR EACH
*           RECEPTION TIME.  RECORD 3 CONTAINS GEOMETRY DATA FOR
*           THE FIRST RECEPTION TIME, RECORD 4 FOR THE SECOND
*           RECEPTION TIME,... RECORD N+2 FOR THE N TH RECEPTION
*           TIME.
*
*             3                    RECORD FORMAT IS *RS
*                        1         DISTANCE OF SOURCE FROM OBSERVER
*                        2         EMISSION TIME, SEC
*                        3         DIRECTIVITY ANGLE, DEG
*                        4         ELEVATION ANGLE, DEG
*                        5         AZIMUTH ANGLE, DEG
*
```

```
*              4         REPEAT OF RECORD 3 FOR SECOND RECEPTION TIME
*              .         .
*              .         .
*            N+3         RECORD FORMAT IS I,3RS,I,RS
*                    1   OBSERVER INDEX FOR SECOND OBSERVER
*                    2   X COORDINATE OF OBSERVER
*                    3   Y COORDINATE OF OBSERVER
*                    4   Z COORDINATE OF OBSERVER
*                    5   NUMBER OF RECEPTION TIMES ASSOCIATED WITH
*                        THIS OBSERVER (ASSUME VALUE IS M)
*
*            N+4         RECORD FORMAT IS *RS
*                    1
*                    .   RECEPTION TIMES FOR CURRENT OBSERVER
*                    .   INDEX
*                    M
*         RECORD   N+5 THROUGH RECORD N+M+4 CONTAIN GEOMETRY DATA
*         FOR EACH RECEPTION TIME STORED IN THE SAME MANNER AS
*         DESCRIBED ABOVE IN RECORDS 3 THROUGH N+2.
*
*
*         THE PATTERN AS SEEN IN RECORDS 1 THROUGH N+2 AND RECORDS
*         N+3 THROUGH N+M+4 CONTINUES FOR ALL OBSERVERS
**
*         THE FORMAT OF PRO(PRES) AND WING (PRES) IS AS FOLLOWS:
*
*            RECORD    WORD              DESCRIPTION
*              1         RECORD FORMAT IS I,*A8
*                    1   NUMBER OF NOISE SOURCES PROPAGATED TO
*                        THE OBSERVERS, NS.
*              2-(NS+1)  MODULE NAMES OF NOISE SOURCES PROPAGATED
*                        TO THE OBSERVERS
*
*              2         RECORD FORMAT IS 2I,2RS
*                    1   OBSERVER INDEX FOR THE FIRST OBSERVER
*                    2   NUMBER OF RECEPTION TIMES ASSOCIATED WITH
*                        THIS OBSERVER (ASSUME VALUE IS N)
*                    3   AIR DENSITY AT THE OBSERVER   (RE RHO )
*                                                             R
*                    4   SPEED OF SOUND AT THE OBSERVER (RE C )
*                                                            R
*              3         RECORD FORMAT IS *RS
*                    1
*                    .   RECEPTION TIMES FOR CURRENT OBSERVER
*                    .   INDEX
*                    N
*
*              4         RECORD FORMAT IS *RS
*                    1   DIMENSIONLESS MEAN SQUARE PRESSURE FOR
*                        THE FIRST FREQUENCY AND THE FIRST
*                        RECEPTION TIME
```

```
*            2       DIMENSIONLESS MEAN SQUARE PRESSURE FOR
*                    THE SECOND FREQUENCY AND THE FIRST
*                    RECEPTION TIME
*                .
*                .
*            NF       DIMENSIONLESS MEAN SQUARE PRESSURE FOR
*                    THE LAST FREQUENCY AND THE FIRST
*                    RECEPTION TIME
*
*      5             RECORD FORMAT IS *RS
*            1       DIMENSIONLESS MEAN SQUARE PRESSURE FOR
*            .       ALL FREQUENCIES FOR THE SECOND
*            .       RECEPTION TIME
*            NF
*
*      6             RECORD FORMAT IS *RS
*            1       DIMENSIONLESS MEAN SQUARE PRESSURE FOR
*            .       ALL FREQUENCIES FOR THE THIRD
*            .       RECEPTION TIME
*            NF
*        .
*        .
*      N+4     SAME AS RECORD 2 BUT DATA IS FOR SECOND
*             OBSERVER
*
*      N+5     SAME AS RECORD 3 BUT DATA IS FOR SECOND
*             OBSERVER
*
*     RECORDS 2 THROUGH N+3 REPEAT FOR ALL OBSERVERS.  THE
*     VALUE OF N DIFFERS FOR EACH OBSERVER.
*
*  ERRORS
*    NON-FATAL
*
*      FUNCTIONAL MODULE ERRORS
*        1. REQUIRED UNIT MEMBER NOT AVAILABLE
*        2. INSUFFICIENT LDS DYNAMIC STORAGE
*        3. UNIT MEMBER NOT OF CORRECT FORMAT
*        4. MEMBER MANAGER ERROR OCCURRED ON READING OR OPENING
*           A UNIT MEMBER
*        7. ERROR ENCOUNTERED IN BUILDING A UNIT MEMBER
**
*      FATAL - NONE
*
*  LDS REQUIREMENTS
*
*    LENGTH = 9*NFREQ + (2+NFREQ)*NTIME
*
*             WHERE NFREQ = NUMBER OF FREQUENCIES
*                   NTIME = LARGEST NUMBER OF OBSERVER TIMES
*
*  GDS REQUIREMENTS - NONE
*
```

APPENDIX III

ANOPP
WING GEOMETRIC EFFECTS MODULE
TEST CASE INPUT AND OUTPUT

```
ANOPP JECHO=.FALSE. JLOG=.FALSE. NLPPM=60 $
   STARTCS $
   SETSYS JECHO=.FALSE. $
   $
   $
   $  THIS JOB COMPUTES THE CERTIFICATION NOISE LEVELS FOR THE 1992
   $  AST TECHNOLOGY BASELINE BUSINESS JET.   THE INPUT
   $  DECK IS SET UP TO TAKE INPUT PARAMETERS THAT MATCH THE INPUT
   $  TO THE GASP PROGRAM TO MAKE IT EASY TO TRANSFER DATA FROM THE
   $  GASP INPUT DECK TO THE ANOPP JOB STREAM.   FURTHER EXPLANATION
   $  OF HOW THIS WORKS WILL BE PROVIDED AS THE DATA ARE ENTERED.
   $
   $
   $  THE FIRST STEP IS TO ENTER THE GASP NAMLIST DATA.   EVERY EFFORT
   $  IS MADE TO KEEP THE DATA IN CONSISTENT FORMAT WITH GASP.
   $
   $
   $  NAMELIST "CONT" IS ENTERED FIRST
   $
   $
   PARAM IFAA      = 1          $  CURRENTLY, ONLY OPTIONS 1-4 (APPROACH,
                                $  TAKEOFF, SIDELINE, AND LEVEL FLIGHT) ARE
                                $  VALID OPTIONS
   PARAM ISI       = 0          $  SELECT ENGLISH OR SI UNITS
   $
   $
   $  NOW, NAMELIST "ENV" IS ENTERED
   $
   $
   PARAM TAMB      = 536.67     $  AMBIENT TEMPERATURE, DEG R
   PARAM PAMB      = 2116.22    $  AMBIENT PRESSURE, PSF
   PARAM RH        = 70.        $  RELATIVE HUMIDITY, PERCENT
   PARAM DIST      = 100.       $  DISTANCE FOR STATIC PREDICTIONS, FT
   $
   $
   $  THE ANGLE ARRAY IS NOT ENTERED AS A USER PARAMETER, BUT AS A UNIT
   $  MEMBER (FILE) ALONG WITH THE DESIRED FREQUENCIES AS FOLLOWS:
   $
   $
   UPDATE NEWU=SFIELD SOURCE=* $
   -ADDR OLDM=* NEWM=FREQ  FORMAT=4H*RS$ $  1/3 OCTAVE CENTER FREQUENCIES
                                          50.   63.   80.   100.
       125.  160.  200.  250.  315.  400.  500.  630.  800.  1000.
       1250. 1600. 2000. 2500. 3150. 4000. 5000. 6300. 8000. 10000. $
   -ADDR OLDM=* NEWM=THETA FORMAT=4H*RS$ $   POLAR DIRECTIVITY ANGLES
       10. 20. 30. 40. 50. 60. 70. 80. 90. 100. 110. 120. 130. 140.
       150. 160. $
   -ADDR OLDM=* NEWM=PHI   FORMAT=4H*RS$ $ AZIMUTH DIRECTIVITY ANGLES
        0. $  SOURCES ARE AXISYMMETRIC
   END* $
   $
   $
   $  IN ADDITION, THE TEMPERATURE AND RELATIVE HUMIDITY MUST BE ENTERED
   $  AS A UNIT MEMBER (FILE) BECAUSE ANOPP ASSUMES YOU ALWAYS WANT TO
   $  USE A LAYERED ATMOSPHERE
   $
```

```
$
UPDATE NEWU=ATM SOURCE=* $
-ADDR OLDM=* NEWM=IN FORMAT=4H3RS$ $
     0.  536.67 70. $  ALTITUDE, TEMPERATURE, RELATIVE HUMIDITY
END* $                       (ONLY ONE RECORD IS NEEDED FOR UNIFORM ATMOSPHERE)
$
$
$  THE NAMELIST VARIABLES FOR "SYS" ARE ENTERED NEXT
$
$
PARAM NTYE      = 1          $  ONLY CURRENT OPTION IS TURBOJET (OR MIXED
                            $  STREAM TURBOFAN)
PARAM ICOMP     = 1,4,5      $  ONLY CURRENT OPTIONS ARE FAN, COMBUSTOR,
                            $  OR JET
PARAM ENP       = 2.         $  NUMBER OF ENGINES
PARAM ANENGI    = 0.         $  ANGLE BETWEEN ENGINE INLET AND AIRCRAFT,
                            $  DEGREES
PARAM ANENGE    = 0.         $  ANGLE BETWEEN ENGINE EXHAUST AND AIRCRAFT,
                            $  DEGREES
PARAM WGMAX     = 28700.     $  AIRCRAFT MAX. GROSS WEIGHT AT T/O, LB
PARAM AMACH     = 0.2086     $  AIRCRAFT MACH NUMBER (CAN ALSO SPECIFY
                            $  PARAMETER "VEL" IN FT/SEC)
$
$
$  THE VARIABLES LOCENG, XL, YL, ZL, IPHASE, AND IDOP ARE NOT
$  APPLICABLE TO THE CURRENT ANOPP MODEL
$
$
$  THE NAMELIST "FPRO" IS ENTERED NEXT
$
$
PARAM IDPRO     = 0          $  STRAIGHT LINE PROFILE (USER CAN ALSO
                            $  SPECIFY PROFILE USING UNIT MEMBER)
PARAM FLTANG    = -3.0       $  FLIGHT PATH ANGLE, DEGREES
PARAM ANGAFT    = 4.2        $  AIRCRAFT ANGLE OF ATTACK, DEGREES
PARAM TOROLL    = 4921.3     $  LENGTH OF TAKEOFF ROLL, FT
PARAM APDIST    = 10685.     $  INITIAL AIRCRAFT APPROACH RANGE, FT
PARAM XALT      = 1000.      $  AIRCRAFT ALTITUDE FOR LEVEL FLYOVER, FT
$
$
$  NOW THE ENGINE THERMODYNAMIC DATA ARE ENTERED.  NAMELIST "FAN" FOR
$  PREDICTING FAN NOISE IS ENTERED FIRST
$
$
PARAM IGV       = 0          $  FAN HAS NO INLET GUIDE VANES
PARAM NBF       = 30         $  NUMBER OF FAN BLADES
PARAM NVAN      = 61         $  NUMBER OF STATOR VANES
PARAM RSS       = 170.       $  ROTOR/STATOR SPACING IN
PARAM WAFAN     = 91.455     $  FAN INLET WEIGHT FLOW, LB/S
PARAM RPM       = 6982.      $  FAN PHYSICAL SPEED, RPM
PARAM FPR       = 1.239      $  FAN PRESSURE RATIO
PARAM FANDIA    = 2.455      $  FAN DIAMETER, FT
PARAM TIPMD     = 1.446      $  FAN TIP MACH NUMBER AT DESIGN POINT
PARAM FANEFF    = 0.8104     $  FAN EFFICIENCY
$
$
$  NOW NAMELIST "BURNER" FOR THE COMBUSTOR
```

```
$
$
PARAM WACOMB    = 14.310     $   COMBUSTOR WEIGHT FLOW, LB/S
PARAM T3        = 1002.9     $   COMBUSTOR INLET TEMPERATURE, DEG R
PARAM T4        = 2074.9     $   COMBUSTOR EXIT TEMPERATURE, DEG R
PARAM P3        = 13737.3    $   COMBUSTOR INLET TOTAL PRESSURE, PSF
$
$
$   AND FINALLY "JET" FOR THE MIXED STREAM JET NOISE
$
$
PARAM VJ        = 692.4      $   FULLY EXPANDED JET VELOCITY, FPS
PARAM TJ        = 754.3      $   JET TOTAL TEMPERATURE, DEG R
PARAM DJ        = 1.8507     $   JET OUTER DIAMETER, FT
PARAM GAMJ      = 1.333      $   JET RATIO OF SPECIFIC HEATS
$
$
$   THERE ARE MANY ADDITIONAL PARAMETERS AND NAMELISTS FOR GASP.  HOWEVER,
$   THEY ARE NOT RELEVANT TO ANOPP CABABILITES OR HAVE NOT BEEN IMPLEMENTED
$   IN THIS JOB STREAM.   THE REMAINING STATEMENTS ARE REQUIRED TO CONVERT
$   TO ANOPP INPUT AND TO EXECUTE THE ANOPP MODULES.   THEY NEED NEVER BE
$   CHANGED UNLESS THE JOB STREAM CAPABILITY IS MODIFIED.
$
$
$$$$$$$$$$$$$$$$$$$$$$$$$$$$$$$$$$$$$$$$$$$$$$$$$$$$$$$$$$$$$$$$$$$$$$$$$$$$
$
$   CONVERSION OF GASP USER PARAMETERS TO ANOPP INPUT
$
$$$$$$$$$$$$$$$$$$$$$$$$$$$$$$$$$$$$$$$$$$$$$$$$$$$$$$$$$$$$$$$$$$$$$$$$$$$$
$
$
$   FIRST, THE OBSERVER POSITIONS CORRESPONDING TO THE FOUR FAR 36 FLIGHT
$   PROFILES ARE DEFINED
$
$
IF ( IFAA .GT. 1 ) GOTO A1 $
$
$
$   APPROACH OBSERVER COORDINATES
$
$
UPDATE NEWU=OBSERV SOURCE=* $
-ADDR OLDM=* NEWM=COORD FORMAT=4H3RS$ $
     -7516.  0.  4.  $
END* $
GOTO A4 $
$
A1 CONTINUE $
IF ( IFAA .GT. 2 ) GOTO A2 $
$
$
$   TAKEOFF OBSERVER COORDINATES
$
$
UPDATE NEWU=OBSERV SOURCE=* $
   -ADDR OLDM=* NEWM=COORD FORMAT=4H3RS$ $
```

```
          21325.  0.  4.  $
END* $
GOTO A4 $
$
A2 CONTINUE $
IF ( IFAA .GT. 3 ) GOTO A3 $
$
$
$   SIDELINE OBSERVER COORDINATES
$
$
UPDATE NEWU=OBSERV SOURCE=* $
-ADDR OLDM=* NEWM=COORD FORMAT=4H3RS$ $
      6000. 1476.  4.   $
      7000. 1476.  4.   $
      8000. 1476.  4.   $
      9000. 1476.  4.   $
     10000. 1476.  4.   $
     11000. 1476.  4.   $
END* $
GOTO A4 $
$
A3 CONTINUE $
$
$
$   LEVEL FLYOVER OBSERVER COORDINATES
$
$
UPDATE NEWU=OBSERV SOURCE=* $
-ADDR OLDM=* NEWM=COORD FORMAT=4H3RS$ $
        0.  0.  4.  $
END* $
A4 CONTINUE $
$
$
$   NOW SOME STANDARD CONTROL PARAMETERS ARE DEFINED
$
$
PARAM     PIE     = 3.14159  $  VALUE OF PI
PARAM     AE      = 1.       $  SET REFERENCE AREA TO ONE SQUARE FOOT
PARAM     RS      = DIST     $  SET SOURCE RADIUS DISTANCE INPUT VALUE
PARAM     TA      = TAMB     $  DEFINE AMBIENT TEMPERATURE
EVALUATE RHOA     = PAMB / TAMB / 1716.22
                            $  COMPUTE AMBIENT DENSITY
EVALUATE CA       = 1116.22 * SQRT ( TAMB / 518.67 )
                            $  COMPUTE AMBIENT SPEED OF SOUND
EVALUATE NENG     = INT ( ENP )
                            $  MAKE ENGINE NUMBER INTEGER
PARAM     MA      = AMACH    $  DEFINE MACH NUMBER
PARAM     IOUT    = 1        $  PRINT DB VALUES ONLY
IF ( ISI .NE. 0 ) GOTO B1   $  SET UNITS FLAG
PARAM     IUNITS  = 7HENGLISH $
GOTO B2 $
B1 CONTINUE $
PARAM     IUNITS  = 2HSI $
B2 CONTINUE $
$
```

```
$
$   THE ENGINE PARAMETERS ARE CONVERTED TO ANOPP FORM
$
$   FIRST, THE FAN
$
$
EVALUATE AFAN      = PIE * FANDIA**2 / 4.
                             $   COMPUTE FAN REFERENCE AREA
PARAM      DIAM    = FANDIA  $   DEFINE FAN DIAMETER
PARAM      MD      = TIPMD   $   DEFINE TIP MACH NUMBER AT DESIGN POINT
EVALUATE RSS       = RSS / 100.
                             $   CONVERT ROTOR/STATOR SPACING TO RATIO
EVALUATE MDOT      = WAFAN / 32.17 / RHOA / CA
                             $   NORMALIZE WEIGHT FLOW
EVALUATE DELTAT    = ( FPR**0.2857 - 1. ) / FANEFF
                             $   COMPUTE FAN TEMPERATURE RISE
PARAM      NB      = NBF     $   SET NUMBER OF BLADES
PARAM      NV      = NVAN    $   SET NUMBER OF VANES
EVALUATE IGV       = IGV + 1 $   SET IGV FLAG
EVALUATE N         = ( RPM / 60. ) * DIAM / CA
                             $   COMPUTE NORMALIZED ROTATIONAL SPEED
PARAM      INCT    = .FALSE. $   TURN OFF COMBINATION TONES
$
$
$   NOW THE COMBUSTOR
$
$
EVALUATE A         = 0.1 * AFAN
                             $   ARBITRARY AREA DEFINED
EVALUATE MDOTC     = WACOMB / 32.17 / RHOA / CA
                             $   WEIGHT FLOW NORMALIZED (NOTE: ANOPP USES
                             $   "MDOT" FOR BOTH THE FAN AND COMBUSTOR -
                             $   COMBUSTOR MASS FLOW IS RENAMED TO AVOID
                             $   OVERWRITE
EVALUATE PI        = P3 / PAMB
                             $   NORMALIZE INPUT PRESSURE
EVALUATE TI        = T3 / TAMB
                             $   NORMALIZE INPUT TEMPERATURE
EVALUATE TCJ       = T4 / TAMB
                             $   NORMALIZE OUTPUT TEMPERATURE
PARAM      TDDELT  = 1.0     $   USE THIS PARAMETER - SET TO 1
$
$
$   JET PARAMETERS
$
$
EVALUATE AJ        = PIE * DJ ** 2 / 4.
                             $   COMPUTE JET AREA
EVALUATE TJ        = TJ / TAMB
                             $   NORMALIZE JET TOTAL TEMPERATURE
EVALUATE VJ        = VJ / CA $   NORMALIZE JET VELOCITY
EVALUATE RHOJ      = 1. / ( TJ - ( GAMJ - 1 ) / 2. * VJ**2 )
                             $   COMPUTE NORMALIZED JET DENSITY
PARAM      CIRCLE  = .TRUE.  $   REQUEST SINGLE JET FORM STONE'S METHOD
$
$
$   LOAD UNITS FROM DATA LIBRARY
```

```
$
$
LOAD /LIBRARY/ SAE PROCLIB STNTBL $
$
$
$   PREDICT SOURCE NOISE
$
$
PARAM IDBB = .FALSE. $
PARAM IDRS = .FALSE. $
EXECUTE HDNFAN HDNFAN=FANIN $
PARAM IDBB = .TRUE. $
PARAM IDRS = .TRUE. $
PARAM INRS = .FALSE. $
PARAM INDIS = .FALSE. $
PARAM INBB = .FALSE. $
EXECUTE HDNFAN HDNFAN=FANOUT $
EVALUATE RS = DIST * SQRT ( 10. ) $
EXECUTE GECOR MDOT=MDOTC $
PARAM       RS = DIST $
EXECUTE SGLJET $
$$$$$ EXECUTE STNJET A1=AJ DE1=DJ DH1=DJ V1=VJ T1=TJ RHO1=RHOJ $
$
$
$   NOW, THE ATMOSPHERIC CONDITIONS AND THE ATMOSPHERIC ABSORPTION
$   COEFFICIENTS ARE COMPUTED
$
$
EXECUTE ATM P1=PAMB $
EXECUTE ABS $
$
$
$   THE FLIGHT PATH AND GEOMETRY IS NOW DEFINED
$
$
EVALUATE VA      = AMACH * CA $   DEFINE AIRCRAFT SPEED
IF ( IFAA .GT. 1 ) GOTO C1 $
EVALUATE XA      = 0. - APDIST
                             $   DEFINE STARTING DISTANCE FOR APPROACH
EVALUATE ZA      = - APDIST * SIN ( FLTANG )
                             $   DEFINE ALTITUDE AT BEGINNING OF APPROACH
EVALUATE THW     = 0. - FLTANG
                             $   DEFINE FLIGHT PATH ANGLE
PARAM     PLG    = 4HDOWN    $   LANDING GEAR IS DOWN
PARAM     TLG    = -1.       $   LANDING GEAR CHANGED BEFORE START
PARAM     JF     = 200       $   ALLOW 200 TIME STEPS
PARAM     ZF     = 0.        $   STOP AT TOUCHDOWN
PARAM     START  = 0.        $   START EPNL CALCULATION
PARAM     STOP   = 80.       $   STOP EPNL CALCULATION
GOTO C3 $
C1 CONTINUE $
IF ( IFAA .GT. 3 ) GOTO C2 $
PARAM     XA     = TOROLL
                             $   DEFINE STARTING DISTANCE FOR TAKEOFF
PARAM     ZA     = 0.
                             $   DEFINE ALTITUDE AT BEGINNING OF TAKEOFF
PARAM     THW    = FLTANG
```

```
                                      $  DEFINE FLIGHT PATH ANGLE
PARAM     PLG     = 4HUP              $  LANDING GEAR IS UP
PARAM     TLG     = -1.              $  LANDING GEAR CHANGED BEFORE START
PARAM     JF      = 200              $  ALLOW 200 TIME STEPS
PARAM     ZF      = 32000.           $  STOP AT 32000. FT
PARAM     XF      = 32000.           $
GOTO C3 $
C2 CONTINUE $
EVALUATE XA       = XALT * SIN ( -5. )
                                      $  DEFINE STARTING DISTANCE FOR LEVEL FLIGHT
PARAM     ZA      = XALT
                                      $  DEFINE ALTITUDE FOR LEVEL FLYOVER
PARAM     THW     = 0.
                                      $  DEFINE FLIGHT PATH ANGLE
PARAM     PLG     = 4HUP              $  LANDING GEAR IS UP
PARAM     TLG     = -100.            $  LANDING GEAR CHANGED BEFORE START
PARAM     JF      = 200              $  ALLOW 200 TIME STEPS
EVALUATE XF       = 0. - XA          $  STOP AT SAME DISTANCE FROM MIC.
PARAM     START   = -9999.           $  SET ARBITRARY START TIME
C3 CONTINUE $
PARAM     ALPHA   = ANGAFT           $  SET ANGLE OF ATTACK
PARAM     ENGNAM  = 3HXXX            $  SET DEFAULT ENGINE NAME IN SFO
PARAM     ICOORD  = 1                $  REQUEST BODY AXIS
$
$
$   NOW GENERATE GEOMETRY
$
$
PARAM IPRINT = 1 $   PRINT INPUT ONLY
$
EXECUTE SFO VI=VA XI=XA ZI=ZA VF=VA $
EXECUTE GEO $
$
$
$   NOW ENTER PROPAGATION PARAMETERS
$
$
PARAM     NCOMP   = 1       $  NUMBER OF NOISE COMPONENTS TO BE PROPAGATED
PARAM     ABSORP  = .TRUE. $  INCLUDE ABSORPTION
PARAM     GROUND  = .TRUE. $  INCLUDE GROUND EFFECTS
PARAM     PROSUM  = 6HFANOUT
                          $  FOUR NOISE SOURCES
PARAM     IOSPL   = .TRUE. $  COMPUTE OVERALL SPL
PARAM     IAWT    = .TRUE. $  COMPUTE A-WEIGHTED OASPL
PARAM     IPNL    = .TRUE. $  COMPUTE PNL
PARAM     PROPRT  = 1       $  ONLY PRINT PROPAGATION MODULE INPUT
PARAM     LEVPRT  = 1       $  ONLY PRINT NOISE LEVELS MODULE INPUT
PARAM     EFFPRT  = 1       $  ONLY PRINT EFFECTIVE NOISE MODULE INPUT
$
$
$   UNIT FLI MUST BE MODIFIED TO SET ONLY ONE SOURCE TIME
$
$
UPDATE NEWU=FLIMOD OLDU=FLI ALL SOURCE=* $
    -OMIT FLIXXX $
    -ADDR OLDM=* NEWM=FLIXXX FORMAT=11H6RS,A4,2RS$ $
        0. 0.2 1. 1116. .00238 .1 4HUP   0. 0. $
```

```
END* $
$
$
$   AND CALL PROPAGATION MODULE
$
$
$
EXECUTE PRO GEOM=BODY FLI=FLIMOD $
$
PARAM ROOTLE =    4.6,-4.8,-17.1 $  WING ROOT LEADING EDGE
PARAM ROOTTE =   -8.2,-4.3,-17.1 $  WING ROOT TRAILING EDGE
PARAM TIPLE  =   -7.4,-4.3, 21.0 $  WING TIP LEADING EDGE
PARAM TIPTE  =  -12.6,-4.3, 21.0 $  WING TIP TRAILING EDGE
PARAM FLPRLE =   -7.7,-3.9,-16.9 $  FLAP ROOT LEADING EDGE
PARAM FLPRTE =  -10.1,-2.5,-16.9 $  FLAP ROOT TRAILING EDGE
PARAM FLPTLE =  -11.2,-4.0, 11.4 $  FLAP TIP LEADING EDGE
PARAM FLPTTE =  -12.5,-3.3, 11.6 $  FLAP TIP TRAILING EDGE
PARAM TABRLE =  -10.3,-2.5,-16.9 $  FLAP TAB ROOT LEADING EDGE
PARAM TABRTE =  -11.4,-0.9,-16.9 $  FLAP TAB ROOT TRAILING EDGE
PARAM TABTLE =  -12.7,-3.2, 11.6 $  FLAP TAB TIP LEADING EDGE
PARAM TABTTE =  -13.3,-2.4, 11.8 $  FLAP TAB TIP TRAILING EDGE
PARAM METHOD = 2, IPRINT = 3, NPANEL = 3 $
$
EXECUTE WING $
$
$ MEMLIST LIST=FULL WING(PRES) FORMAT=4H*RS$ $
$ PARAM MEMSUM=4HPRO  4HPRES $
$ EXECUTE LEV $
PARAM MEMSUM=4HWING 4HPRES $
EXECUTE LEV $
$
$   END OF JOB
$
$
ENDCS $
```

ANOPP INITIALIZATION PHASE

ANOPP JECHO=.FALSE. JLOG=.FALSE. NLPPM=60 $
STARTCS $

ANOPP EXECUTIVE PARAMETERS

NOGO = F   JECHO = F   JLOG = F

MAXIMUM TABLE DIRECTORY ENTRIES   = 10

MAXIMUM UNIT DIRECTORY ENTRIES   = 25

CHECKPOINT FILE (IF REQUESTED)   = CPFILE

NUMBER OF LINES PER PAGE   = 60

MAXIMUM NUMBER OF CARDS IN PRIMARY INPUT STREAM   = 10000

MAXIMUM LENGTH OF GLOBAL DYNAMIC STORAGE   = 12000

*************** DBM INFORMATIVE MESSAGE 76 *** XUPNEW - UNIT SFIELD IS BEING CREATED DYNAMICALLY. *********************
APPLICABLE DIAGNOSTIC MESSAGES PRECEDE CARD IMAGE

HEADER SECTION

UPDATE PROCESSING BEGINNING WITH THE FOLLOWING PARAMETERS
CREATE MODE   NEW DATA UNIT = SFIELD   OLD DATA UNIT = NONE
SOURCE OF UPDATE DIRECTIVES IS PRIMARY INPUT STREAM   LIST = NONE

*************** DBM INFORMATIVE MESSAGE 76 *** XUPNEW - UNIT ATM IS BEING CREATED DYNAMICALLY. *********************
APPLICABLE DIAGNOSTIC MESSAGES PRECEDE CARD IMAGE

HEADER SECTION

UPDATE PROCESSING BEGINNING WITH THE FOLLOWING PARAMETERS
CREATE MODE   NEW DATA UNIT = ATM   OLD DATA UNIT = NONE
SOURCE OF UPDATE DIRECTIVES IS PRIMARY INPUT STREAM   LIST = NONE

*************** DBM INFORMATIVE MESSAGE 76 *** XUPNEW - UNIT OBSERV IS BEING CREATED DYNAMICALLY. *********************

III-10

APPLICABLE DIAGNOSTIC MESSAGES PRECEDE CARD IMAGE

UPDATE PROCESSING BEGINNING WITH THE FOLLOWING PARAMETERS
CREATE   MODE   NEW DATA UNIT = OBSERV   OLD DATA UNIT = NONE
SOURCE OF UPDATE DIRECTIVES IS PRIMARY INPUT STREAM   LIST = NONE

HEADER SECTION

1   1/21/**   ANOPP LEVEL 03/02/11   PAGE 2

FAN NOISE MODULE

INPUT PARAMETERS

```
AE     = .10000000E+01     RS     = .10000000E+03     AFAN   = .47336104E+01     DIAM   = .24550000E+01
MD     = .14460000E+01     RSS    = .17000000E+01     MDOT   = .10897276E+01     MA     = .20860000E+00
N      = .25160670E+00     DELTAT = .77912184E-01     CA     = .11354235E+04     RHOA   = .22976323E-02
NBANDS = 0                 METHOD = 1                 NENG   = 2                 NB     = 30
NV     = 61
IGV    = 1                 DIS    = 1                 IOUT   = 1                 IPRINT = 3
INRS   = T                 INCT   = F                 INDIS  = F                 IDBB   = F
IDRS   = F                 INBB   = T                 SCRNNN = 1                 SCRXXX = XXX
IUNITS = ENGLISH           STIME  = .00000000E+00
```

UNIT MEMBERS

```
SFIELD (FREQ    ) IS ALTERNATE NAME OF SFIELD (FREQ   )
FANIN  (XXX001  ) IS ALTERNATE NAME OF HDNFAN (XXX001 )
SFIELD (PHI     ) IS ALTERNATE NAME OF SFIELD (PHI    )
SFIELD (THETA   ) IS ALTERNATE NAME OF SFIELD (THETA  )
```

1   1/21/**   ANOPP LEVEL 03/02/11   PAGE 4

FAN NOISE MODULE

INPUT PARAMETERS

```
AE     = .10000000E+01     RS     = .10000000E+03     AFAN   = .47336104E+01     DIAM   = .24550000E+01
MD     = .14460000E+01     RSS    = .17000000E+01     MDOT   = .10897276E+01     MA     = .20860000E+00
N      = .25160670E+00     DELTAT = .77912184E-01     CA     = .11354235E+04     RHOA   = .22976323E-02
NBANDS = 0                 METHOD = 1                 NENG   = 2                 NB     = 30
NV     = 61
IGV    = 1                 DIS    = 1                 IOUT   = 1                 IPRINT = 3
INRS   = F                 INCT   = F                 INDIS  = F                 IDBB   = T
```

III-11

```
IDRS   = T              INBB  = F                  SCRNNN = 1            SCRXXX = XXX
IUNITS = ENGLISH        STIME = .00000000E+00

                                    UNIT MEMBERS

        SFIELD  (FREQ    ) IS ALTERNATE NAME OF SFIELD  (FREQ    )
        FANOUT  (XXX001  ) IS ALTERNATE NAME OF HDNFAN  (XXX001  )
        SFIELD  (PHI     ) IS ALTERNATE NAME OF SFIELD  (PHI     )
        SFIELD  (THETA   ) IS ALTERNATE NAME OF SFIELD  (THETA   )

 1      1/21/**          ANOPP LEVEL 03/02/11                          PAGE   6


                              COMBUSTION NOISE MODULE

        MODULE GECOR USES THE FOLLOWING INPUT PARAMETERS AND UNIT MEMBERS

AE     = 1.0000         A      = .47336         RS    = 316.23      STIME  = .00000E+00     MDOT   = .17051
MA     = .20860         TI     = 1.8687         TCJ   = 3.8662      CA     = 1135.4         RHOA   = .22976E-02
PI     = 6.4914         TDDELT = 1.0000         IOUT  = 1           NENG   = 2              IPRINT = 3
SCRNNN = 1              SCRXXX = XXX            ICA078 = F           METHOD = 1              IUNITS = ENG

        SFIELD  (FREQ    ) IS ALTERNATE NAME OF SFIELD  (FREQ    )
        GECOR   (XXX001  ) IS ALTERNATE NAME OF GECOR   (XXX001  )
        SFIELD  (PHI     ) IS ALTERNATE NAME OF SFIELD  (PHI     )
        SFIELD  (THETA   ) IS ALTERNATE NAME OF SFIELD  (THETA   )

 1      1/21/**          ANOPP LEVEL 03/02/11                          PAGE   8


                   SINGLE STREAM CIRCULAR JET NOISE MODULE

        MODULE SGLJET USES THE FOLLOWING INPUT PARAMETERS AND UNIT MEMBERS

AJ     = 2.6901         RHOJ   = .74427         TJ    = 1.4055      VJ     = .60982         RS   = 100.00
RHOA   = .22976E-02     IUNITS = ENGLISH        CA    = 1135.4      MA     = .20860         AE   = 1.0000
DELTA  = .00000E+00     NENG   = 2              SCRXXX = XXX        SCRNNN = 1              IOUT = 1
IPRINT = 3              STIME  = .00000E+00     SHOCK = F           METHOD = 1

        SFIELD  (FREQ    ) IS ALTERNATE NAME OF SFIELD  (FREQ    )
        SFIELD  (PHI     ) IS ALTERNATE NAME OF SFIELD  (PHI     )
        SFIELD  (THETA   ) IS ALTERNATE NAME OF SFIELD  (THETA   )
        SAE     (MTH     ) IS ALTERNATE NAME OF SAE     (MTH     )
```

```
                      SAE    (OM     ) IS ALTERNATE NAME OF SAE    (OM     )
                      SAE    (PDF    ) IS ALTERNATE NAME OF SAE    (PDF    )
                      SAE    (NDF    ) IS ALTERNATE NAME OF SAE    (NDF    )
                      SAE    (SJC    ) IS ALTERNATE NAME OF SAE    (SJC    )
                      SAE    (SCF    ) IS ALTERNATE NAME OF SAE    (SCF    )
                      SGLJET (XXX001 ) IS ALTERNATE NAME OF SGLJET (XXX001 )
```

1   1/21/**   ANOPP LEVEL 03/02/11   PAGE   10

ATMOSPHERIC MODEL FOR AIRCRAFT NOISE PREDICTION

PARAMETERS RETRIEVED FROM USER PARAMETER TABLE

```
DELH  =   328.08      H1  =       .00      IUNITS = ENGLISH
NHO   =   1           P1  =   2116.22      IPRINT = 3
```

*************** DBM INFORMATIVE MESSAGE   76 *** MMOPWD - UNIT SCRATCH   IS BEING CREATED DYNAMICALLY.*********************

ATMOSPHERIC PROPERTIES OUTPUT
TABLE TMOD   ON UNIT ATM   CONVERTED TO DIMENSIONAL UNITS
ALTITUDE IS RELATIVE TO GROUND LEVEL OF   0.   FEET

ALTITUDE	PRESSURE	DENSITY	TEMPERATURE	SOUND SPEED	AVERAGE SOUND SPEED	HUMIDITY	VISCOSITY	THERMAL CONDUCTIVITY	CHARACTERISTIC IMPEDANCE
FEET	LB/FT**2	SLUG/FT**3	DEG R	FT/S	FT/S	% MOLE FRACTION	SLUG/(FT S)	BTU(DEG R M S)	SLUG(S FT**2)
0.	.211622E+04	.229718E-02	.536670E+03	.113566E+04	.113566E+04	.218960E+01	.383694E-06	.419313E-05	.260881E+01

1   1/21/**   ANOPP LEVEL 03/02/11   PAGE   11

ATMOSPHERIC ABSORPTION MODULE

INPUT VALUES READ FROM USER PARAMETER TABLE
```
                ABSINT = 5            IPRINT = 3                    ISAE = 2

                IUNITS = ENGLISH

                24 FREQUENCY VALUES READ FROM UNIT MEMBER SFIELD  (FREQ    )
      50.00       63.00       80.00      100.00      125.00      160.00      200.00      250.00
     315.00      400.00      500.00      630.00      800.00     1000.00     1250.00     1600.00
    2000.00     2500.00     3150.00     4000.00     5000.00     6300.00     8000.00    10000.00
```

*** ATM   (AAC   ) *** TMEDI1 - LINEAR EXTRAP ATTEMPTED ON INDEPENDENT VARIABLE 1 WILL RESULT IN CLOSEST VALUE METHOD

ATMOSPHERIC ABSORPTION COEFFICIENT IN DECIBELS/WAVELENGTH
ANSI STANDARD METHOD
TABLE AAC ON UNIT ATM CONVERTED.

ALTITUDE FEET	FREQUENCIES									
	50.00	63.00	80.00	100.00	125.00	160.00	200.00	250.00	315.00	400.00
0.	.11775E-04	.18654E-04	.29971E-04	.46581E-04	.72187E-04	.11658E-03	.17848E-03	.27037E-03	.40899E-03	.61212E-03

ALTITUDE FEET	FREQUENCIES									
	500.00	630.00	800.00	1000.00	1250.00	1600.00	2000.00	2500.00	3150.00	4000.00
0.	.86553E-03	.11928E-02	.15877E-02	.19912E-02	.24182E-02	.29324E-02	.34813E-02	.41930E-02	.52386E-02	.68795E-02

ALTITUDE FEET	FREQUENCIES			
	5000.00	6300.00	8000.00	10000.00
0.	.92515E-02	.13077E-01	.19353E-01	.28570E-01

SFO   USES DEFAULT VALUES FOR FOLLOWING PARAMETERS

NAME	TYPE	CODE	ELEMENT	VALUE
DELTA	RS	2	(1)	.00000000000000E+00
DELMACH	RS	2	(1)	.50000000000000E-01
TF	RS	2	(1)	.10000000000000E+03
TSTEP	RS	2	(1)	.50000000000000E+00
THROT	RS	2	(1)	.10000000000000E+01
XF	RS	2	(1)	.00000000000000E+00
YF	RS	2	(1)	.00000000000000E+00
YI	RS	2	(1)	.00000000000000E+00
ZGR	RS	2	(1)	.00000000000000E+00

*************** FUNCTIONAL MODULE ERROR   10 OCCURRED IN MODULE SFO   ***

USER PARAMETER TLG   HAS VALUE   -.10000000E+01 THAT IS OUT OF RANGE - DEFAULT VALUE   .00000000E+00 WILL BE USED.

SFO   USES DEFAULT VALUES FOR FOLLOWING PARAMETERS

NAME	TYPE	CODE	ELEMENT	VALUE
ZOPT	I	1	(1)	1
J	I	1	(1)	1
APPEND	L	6	(1)	F

STEADY FLYOVER MODULE

MODULE SFO USES THE FOLLOWING INPUT PARAMETERS AND UNIT MEMBERS

ALPHA	=	4.20	TLG	=	.00	PLG	=	DOWN	
DELTA	=	.00	ZGR	=	.00	ENGNAM	=	XXX	
THW	=	3.00	TSTEP	=	.50	IUNITS	=	ENGLISH	
THROT	=	1.00	IPRINT	=	1	APPEND	=	F	
DELMACH=		.05	ZOPT	=	1	J	=	1	

TI	=	1.87	TF	=	100.00
VI	=	236.85	VF	=	236.85
XI	=	-10685.00	XF	=	.00
YI	=	.00	YF	=	.00
ZI	=	559.21	ZF	=	.00

ATM	(TMOD) IS ALTERNATE NAME OF ATM	(TMOD)
FLI	(PATH) IS ALTERNATE NAME OF FLI	(PATH)
FLI	(FLIXXX) IS ALTERNATE NAME OF FLI	(FLIXXX)

*************** DBM INFORMATIVE MESSAGE   76 *** MMOPWD - UNIT FLI   IS BEING CREATED DYNAMICALLY. ***********************

************************************ STEADY FLYOVER MODULE ***

NORMAL TERMINATION - FINAL CONDITIONS REACHED

GEO   USES DEFAULT VALUES FOR FOLLOWING PARAMETERS

NAME	TYPE	CODE	ELEMENT	VALUE
DIRECT	L	6	(1)	F
GEOERR	L	6	(1)	F

GEO   USES DEFAULT VALUES FOR FOLLOWING PARAMETERS

NAME	TYPE	CODE	ELEMENT	VALUE
AW	RS	2	(1)	.32808000000000000E+01
CTK	RS	2	(1)	.10000000000000000E+01
DELDB	RS	2	(1)	.20000000000000000E+02
MASSAC	RS	2	(1)	.28559900000000000E+02
DTIME	RS	2	(1)	.50000000000000000E+00
DELTH	RS	2	(1)	.10000000000000000E+02

SOURCE TO OBSERVER GEOMETRY

III-15

GEO USER PARAMETER INPUT

AW   = 3.2808   FT**2   CTK   = 1.0000   SEC   DELB = 20.000   SEC   DB   MASSAC = 28.560   SLUGS
START = .00000E+00 SEC   STOP = 80.000   SEC   DTIME = .50000   SEC   DELTH = 10.000   DEGREES
ICOORD = 1   IPRINT = 1   IUNITS = ENGLISH   DIRECT = F

*************** DBM INFORMATIVE MESSAGE   76 *** MMOPWS - UNIT GEO   IS BEING CREATED DYNAMICALLY.********************
1   ANOPP LEVEL 03/02/11   PAGE   15
                               1/21/**

                               SOURCE TO OBSERVER GEOMETRY

                       SOURCE COORDINATE SYSTEM DESCRIPTION

                                                                        EULER ANGLES
                       ORIGIN OFFSET   (DEGREES)
                       (FEET)
INDEX NAME   X   Y   Z   PSI   THETA   PHI
                       .00   .00   .00   .00   .00   .00
  1   BODY

                               OBSERVER COORDINATES

                       NO.   X   Y   Z
                        1   -7516.00   .00   4.00

*************** DBM INFORMATIVE MESSAGE   76 *** XUPNEW - UNIT FLIMOD   IS BEING CREATED DYNAMICALLY.********************
APPLICABLE DIAGNOSTIC MESSAGES PRECEDE CARD IMAGE

                               HEADER SECTION

UPDATE PROCESSING BEGINNING WITH THE FOLLOWING PARAMETERS
REVISE MODE   NEW DATA UNIT = FLIMOD   OLD DATA UNIT = FLI
SOURCE OF UPDATE DIRECTIVES IS PRIMARY INPUT STREAM   LIST = NONE

PRO   USES DEFAULT VALUES FOR FOLLOWING PARAMETERS

NAME   TYPE   CODE   ELEMENT   VALUE

NBAND   I   1   (1)   5
STATIC   L   6   (1)   F
SIDELN   L   6   (1)   T

PRO   USES DEFAULT VALUES FOR FOLLOWING PARAMETERS

III-16

```
        NAME     TYPE   CODE  ELEMENT      VALUE
        ----     ----   ----  -------      -----
        COH      RS      2    (  1)        .10000000000000E-01
        SIGMA    RS      2    (  1)        .48508000000000E+03
        RO       RS      2    (  1)        .65616800000000E+01
        ZS       RS      2    (  1)        .32808400000000E+01
        ZO       RS      2    (  1)        .32808400000000E+01
        PROTIME  A      -3    (  1)        XXX
        SURFACE  A      -4    (  1)        SOFT

1                              1/21/**        ANOPP LEVEL 03/02/11                    PAGE   16


                                         PROPAGATION MODULE


        MODULE PRO USES THE FOLLOWING INPUT PARAMETERS AND UNIT MEMBERS


SIGMA   = 485.08         RS       =  100.00      RO      =  6.5617       ZS      =  3.2808
COH     = .10000E-01     IPRINT   =  1           IOUT    =  1            NBAND   =  5          PROTIME = XXX
SURFACE = SOFT           GROUND   =  T           ABSORP  =  T            STATION =  F          SIDELINE= T
IUNITS  = ENGLISH


********** FOR MOVING NOISE SOURCE, PARAMETERS RS, RO, ZS, ZO, AND SIDELINE ARE IGNORED **********


                    ATM     (AAC      )   IS ALTERNATE NAME OF ATM     (AAC      )
                    ATM     (TMOD     )   IS ALTERNATE NAME OF ATM     (TMOD     )
                    GEO     (BODY     )   IS ALTERNATE NAME OF GEO     (GEOM     )
                    FLIMOD  (FLIXXX   )   IS ALTERNATE NAME OF FLI     (FLIXXX   )
                    PRO     (PRES     )   IS ALTERNATE NAME OF PRO     (PRES     )
                    SCRATCH (XXXNNN   )   IS ALTERNATE NAME OF SCRATCH (XXXNNN   )

THE FOLLOWING NOISE UNITS WILL BE USED
    FANOUT


****************** DBM INFORMATIVE MESSAGE    76 *** MMOPWD - UNIT PRO       IS BEING CREATED DYNAMICALLY. ******************
1                              1/21/**        ANOPP LEVEL 03/02/11                    PAGE   17


                                      WING GEOMETRIC EFFECTS MODULE


        MODULE WING USES THE FOLLOWING INPUT PARAMETERS AND UNIT MEMBERS


IPRINT  =  3            METHOD  =  2            NPANEL  =  3            IUNITS  = ENGLISH


ROOTLE  =    4.60000      -4.80000    -17.10000
ROOTTE  =   -8.20000      -4.30000    -17.10000
TIPLE   =   -7.40000      -4.30000     21.00000
TIPTE   =  -12.60000      -4.30000     21.00000
FLPRLE  =   -7.70000      -3.90000    -16.90000
```

```
FLPRTE  = -10.10000    -2.50000   -16.90000
FLPTLE  = -11.20000    -4.00000    11.40000
FLPTTE  = -12.50000    -3.30000    11.60000
TABRLE  = -10.30000    -2.50000   -16.90000
TABRTE  = -11.40000     -.90000   -16.90000
TABTLE  = -12.70000    -3.20000    11.60000
TABTTE  = -13.30000    -2.40000    11.80000
```

```
              GEO     (BODY  )   IS ALTERNATE NAME OF GEO    (BODY  )
              PRO     (PRES  )   IS ALTERNATE NAME OF PRO    (PRES  )
              SFIELD  (FREQ  )   IS ALTERNATE NAME OF SFIELD (FREQ  )
              WING    (PRES  )   IS ALTERNATE NAME OF WING   (PRES  )
```

```
****************** DBM INFORMATIVE MESSAGE   76 *** MMOPWD - UNIT WING   IS BEING CREATED DYNAMICALLY. ******************
 1                       1/21/**                  ANOPP LEVEL 03/02/11                              PAGE    18

                                            WING GEOMETRIC EFFECTS MODULE

            OBSERVER   1 LOCATED AT X=  -7516.0000     Y=   .00000000E+00     Z=   4.0000000
```

```
FREQUENCIES   .50000E+02  .63000E+02  .80000E+02  .10000E+03  .12500E+03  .16000E+03  .20000E+03  .25000E+03
              .31500E+03  .40000E+03  .50000E+03  .63000E+03  .80000E+03  .10000E+04  .12500E+04  .16000E+04
              .20000E+04  .25000E+04  .31500E+04  .40000E+04  .50000E+04  .63000E+04  .80000E+04  .10000E+05
```

```
                                       WING GEOMETRY SPL CORRECTION FOR EACH FREQUENCY
OBS. TIME
  5.20 SPL     .00       .00       .00       .00       .00       .00       .00
       SPL     .00       .00       .00       .00       .00       .00       .00
       SPL     .00       .00       .00       .00       .00       .00       .00
```

```
                                       WING GEOMETRY SPL CORRECTION FOR EACH FREQUENCY
OBS. TIME
  5.70 SPL     .00       .00       .00       .00       .00       .00       .00
       SPL     .00       .00       .00       .00       .00       .00       .00
       SPL     .00       .00       .00       .00       .00       .00       .00
```

```
                                       WING GEOMETRY SPL CORRECTION FOR EACH FREQUENCY
OBS. TIME
  6.20 SPL     .00       .00       .00       .00       .00       .00       .00
       SPL     .00       .00       .00       .00       .00       .00       .00
       SPL     .00       .00       .00       .00       .00       .00       .00
```

```
                                       WING GEOMETRY SPL CORRECTION FOR EACH FREQUENCY
OBS. TIME
  6.70 SPL     .00       .00       .00       .00       .00       .00       .00
       SPL     .00       .00       .00       .00       .00       .00       .00
       SPL     .00       .00       .00       .00       .00       .00       .00
```

```
                                       WING GEOMETRY SPL CORRECTION FOR EACH FREQUENCY
OBS. TIME
```

III-18

WING GEOMETRIC EFFECTS MODULE

WING GEOMETRY SPL CORRECTION FOR EACH FREQUENCY

```
           7.20 SPL      .00    .00    .00    .00    .00    .00    .00    .00
                SPL      .00    .00    .00    .00    .00    .00    .00    .00
                SPL      .00    .00    .00    .00    .00    .00    .00    .00

OBS. TIME  7.70 SPL      .00    .00    .00    .00    .00    .00    .00    .00
                SPL      .00    .00    .00    .00    .00    .00    .00    .00
                SPL      .00    .00    .00    .00    .00    .00    .00    .00

OBS. TIME  8.20 SPL      .00    .00    .00    .00    .00    .00    .00    .00
                SPL      .00    .00    .00    .00    .00    .00    .00    .00
                SPL      .00    .00    .00    .00    .00    .00    .00    .00

OBS. TIME  8.70 SPL      .00    .00    .00    .00    .00    .00    .00    .00
                SPL      .00    .00    .00    .00    .00    .00    .00    .00
                SPL      .00    .00    .00    .00    .00    .00    .00    .00
```

ANOPP LEVEL 03/02/11   PAGE 19

1/21/**

1

WING GEOMETRIC EFFECTS MODULE

WING GEOMETRY SPL CORRECTION FOR EACH FREQUENCY

```
OBS. TIME  9.20 SPL      .00    .00    .00    .00    .00    .00    .00    .00
                SPL      .00    .00    .00    .00    .00    .00    .00    .00
                SPL      .00    .00    .00    .00    .00    .00    .00    .00

OBS. TIME  9.70 SPL      .00    .00    .00    .00    .00    .00    .00    .00
                SPL      .00    .00    .00    .00    .00    .00    .00    .00
                SPL      .00    .00    .00    .00    .00    .00    .00    .00

OBS. TIME 10.20 SPL      .00    .00    .00    .00    .00    .00    .00    .00
                SPL      .00    .00    .00    .00    .00    .00    .00    .00
                SPL      .00    .00    .00    .00    .00    .00    .00    .00

OBS. TIME 10.70 SPL      .00    .00    .00    .00    .00    .00    .00    .00
                SPL      .00    .00    .00    .00    .00    .00    .00    .00
                SPL      .00    .00    .00    .00    .00    .00    .00    .00

OBS. TIME 11.20 SPL      .00    .00    .00    .00    .00    .00    .00    .00
                SPL      .00    .00    .00    .00    .00    .00    .00    .00
```

```
                                              SPL       .00       .00       .00       .00       .00       .00       .00

OBS. TIME  11.70  SPL       .00       .00       .00       .00       .00       .00       .00       .00
                  SPL       .00       .00       .00       .00       .00       .00       .00       .00
                  SPL       .00       .00       .00       .00       .00       .00       .00       .00
                        WING GEOMETRY SPL CORRECTION FOR EACH FREQUENCY

OBS. TIME  12.20  SPL       .00       .00       .00       .00       .00       .00       .00       .00
                  SPL       .00       .00       .00       .00       .00       .00       .00       .00
                  SPL       .00       .00       .00       .00       .00       .00       .00       .00
                        WING GEOMETRY SPL CORRECTION FOR EACH FREQUENCY

OBS. TIME  12.70  SPL       .00       .00       .00       .00       .00       .00       .00       .00
                  SPL       .00       .00       .00       .00       .00       .00       .00       .00
                  SPL       .00       .00       .00       .00       .00       .00       .00       .00
                        WING GEOMETRY SPL CORRECTION FOR EACH FREQUENCY

OBS. TIME  13.20  SPL       .00       .00       .00       .00       .00       .00       .00       .00
                  SPL       .00       .00       .00       .00       .00       .00       .00       .00
                  SPL       .00       .00       .00       .00       .00       .00       .00       .00
```

ANOPP LEVEL 03/02/11   PAGE   20

1/21/**   1

WING GEOMETRIC EFFECTS MODULE

```
OBS. TIME  13.70  SPL       .00       .00       .00       .00       .00       .00
                  SPL       .00       .00       .00       .00       .00       .00
                  SPL       .00       .00       .00       .00       .00       .00
                        WING GEOMETRY SPL CORRECTION FOR EACH FREQUENCY

OBS. TIME  14.20  SPL       .00       .00       .00       .00       .00       .00
                  SPL       .00       .00       .00       .00       .00       .00
                  SPL       .00       .00       .00       .00       .00       .00
                        WING GEOMETRY SPL CORRECTION FOR EACH FREQUENCY

OBS. TIME  14.45  SPL       .00       .00       .00       .00       .00       .00
                  SPL       .00       .00       .00       .00       .00       .00
                  SPL       .00       .00       .00       .00       .00       .00
                        WING GEOMETRY SPL CORRECTION FOR EACH FREQUENCY

OBS. TIME  14.70  SPL       .00     29.57     38.11       .00      5.09      8.93     12.14     11.95     16.76
                  SPL     42.55     56.16     56.85     41.62     45.05     51.43     49.29     53.93
                  SPL     59.84     56.69     53.37     53.89     46.92     35.09
                        WING GEOMETRY SPL CORRECTION FOR EACH FREQUENCY
```

III-20

OBS. TIME 14.95
WING GEOMETRY SPL CORRECTION FOR EACH FREQUENCY
SPL   .00   .00   .00   .00   .00   .00   .00   .00
SPL   .00   .00   .00   .00   .00   .00   .00   .00
SPL   .00   .00   .00   .00   .00   .00   .00   .00

OBS. TIME 15.20
WING GEOMETRY SPL CORRECTION FOR EACH FREQUENCY
SPL   .00   .00   .00   .00   .00   .00   .00   .00
SPL   .00   .00   .00   .00   .00   .00   .00   .00
SPL   .00   .00   .00   .00   .00   .00   .00   .00

OBS. TIME 15.45
WING GEOMETRY SPL CORRECTION FOR EACH FREQUENCY
SPL   .00   .00   .00   .00   .00   .00   .00   .00
SPL   .00   .00   .00   .00   .00   .00   .00   .00
SPL   .00   .00   .00   .00   .00   .00   .00   .00

OBS. TIME 15.70
WING GEOMETRY SPL CORRECTION FOR EACH FREQUENCY
SPL   .00   .00   .00   .00   .00   .00   .00   .00
SPL   .00   .00   .00   .00   .00   .00   .00   .00
SPL   .00   .00   .00   .00   .00   .00   .00   .00

OBS. TIME 15.95
WING GEOMETRY SPL CORRECTION FOR EACH FREQUENCY
SPL   .00   .00   .00   11.44   20.14   25.63   20.70   37.70
SPL   40.92 48.87 49.22 53.79   59.69   61.50   64.75   67.55
SPL   69.48 71.01 75.10 73.09   72.76   76.14   70.74   69.10

ANOPP LEVEL 03/02/11   PAGE 21

1/21/**

1

WING GEOMETRIC EFFECTS MODULE

OBS. TIME 16.20
WING GEOMETRY SPL CORRECTION FOR EACH FREQUENCY
SPL   .00   .00   .00   10.85   20.79   27.48   24.64   36.80
SPL   42.68 47.85 47.58 53.41   58.32   62.88   65.16   67.91
SPL   69.92 71.22 75.43 73.35   73.02   76.45   70.86   69.14

OBS. TIME 16.45
WING GEOMETRY SPL CORRECTION FOR EACH FREQUENCY
SPL   .00   .00   .00   10.03   20.76   28.51   28.96   34.40
SPL   44.60 44.95 50.63 56.46   59.13   62.17   65.40   67.72
SPL   70.01 71.18 75.36 73.24   72.84   76.14   70.44   68.46

OBS. TIME 16.70
WING GEOMETRY SPL CORRECTION FOR EACH FREQUENCY
SPL   .00   .00   .00   8.30   19.99   28.84   31.74   29.41
SPL   44.94 41.81 53.33 56.91   60.24   62.66   64.90   67.78
SPL   69.49 70.80 74.82 72.79   72.29   75.39   69.62   67.29

OBS. TIME 16.95
WING GEOMETRY SPL CORRECTION FOR EACH FREQUENCY
SPL   .00   .00   .00   5.39   18.04   28.00   32.71   27.73

III-21

WING GEOMETRY SPL CORRECTION FOR EACH FREQUENCY

```
     SPL     66.91  64.46  61.47  57.25  53.05  52.47  45.11  43.08
     SPL     65.33  68.04  73.93  71.00  71.63  73.56  69.70  68.26

OBS. TIME 17.20
     WING GEOMETRY SPL CORRECTION FOR EACH FREQUENCY
     SPL     31.72  32.21  26.35  15.59   3.03    .00    .00    .00
     SPL     65.61  63.29  60.34  56.41  52.48  49.65  46.11  39.98
     SPL     63.17  66.22  72.19  69.35  70.06  72.06  68.19  67.02

OBS. TIME 17.70
     WING GEOMETRY SPL CORRECTION FOR EACH FREQUENCY
     SPL     33.48  29.39  21.22   8.07    .00    .00    .00    .00
     SPL     62.25  59.02  57.29  53.96  50.96  45.06  43.62  31.24
     SPL     57.39  61.95  67.62  65.02  65.90  68.14  64.56  63.50

OBS. TIME 18.20
     WING GEOMETRY SPL CORRECTION FOR EACH FREQUENCY
     SPL     31.25  24.29  13.75    .00    .00    .00    .00    .00
     SPL     58.26  54.46  52.44  50.70  43.94  44.46  33.84  33.56
     SPL     50.89  57.85  62.55  60.23  61.35  64.03  60.13  58.72

OBS. TIME 18.70
     WING GEOMETRY SPL CORRECTION FOR EACH FREQUENCY
     SPL     27.36  17.93   4.31    .00    .00    .00    .00    .00
     SPL     53.62  52.66  48.61  44.21  45.19  36.89  32.42  33.22
     SPL     44.60  53.12  58.00  55.98  57.64  60.14  56.15  55.37

OBS. TIME 19.20
     WING GEOMETRY SPL CORRECTION FOR EACH FREQUENCY
     SPL       .00    .00    .00    .00    .00    .00    .00    .00
     SPL       .00    .00    .00    .00    .00    .00    .00    .00
     SPL       .00    .00    .00    .00    .00    .00    .00    .00
```

1   ANOPP LEVEL 03/02/11   1/21/**

WING GEOMETRIC EFFECTS MODULE   PAGE 22

```
OBS. TIME 19.70
     WING GEOMETRY SPL CORRECTION FOR EACH FREQUENCY
     SPL       .00    .00    .00    .00    .00    .00
     SPL       .00    .00    .00    .00    .00    .00
     SPL       .00    .00    .00    .00    .00    .00

OBS. TIME 20.20
     WING GEOMETRY SPL CORRECTION FOR EACH FREQUENCY
     SPL       .00    .00    .00    .00    .00    .00
     SPL       .00    .00    .00    .00    .00    .00
     SPL       .00    .00    .00    .00    .00    .00

OBS. TIME 20.70
     WING GEOMETRY SPL CORRECTION FOR EACH FREQUENCY
     SPL       .00    .00    .00    .00    .00    .00
     SPL       .00    .00    .00    .00    .00    .00
```

WING GEOMETRY SPL CORRECTION FOR EACH FREQUENCY

SPL   .00   .00   .00   .00   .00   .00   .00

OBS. TIME
21.20 SPL   .00   .00   .00   .00   .00   .00   .00
      SPL   .00   .00   .00   .00   .00   .00   .00
      SPL   .00   .00   .00   .00   .00   .00   .00

WING GEOMETRY SPL CORRECTION FOR EACH FREQUENCY

OBS. TIME
21.70 SPL   .00   .00   .00   .00   .00   .00   .00
      SPL   .00   .00   .00   .00   .00   .00   .00
      SPL   .00   .00   .00   .00   .00   .00   .00

WING GEOMETRY SPL CORRECTION FOR EACH FREQUENCY

OBS. TIME
22.20 SPL   .00   .00   .00   .00   .00   .00   .00
      SPL   .00   .00   .00   .00   .00   .00   .00
      SPL   .00   .00   .00   .00   .00   .00   .00

WING GEOMETRY SPL CORRECTION FOR EACH FREQUENCY

OBS. TIME
22.70 SPL   .00   .00   .00   .00   .00   .00   .00
      SPL   .00   .00   .00   .00   .00   .00   .00
      SPL   .00   .00   .00   .00   .00   .00   .00

WING GEOMETRY SPL CORRECTION FOR EACH FREQUENCY

OBS. TIME
23.20 SPL   .00   .00   .00   .00   .00   .00   .00
      SPL   .00   .00   .00   .00   .00   .00   .00
      SPL   .00   .00   .00   .00   .00   .00   .00

WING GEOMETRY SPL CORRECTION FOR EACH FREQUENCY

OBS. TIME
23.70 SPL   .00   .00   .00   .00   .00   .00   .00
      SPL   .00   .00   .00   .00   .00   .00   .00
      SPL   .00   .00   .00   .00   .00   .00   .00

1   ANOPP LEVEL 03/02/11   1/21/**   PAGE   23

WING GEOMETRIC EFFECTS MODULE

WING GEOMETRY SPL CORRECTION FOR EACH FREQUENCY

OBS. TIME
24.20 SPL   .00   .00   .00   .00   .00   .00   .00
      SPL   .00   .00   .00   .00   .00   .00   .00
      SPL   .00   .00   .00   .00   .00   .00   .00

WING GEOMETRY SPL CORRECTION FOR EACH FREQUENCY

OBS. TIME
24.70 SPL   .00   .00   .00   .00   .00   .00   .00
      SPL   .00   .00   .00   .00   .00   .00   .00
      SPL   .00   .00   .00   .00   .00   .00   .00

III-23

```
OBS. TIME    WING GEOMETRY SPL CORRECTION FOR EACH FREQUENCY
25.20 SPL      .00    .00    .00    .00    .00    .00    .00
      SPL      .00    .00    .00    .00    .00    .00    .00
      SPL      .00    .00    .00    .00    .00    .00    .00

OBS. TIME    WING GEOMETRY SPL CORRECTION FOR EACH FREQUENCY
25.70 SPL      .00    .00    .00    .00    .00    .00    .00
      SPL      .00    .00    .00    .00    .00    .00    .00
      SPL      .00    .00    .00    .00    .00    .00    .00

OBS. TIME    WING GEOMETRY SPL CORRECTION FOR EACH FREQUENCY
26.20 SPL      .00    .00    .00    .00    .00    .00    .00
      SPL      .00    .00    .00    .00    .00    .00    .00
      SPL      .00    .00    .00    .00    .00    .00    .00

OBS. TIME    WING GEOMETRY SPL CORRECTION FOR EACH FREQUENCY
26.70 SPL      .00    .00    .00    .00    .00    .00    .00
      SPL      .00    .00    .00    .00    .00    .00    .00
      SPL      .00    .00    .00    .00    .00    .00    .00

OBS. TIME    WING GEOMETRY SPL CORRECTION FOR EACH FREQUENCY
27.20 SPL      .00    .00    .00    .00    .00    .00    .00
      SPL      .00    .00    .00    .00    .00    .00    .00
      SPL      .00    .00    .00    .00    .00    .00    .00

OBS. TIME    WING GEOMETRY SPL CORRECTION FOR EACH FREQUENCY
27.70 SPL      .00    .00    .00    .00    .00    .00    .00
      SPL      .00    .00    .00    .00    .00    .00    .00
      SPL      .00    .00    .00    .00    .00    .00    .00

OBS. TIME    WING GEOMETRY SPL CORRECTION FOR EACH FREQUENCY
28.20 SPL      .00    .00    .00    .00    .00    .00    .00
      SPL      .00    .00    .00    .00    .00    .00    .00
      SPL      .00    .00    .00    .00    .00    .00    .00

 1             ANOPP LEVEL 03/02/11                    PAGE    24

OBS. TIME    WING GEOMETRY SPL CORRECTION FOR EACH FREQUENCY
28.70 SPL      .00    .00    .00    .00    .00    .00    .00
      SPL      .00    .00    .00    .00    .00    .00    .00
      SPL      .00    .00    .00    .00    .00    .00    .00

OBS. TIME    WING GEOMETRY SPL CORRECTION FOR EACH FREQUENCY
29.20 SPL      .00    .00    .00    .00    .00    .00    .00
```

1/21/**

WING GEOMETRIC EFFECTS MODULE

OBS. TIME 29.70 SPL .00 .00 .00 .00 .00 .00 .00 .00
                 SPL .00 .00 .00 .00 .00 .00 .00
                 SPL .00 .00 .00 .00 .00 .00 .00

WING GEOMETRY SPL CORRECTION FOR EACH FREQUENCY

OBS. TIME 30.20 SPL .00 .00 .00 .00 .00 .00 .00 .00
                 SPL .00 .00 .00 .00 .00 .00 .00
                 SPL .00 .00 .00 .00 .00 .00 .00

WING GEOMETRY SPL CORRECTION FOR EACH FREQUENCY

OBS. TIME 30.70 SPL .00 .00 .00 .00 .00 .00 .00 .00
                 SPL .00 .00 .00 .00 .00 .00 .00
                 SPL .00 .00 .00 .00 .00 .00 .00

WING GEOMETRY SPL CORRECTION FOR EACH FREQUENCY

OBS. TIME 31.20 SPL .00 .00 .00 .00 .00 .00 .00 .00
                 SPL .00 .00 .00 .00 .00 .00 .00
                 SPL .00 .00 .00 .00 .00 .00 .00

WING GEOMETRY SPL CORRECTION FOR EACH FREQUENCY

OBS. TIME 31.70 SPL .00 .00 .00 .00 .00 .00 .00 .00
                 SPL .00 .00 .00 .00 .00 .00 .00
                 SPL .00 .00 .00 .00 .00 .00 .00

WING GEOMETRY SPL CORRECTION FOR EACH FREQUENCY

OBS. TIME 32.20 SPL .00 .00 .00 .00 .00 .00 .00 .00
                 SPL .00 .00 .00 .00 .00 .00 .00
                 SPL .00 .00 .00 .00 .00 .00 .00

WING GEOMETRY SPL CORRECTION FOR EACH FREQUENCY

OBS. TIME 32.70 SPL .00 .00 .00 .00 .00 .00 .00 .00
                 SPL .00 .00 .00 .00 .00 .00 .00
                 SPL .00 .00 .00 .00 .00 .00 .00

1   1/21/**   ANOPP LEVEL 03/02/11   PAGE 25

WING GEOMETRIC EFFECTS MODULE

WING GEOMETRY SPL CORRECTION FOR EACH FREQUENCY

OBS. TIME 33.20 SPL .00 .00 .00 .00 .00 .00
                 SPL .00 .00 .00 .00 .00 .00
                 SPL .00 .00 .00 .00 .00 .00

III-25

OBS. TIME
33.70   WING GEOMETRY SPL CORRECTION FOR EACH FREQUENCY
        SPL   .00   .00   .00   .00   .00
        SPL   .00   .00   .00   .00   .00
        SPL   .00   .00   .00   .00   .00

OBS. TIME
34.20   WING GEOMETRY SPL CORRECTION FOR EACH FREQUENCY
        SPL   .00   .00   .00   .00   .00
        SPL   .00   .00   .00   .00   .00
        SPL   .00   .00   .00   .00   .00

OBS. TIME
34.70   WING GEOMETRY SPL CORRECTION FOR EACH FREQUENCY
        SPL   .00   .00   .00   .00   .00
        SPL   .00   .00   .00   .00   .00
        SPL   .00   .00   .00   .00   .00

LEV   USES DEFAULT VALUES FOR FOLLOWING PARAMETERS

NAME	TYPE	CODE	ELEMENT	VALUE
IDWT	L	6	(1)	F
IPNLT	L	6	(1)	T
NAWT	L	6	(1)	F
NDWT	L	6	(1)	F
NOSPL	L	6	(1)	F

NOISE LEVELS MODULE

MODULE LEV USES THE FOLLOWING INPUT PARAMETERS AND UNIT MEMBERS

IDWT   = F   IOSPL = T   IPNL   = T   IPNLT = T
NDWT   = F   NOSPL = F   IPRINT = 3
WING   = PRES

OBSERV (COORD)   IS ALTERNATE NAME OF OBSERV (COORD)
LEV   (AWGT   )   IS ALTERNATE NAME OF LEV   (AWGT   )
LEV   (PNLT   )   IS ALTERNATE NAME OF LEV   (PNLT   )
LEV   (PRES   )   IS ALTERNATE NAME OF LEV   (PRES   )
SFIELD (FREQ   )   IS ALTERNATE NAME OF SFIELD (FREQ   )
WING   (PRES   )   IS ALTERNATE NAME OF WING   (PRES   )

IAWT   = T
NAWT   = F
MEMSUM =

***************** DBM INFORMATIVE MESSAGE   76 *** MMOPWS - UNIT LEV   IS BEING CREATED DYNAMICALLY. *************************

NOISE LEVELS MODULE

NOISE SOURCES USED IN CALCULATING THE NOISE LEVELS

FANOUT

NOISE LEVELS MODULE

TIME HISTORIES OF THE NOISE LEVELS AT THE OBSERVER POSITIONS
(0.00 MEANS VALUE WAS NOT COMPUTED)

OBSERVER   1   (-7516.0000   .00000000E+00   4.0000000   )

OBSERVER TIME	OVERALL SPL (DB)	A-WEIGHTED SPL (DB(A))	D-WEIGHTED SPL (DB(D))	PERCEIVED NOISE LEVEL (PNL) (PNDB)	TONE-CORRECTED PNL (PNLT) (PNDB)
5.20	15.97	15.33	.00	11.32	12.10
5.70	16.70	16.37	.00	14.56	15.51
6.20	17.60	17.56	.00	18.03	19.31
6.70	18.39	18.51	.00	20.75	22.20
7.20	18.88	19.09	.00	22.60	24.19
7.70	19.83	20.20	.00	25.33	26.90
8.20	21.81	22.42	.00	29.64	31.05
8.70	23.25	23.97	.00	31.75	33.27
9.20	24.28	25.04	.00	33.29	34.99
9.70	26.28	27.10	.00	36.24	37.69
10.20	27.97	28.81	.00	38.67	40.26
10.70	30.37	31.26	.00	41.69	43.58
11.20	32.74	33.60	.00	45.11	46.82
11.70	35.84	36.68	.00	48.76	50.83
12.20	38.92	39.70	.00	52.05	53.60
12.70	42.33	43.05	.00	55.69	57.66
13.20	47.10	47.74	.00	60.65	62.02
13.70	51.71	52.27	.00	65.37	66.87
14.20	57.97	58.46	.00	71.47	72.65
14.45	61.69	62.12	.00	75.23	76.93
14.70	68.22	68.88	.00	81.58	82.63
14.95	69.65	70.02	.00	82.97	83.99
15.20	73.65	73.99	.00	86.90	87.92
15.45	77.33	77.70	.00	89.98	91.76

1

15.70	80.15	80.58	.00	93.13	94.93
15.95	84.93	85.40	.00	97.97	98.97
16.20	85.45	85.93	.00	98.51	99.55
16.45	85.38	85.89	.00	98.53	99.58
16.70	84.88	85.41	.00	98.12	99.48
16.95	83.89	84.46	.00	97.18	98.63
17.20	82.33	82.92	.00	95.65	96.58
17.70	78.56	79.20	.00	92.03	93.34
18.20	74.27	74.95	.00	87.87	88.82
18.70	70.46	71.17	.00	84.24	85.41
19.20	65.32	66.05	.00	79.04	80.58
19.70	62.37	63.14	.00	76.08	78.66
20.20	60.34	61.15	.00	74.18	75.39
20.70	59.41	60.27	.00	73.14	75.59
21.20	57.40	58.23	.00	71.33	72.63
21.70	56.96	57.87	.00	70.69	72.26
22.20	55.33	56.22	.00	68.92	70.77
22.70	54.39	55.29	.00	68.24	69.61
23.20	53.59	54.52	.00	67.24	68.49
23.70	52.40	53.33	.00	65.37	67.09

1/21/**   ANOPP LEVEL 03/02/11   PAGE   37

NOISE LEVELS MODULE

24.20	51.58	52.50	.00	65.19	66.70
24.70	50.64	51.59	.00	64.59	66.70
25.20	49.77	50.70	.00	63.15	64.54
25.70	48.79	49.72	.00	61.30	63.09
26.20	48.18	49.12	.00	60.65	62.28
26.70	47.81	48.75	.00	61.11	62.82
27.20	47.17	48.11	.00	60.55	63.31
27.70	46.25	47.16	.00	59.40	62.09
28.20	45.22	46.09	.00	57.72	59.61
28.70	44.26	45.09	.00	55.45	57.04
29.20	43.51	44.32	.00	55.26	56.92
29.70	43.00	43.81	.00	54.97	56.20
30.20	42.66	43.48	.00	54.42	55.58
30.70	42.35	43.18	.00	54.44	56.33
31.20	41.99	42.82	.00	54.26	56.72
31.70	41.54	42.36	.00	53.86	56.35
32.20	41.00	41.80	.00	53.21	55.63

1

ENTERING ANOPP NORMAL TERMINATION PHASE
ANOPP IS TERMINATING NORMALLY

REPORT DOCUMENTATION PAGE		Form Approved OMB No. 0704-0188

Public reporting burden for this collection of information is estimated to average 1 hour per response, including the time for reviewing instructions, searching existing data sources, gathering and maintaining the data needed, and completing and reviewing the collection of information. Send comments regarding this burden estimate or any other aspect of this collection of information, including suggestions for reducing this burden, to Washington Headquarters Services, Directorate for Information Operations and Reports, 1215 Jefferson Davis Highway, Suite 1204, Arlington, VA 22202-4302, and to the Office of Management and Budget, Paperwork Reduction Project (0704-0188), Washington, DC 20503.

1. AGENCY USE ONLY (Leave blank)	2. REPORT DATE November 2000	3. REPORT TYPE AND DATES COVERED Contractor Report

4. TITLE AND SUBTITLE Small Engine Technology (SET) Task 23 ANOPP Noise Prediction for Small Engines, Wing Reflection Code	5. FUNDING NUMBERS C NAS3-27483 TA 23
6. AUTHOR(S) Lysbeth Lieber and Daniel Brown	WU 522-81-13-01

7. PERFORMING ORGANIZATION NAME(S) AND ADDRESS(ES) Honeywell Engines and Systems 111 S. 34th Street P.O. Box 52180 Phoenix, AZ 85072-2180	8. PERFORMING ORGANIZATION REPORT NUMBER 21-11144

9. SPONSORING/MONITORING AGENCY NAME(S) AND ADDRESS(ES) National Aeronautics and Space Administration Langley Research Center Hampton, VA 23681-2199	10. SPONSORING/MONITORING AGENCY REPORT NUMBER NASA/CR-2000-210630

11. SUPPLEMENTARY NOTES
This final report was prepared for Langley Research Center under Task 23 of Contract NAS3-27483.
Contracting Officer: Linda M. Kendrick, NASA Glenn Research Center, Cleveland, Ohio
Technical Monitor: Robert A. Golub, NASA Langley Research Center, Hampton, Virginia

12a. DISTRIBUTION/AVAILABILITY STATEMENT Unclassified-Unlimited Subject Category 71 Distribution: Nonstandard Availability: NASA CASI (301) 621-0390	12b. DISTRIBUTION CODE

13. ABSTRACT (Maximum 200 words)

The work performed under Task 23 consisted of the development and demonstration of improvements for the NASA Aircraft Noise Prediction Program (ANOPP), specifically targeted to the modeling of engine noise enhancement due to wing reflection. This report focuses on development of the model and procedure to predict the effects of wing reflection, and the demonstration of the procedure, using a representative wing/engine configuration.

14. SUBJECT TERMS Noise reduction; Simulation			15. NUMBER OF PAGES 108
			16. PRICE CODE A06

17. SECURITY CLASSIFICATION OF REPORT Unclassified	18. SECURITY CLASSIFICATION OF THIS PAGE Unclassified	19. SECURITY CLASSIFICATION OF ABSTRACT Unclassified	20. LIMITATION OF ABSTRACT UL

NSN 7540-01-280-5500

Standard Form 298 (Rev. 2-89)
Prescribed by ANSI Std. Z-39-18
298-102